DE-AC22-91PC91042-TPR-3

Effects of Low-Temperature Catalytic Pretreatments on Coal Structure and Reactivity in Liquefaction

DOE/PC/91042--T2

DE93 004362

Technical Progress Report
April 1992 - July 1992

C. Song, A.K. Saini, L. Huang, K. Wenzel, L. Hou, P.G. Hatcher and H.H. Schobert

Fuel Science Program
Department of Materials Science and Engineering
The Pennsylvania State University
209 Academic Projects Building, University Park, Pennsylvania, PA 16802

August 1992

Prepared for the U.S. Department of Energy
under Contract No.
DE-AC22-91PC91042

DISCLAIMER

ACKNOWLEDGEMENTS

This on-going project is supported by the U.S. Department of Energy, Pittsburgh Energy Technology Center, in Advanced Coal Research Program. Dr. Michael J. Baird is DOE/PETC Project Manager, and Drs. H.H. Schobert, C. Song and P.G. Hatcher are the Co-Principal Investigators at Penn State. The authors wish to express their appreciation to Drs. M. J. Baird, S. Lee, and E. B. Klunder of DOE/PETC for their support of this effort. The authors would also like to thank Dr. A. Davis and Mr. D. Glick for providing samples and data of the Department of Energy Coal Sample (DECS) from DOE/Penn State Coal Sample Bank, and Mr. R.M. Copenhaver for the fabrication of tubing bomb reactors.

TABLE OF CONTENTS

ABSTRACT

Low-temperature catalytic pretreatment is a promising approach to the development of an improved liquefaction process. This work is a fundamental study on effects of pretreatments on coal structure and reactivity in liquefaction. The main objectives of this project are to study the coal structural changes induced by low-temperature catalytic and thermal pretreatments by using spectroscopic techniques; and to clarify the pretreatment-induced changes in reactivity or convertibility of coals in the subsequent liquefaction. This report describes the recent progress of our work.

Substantial progress has been made in the spectroscopic characterization of structure and pretreatment-liquefaction reactions of a Montana subbituminous Coal (DECS-9), and thermochemical analysis of three raw and reacted bituminous coals. Temperature programmed liquefaction has been performed on three low-rank coals both in the presence and absence of dispersed molybdenum sulfide catalyst. We also performed a detailed study of the effects of mild thermal pretreatment- drying in air and in vacuum - on thermal and catalytic liquefaction of a Wyodak subbituminous coal.

Important information on structure andstructural transformation during thermal pretreatment and liquefaction reactions of low-rank coals has been derived by applying solid-state CPMAS ^{13}C NMR and flash pyrolysis-GC-MS (Py-GC-MS) for characterization of the macromolecular network of a Montana subbituminous coal and its residues from temperature-programmed and non-programmed liquefaction (TPL and N-PL) at .al temperatures ranging from 300 to 425°C in H-donor and non-donor solvents. The results revealed that this coal contains significant quantities of oxygen-bearing structures, corresponding to about 18 O-bound C per 100 C atoms and one O-bound C per every 5 to 6 aromatic C. The oxygen-bearing components in the coal include catechol-like structures, which seem to disappear from the liquefaction residues above 300°C; carboxyl groups, which almost disappear after 350°C; and phenolic structures, which are most important in the original coal but diminish in concentration with increasing temperature. These results point to the progressive loss of oxygen functional groups and aliphatic-rich species from the macromolecular network of the coal during programmed heat-up under TPL conditions. The higher conversions in TPL runs in H-donor tetralin (relative to the conventional N-PL runs) suggest that the removal of carboxylic and catechol groups from the coal and the capping of the reactive sites by H-transfer from H-donors during low temperature ($\leq$ 350°C) pretreatments have contributed to minimizing the retrogressive crosslinking at higher temperatures. Quantitative calculation of NMR data and mathematical correlation were also attempted in this work. For 24 liquefaction residues

derived under significantly different conditions, linear correlations between C-distribution and reaction temperature (≥300°C) have been found, which can be expressed by a simple equation, $C_i = \alpha f_i + \beta T$, where f_i and C_i represent content of aromatic, aliphatic, or oxygen-bound carbons in the original coal and residue, respectively; T stands for the reaction temperature; α and β are constants.

Thermogravimetric analysis (TGA) of three bituminous coals has revealed the differences in their devolatilization behavior. Py-GC-MS of these coals at different pyrolysis temperatures and the Py-GC-MS of thermally pretreated samples provided some new information on their structures and structural transformations. For three low-rank coals, swelling and impregnation of catalyst precursors by preswelling were attempted. The results of their temperature-programmed catalytic and non-catalytic liquefaction are described in this report. We also studied the effects of non-oxidative and oxidative drying on the structure and on the thermal and catalytic liquefaction of Wyodak subbituminous coal (DECS-8). The structural changes due to air-drying were followed by using CPMAS ^{13}C NMR and FT-IR; the changes in the reactivity and convertibility were evaluated by changes in coal conversion and product distribution. An interesting observation is that for catalytic liquefaction, oxidative drying appeared to be better than vacuum-drying for liquefaction under certain conditions.

INTRODUCTION

The conventional concept for high-severity conversion of coal is that coal must be heated to high temperatures (400-450°C) causing thermal cleavage of bonds in organic matrix of coal to yield free radicals, which are capped by hydrogen to form low-molecular-weight products. However, recent fundamental research in coal liquefaction and pyrolysis has revealed that coal is more reactive than had been thought previously. The thermally initiated reactions of coal can take place very rapidly (Whitehurst et al., 1980a, 1980b) and, especially for low-rank coals, can occur at lower temperatures (Neavel, 1982; Suuberg et al., 1985, 1987). Temperature-programmed pyrolysis (TPP) of different coals ranging from brown to bituminous coals clearly showed that more bonds in low-rank coals are thermally broken at lower temperatures as compared to bituminous coals, and a concept of bond energy distribution has been developed from TPP (Song et al., 1991a; Song and Schobert, 1992). Considerable work at Penn State (Davis et al., 1986, 1989; Derbyshire et al., 1986a, 1986b, 1989; Stansberry et al., 1987; Burgess and Schobert, 1990; Burgess et al., 1991) has demonstrated that the combination of low-temperature catalytic reaction followed by the high temperature catalytic reaction using dispersed molybdenum catalysts significantly enhanced coal conversion and oil production. More recent work in this laboratory has shown that temperature-programmed liquefaction using programmed heat-up is more effective for converting low-rank coals (Song et al., 1991b; Song and Schobert, 1992; Huang et al., 1992). All these results point to the beneficial effects of reactions at lower temperatures as compared to conventional high-severity processes.

The above results strongly suggest that low-temperature catalytic pretreatment or preconversion is a promising approach and deserves further detailed study. An important fact noted from previous work is that the low temperature pretreatments using dispersed catalyst do not appreciably alter the solubility of coal in THF, and the main effects become apparent only upon subsequent reaction at higher temperature (Derbyshire, 1988; DOE COLIRN, 1989). Probably the catalytic pretreatment affects the early reaction stage most significantly. The importance of, and potential problems, associated with early steps in direct liquefaction has been discussed in relation to the catalytic pretreatments in the previous report (Song et al., 1992d). Briefly, the most important issue in the early stage of coal dissolution is to suppress the retrograde reactions to produce higher yields of less refractory liquids for the down-stream catalytic upgrading. The appropriate low-temperature catalytic pretreatments followed by high-temperature catalytic reactions could improve yield and quality of distillate products and increase coal conversion and the efficiency of hydrogen utilization, provided that the pretreatment can induce desirable structural

modification in coal that will improve its reactivity and reduce retrograde reactions upon liquefaction. Recently, we have demonstrated that the combined use of solid-state NMR and pyrolysis-GC-MS has the potential to reveal the major and minor structural changes in the macromolecular network of coal induced by low-temperature liquefaction (Song et al., 1991b, 1992b). The study of coal structure and reactivity associated with catalytic pretreatment and subsequent liquefaction could lead to the development of most effective preconversion and liquefaction procedures. These advantages are of great importance to the potential commercial applications, not only in coal hydroliquefaction, but also in coal co-processing as well as coal hydropyrolysis. An apparent disadvantage of introducing catalytic pretreatment is that it increases the process units, equipment costs and complexity of operation. This disadvantage can be offset by the prospective gains in yields and quality of distillate products and suppression of unnecessary H_2 consumption. It is undisputable that the development of a low-severity catalytic liquefaction process has great potential to improve overall process efficiency and to reduce operating costs for producing transportation fuels from coal.

PROJECT OBJECTIVES

This work is a fundamental study of catalytic pretreatments as a potential preconversion step to low-severity liquefaction. The ultimate goal of this work is to provide the basis for the design of an improved liquefaction process and to facilitate our understanding of those processes that occur when coals are initially dissolved. The main objectives of this project are to study the effects of low-temperature pretreatments on coal structure and their impacts on the subsequent liquefaction. The effects of pretreatment temperatures, catalyst type, coal rank and influence of solvent will be examined.

The specific objectives are to identify the basic changes in coal structure induced by catalytic and thermal pretreatments by using spectroscopic, thermochemical and chemical techniques; and to determine the reactivity of the catalytically and thermally treated coals for coal liquefaction. Combining the two lines of information will allow us to identify the pretreatment-induced desirable/undesirable basic changes in coal structure; to clarify the impacts of pretreatments on coal liquefaction; to identify the structures responsible for retrograde reactions; to evaluate the structural differences resulting from different catalytic actions in relation to the overall catalytic effects in liquefaction; and ultimately, to develop a structure-reactivity relationship for liquefaction associated with catalyst type, coal rank and solvent. Furthermore, this research will contribute greatly to the development of effective pretreatment procedures which will allow coals to be liquefied more efficiently than the current practice. Finally, much of the knowledge to be generated from this research is not only critical for developing advanced hydroliquefaction processes, but also very useful to development of coal/petroleum resid co-processing, pyrolysis and hydropyrolysis processes.

TECHNICAL PROGRESS

1. CPMAS ^{13}C NMR and Pyrolysis-GC-MS Studies of Structure and Liquefaction Reactions of Montana Subbituminous Coal

INTRODUCTION

Modern solid state ^{13}C nuclear magnetic resonance (NMR) spectroscopy originated in the 1970's when cross-polarization (CP) and magic angle spinning (MAS) techniques were developed and combined (CPMAS) [Pines et al., 1972, 1973; Schaefer, 1976; Andrew, 1977; Yannoni, 1982]. Since the first paper on ^{13}C NMR of coals was published by VanderHart and Retcofsky in 1976, solid-state NMR has been applied extensively in characterization of coals [VanderHart, 1976]. The techniques of CPMAS and dipolar dephasing MAS (DDMAS) ^{13}C NMR can provide useful structural information on insoluble organic solids. In recent years, solid-state NMR has rapidly become one of the most important non-destructive techniques for studying the structure of solid coal, coal macerals, coal-derived products, geochemical samples, and other organic solids [Alemany et al., 1983; Wilson et al., 1984; Dennis et al., 1982; Hatcher et al., 1989; Yoshida et al., 1987, 1984; Supaluknari et al., 1989; Solum, 1989; Botto, 1987]. As long as one recognizes the important experimental variables necessary for quantitative measurements, it can make a major contribution to the structural characterization of insoluble carbonaceous materials [Davidson, 1980; Wilson et al., 1984; Snape et al., 1989; Meiler & Meusinger, 1991].

Flash pyrolysis-gas chromatography-mass spectrometry (Py-GC-MS) is also an important analytical technique for structural study of polymeric materials [Nip et al., 1985; Philp, 1987; Saiz-Jimenez et al., 1986; Saiz-Jimenez & Leeuw, 1986; Hatcher et al., 1988, Nomura et al., 1989]. Py-GC-MS is relatively simple in theory, and can be viewed as a combination of the well known MS techniques with pyrolysis-GC [Gallegos, 1979; Meuzelaar, 1982; Maswadeh et al., 1992; Winans et al., 1992]. While these techniques have been applied in many investigations, very few applications have been made in coal liquefaction studies. Yoshida et al. [1987, 1992] analyzed several different coals by using CPMAS ^{13}C NMR and attempted correlating their liquefaction reactivity with structural characteristics. Franco et al. [1991] characterized the structural changes of two coals before and after chemical treatments using CPMAS ^{13}C NMR. Fatemi-Badi et al. [1990] examined a lignite and its liquefaction residues using solid state NMR and IR. Recently, Song et al. [1991, 1992] and Saini et al. [1992] reported preliminary studies of coal structure, pretreatments and liquefaction using CPMAS ^{13}C NMR, pyrolysis-GC-MS and FT-IR.

The present work is a part of an on-going program to examine the structure and temperature-programmed liquefaction of low-rank coals, and involves the spectroscopic study of coals and their

residues from liquefaction at different temperatures by using the combination of CPMAS ^{13}C NMR and Py-GC-MS techniques [Song et al., 1991b, 1992a, 1992b; Song and Schobert, 1992; Saini et al., 1992]. The NMR technique has an advantage of providing the information related to the type and distribution of aromatic and aliphatic carbons in a non-destructive and quantitative fashion. Its disadvantage is that the information from NMR does not provide a direct picture of the molecular components and their environments. This is partly because the coal organic matrix is a complex mixture, whose individual components can not be resolved by NMR. Py-GC-MS is a very useful technique for studying the molecular components or structural units of polymeric organic solids. However, the major drawback to Py-GC-MS is that the proportion of coal that can be volatilized and analyzed by GC-MS is relatively small. For many coals more than half of the organic material remains as a residue. Since each technique has advantages and disadvantages, we can make complementary use of these techniques by using them in tandem. The combined use of solid state NMR and Py-GC-MS has the potential to provide both average structural information and specific molecular components, and when applied to properly selected samples, can provide insights into the major and minor changes in coal structures and structural transformations involved in coal liquefaction processes [Song et al., 1991b, 1992a].

The objectives of the present work are 1) to characterize the structural features and structural components of a subbituminous coal, 2) to delineate the chemical reactions occurring during coal liquefaction by characterizing the resultant structural changes in coal macromolecular network using CPMAS ^{13}C NMR and Py-GC-MS, and 3) to make quantitative evaluation of changes in carbon distribution of coal macromolecular network as a function of reaction temperature. Mathematical correlation of CPMAS ^{13}C NMR data with reaction temperature was also attempted in the present work, and the results are reported in this report.

EXPERIMENTAL

Sample Preparation

The coal used was a Montana subbituminous coal obtained from the DOE/Penn State Coal Sample Bank (DECS-9 or PSOC-1546). This sample was collected from Dietz seam in Bighorn County of Montana state in June 1990, and it was stored in a multi-layer laminated bag under argon atmosphere. The proximate and ultimate analysis of this coal are as follows: 33.5% volatile matter, 37.1% fixed carbon, 4.8% ash, 24.6% moisture, on a raw coal basis; 76.1% C, 5.1% H, 0.9% N, 0.3% organic S, and 17.5% O, on a dmmf basis. The coal was dried in a vacuum oven at 95°C for 2 h before use. The liquefaction vehicles used were tetralin, a known H-donor, and non-donors such as 1-methylnaphthalene and naphthalene as well as process solvent, which is a middle distillate

fraction from two-stage catalytic liquefaction of Pittsburgh #8 bituminous coal at the Advanced Coal Liquefaction Research and Development Facility in Wilsonville in Run 259E (WI-MD) [Gollakota et al., 1990; 129-158; Lai et al., 1992]. Liquefaction was carried out in 25 mL microautoclaves using 4 g coal (< 60 mesh) and 4 g solvent under 6.9 MPa (cold) H_2. After the reaction, the liquid and solid products were separated by sequential extraction with hexane, toluene and tetrahydrofuran (THF). More details about liquefaction experiments may be found elsewhere [Song and Schobert, 1992; Song et al., 1992].

In order to derive structural information related to the macromolecular network, the low molecular weight species in the coal and coal liquefaction products were removed by THF extraction, and the THF-insoluble residues were analyzed by CPMAS ^{13}C NMR and Py-GC-MS. Our preliminary tests showed that a trace amount of THF remains in the residue even after vacuum drying at 100 °C for over 6 h, which significantly interferes with the characterization using Py-GC-MS and NMR. Therefore, prior to analyses, all the THF-insoluble residues were washed first by using acetone and then n-pentane, followed by vacuum drying at 100°C for 6 h. This procedure was found to be very effective for removing trace amounts of THF, as confirmed by NMR and Py-GC-MS.

CPMAS ^{13}C NMR Spectroscopy

The NMR spectra were acquired on a Chemagnetics M-100 NMR spectrometer by using the combined high power proton decoupling, cross-polarization and magic-angle-spinning (CPMAS) techniques. The measurements were carried out at a carbon frequency of 25.1 MHz. About 0.4-0.6 g of a sample was packed in a 0.4 mL bullet-type rotor made of polychlorotrifluoroethylene (Kel-F); the spinning speed of the rotor was about 3.5 kHz. The experimental conditions for all the samples are as follows: a cross-polarization contact time of 1 ms and a pulse delay time of 1 s. An instrumental calibration test was performed with the rotor containing hexamethylbenzene, which was adjusted to the magic angle (54.7°) to give the correct chemical shifts. To assure good spectra with high signal-to-noise ratios, the number of pulses accumulated for obtaining a spectrum was at least 10,000, and most of the spectra were obtained with numbers of scans between 20,000 to 35,000. Other details concerning solid state NMR may be found elsewhere [Hatcher et al., 1989].

For quantitative evaluation, the NMR spectra were input into computer as graphs by using an automated digitizing system UN-PLOT-IT software developed by Silk Scientific, Inc. in 1990. Further data processing was performed by using LAB CALC software developed by Galactic Industries Co. in 1990. The peak separation and quantitative calculation of specific NMR bands were carried out by using the curve-fitting program of LAB CALC.

Pyrolysis-GC-MS

Py-GC-MS analysis was performed on a Du Pont 490B GC-MS system fitted with a 30 m x 0.25 mm i.d. DB-17 capillary column coated with 50% phenylmethylsilicone stationary phase with a film thickness of 0.25 μm, and interfaced to a Chemical Data Systems Pyroprobe-1000 pyrolyzer. Helium was used as a carrier gas. The data acquisition and processing were controlled through a computer-aided system. In a typical run, about 0.6-1.0 mg of a sample was loaded into a thin quartz tube, which was then inserted into the horizontal filament coil in the pyroprobe. The pyroprobe is then interfaced directly to the capillary GC inlet. Prior to the start of data acquisition, the sample was flash-pyrolyzed (with a nominal heating rate of 5000°C/second) at 610°C for 10 seconds, during which the pyrolyzates (pyrolysis products) were cryotrapped in the close-to-inlet part of the capillary column by cooling with liquid nitrogen. The column temperature was programmed from 30°C to 280°C at a heating rate of 4°C/min. The mass spectrometer was operated in the electron impact mode at 70 eV. It should be noted that our preliminary Py-GC-MS data were obtained by using an old capillary column [Song et al., 1991, 1992a, 1992b]. A new DB-17 column was installed for the Py-GC-MS runs reported here, which exhibited better sensitivity and resolution, especially for catechol and methylcatechol peaks.

RESULTS AND DISCUSSION

CPMAS ^{13}C NMR of DECS-9 Montana Subbituminous Coal

Figure 1 shows the CPMAS ^{13}C NMR spectra of the fresh Montana subbituminous coal and the unreacted but THF-extracted coal. It is interesting to note that the THF-extracted coal, which lost about 8 % THF-soluble materials, gave a spectrum similar to that of the raw coal in terms of the aromaticity and functionality (see below). Integration of the spectra gives only a slightly higher aromaticity (fa) value for the THF-extracted coal than for the raw coal. It should be noted that, for some coals, the THF-extracted samples may display substantially different spectra.

A general observation is that these NMR spectra are relatively poorly resolved, as compared to the spectra of pure materials, primarily because of the presence of a large number of different molecular species that have only slightly different chemical shifts. The representative carbon types are also marked in Figure 1. In general, there two major spectral bands, an aromatic band from 90 to 170 ppm and an aliphatic band from 0 to 90 ppm. Among the aliphatic carbons, methyl groups appear at 0-25 ppm, methylene carbons resonate between 25-50 ppm, methoxyl groups around 50-65 ppm and ether group between 70-80 ppm [Yoshida & Maekawa, 1987; Franco et al., 1991; Song et al., 1992a]. The aromatic region also includes two shoulders which are likely due to

catechol-like carbons and phenolic carbons, respectively. There are some other bands with lower intensities, including carboxyl groups at 170-190 ppm and carbonyl groups between 190-230 ppm.

Py-GC-MS of Montana Coal

Figure 2 shows the retention time (RT) window (0-40 min) of the total ion chromatogram (TIC) obtained from Py-GC-MS of the THF-extracted raw coal. With the aid of computer-based data processing, it is now possible to perform a compound type analysis of coal pyrolysis products by using the selective ion monitoring technique in Py-GC-MS, as has been used for hydrocarbon type analysis of liquid fuels by GC-MS [Song and Hatcher, 1992]. Low-rank coals are known to have higher oxygen funtionalities [Schobert, 1990]. We have examined the oxygen compounds in the pyrolyzates by using the characteristic ion masses for phenol (m/z 94), cresol (m/z 108), xylenol and ethylphenol (m/z 122), catechol (m/z 110) and methylcatechol (m/z 124). Within the RT range of 9-16 min in the TIC, there are five dominant peaks, and all of them are phenolic compounds. Also found in this sample are catechol and methylcatechol between RT of 17-21 min, in relatively high intensities. The relative retention order of 3- and 4-methylcatechol in Figure 2 was determined based on the results of Bergen et al. [Bergen et al., 1991].

There are many other small peaks appearing over the whole RT region, and selective ion monitoring at m/z 71 indicates that many of them are long-chain alkanes and alkenes. Figure 3 shows the whole TIC and selected SICs at ion masses characteristic of alkanes (m/z 71) and alkylbenzenes (m/z 91). In the SIC at m/z 71 there are a number of alkanes ranging from C_4 to C_{31} (the carbon-number indicates the even-numbered alkanes). Several hydrocarbon peaks which appeared as unresolved peaks between RT of 2-3 min in this SIC are C_4-C_6 alkanes plus alkenes. It is interesting to note that this sample still contains long-chain aliphatic components up to n-C_{31} although it was pre-extracted by THF for over 24 h. Prist-1-ene was also found in this sample, as marked between n-C_{17} and n-C_{18} in the SIC at m/z 71. Both pristane and prist-1-ene are known fossil fuel biomarkers [Philp, 1985]. The presence of prist-1-ene but absence of pristane in the pyrolyzates may suggest that pristane is chemically bound into the coal structure. In the SIC for m/z 91, there are only three major peaks. The two relatively large peaks around RT of 4 min and 5 min are toluene and p- and o-xylene, in that order. Another peak appearing around RT of 35 min is n-dodecylbenzene. We also performed Py-GC-MS of the raw coal (undried and unextracted). The Py-GC-MS TIC is similar to that in Figure 3 in that one can found identical peaks in both, but the relative intensities of the peaks eluting before RT of 3 min are higher for the raw coal, which is expected. Overall, the above results show that the DECS-9 coal contains significant amounts of oxygen-containing structural units such as phenol, alkylphenols, catechol (1,2-benzenediol), and methylcatechol, together with small amounts of alkylbenzenes, alkylnaphthalenes and paraffins.

Table 1. Identified Peaks in TIC from Py-GC-MS of DECS-9 Montana Subbituminous Coal

Peak No.	MW	Identified Compounds	Peak No.	MW	Identified Compounds
1	100 + 98	Heptane + Heptene	40	156	Dimethylnaphthalene
2	78	Benzene	41	240	n-Heptadecane (n-C_{17})
3	114 + 112	Octane + Octene	42	238	1-Heptadecene
4	92	Toluene	43	268	Prist-1-ene
5	128 + 126	Nonane + Nonene	44	170	C_3-naphthalene
6	106	p- & m-Xylene	45	254	n-Octadecane (n-C_{18})
7	106	o-Xylene	46	252	1-Octadecene
8	120	C_3-benzene	47	144	2-Naphthol
9	120	C_3-benzene	48	170	C_3-naphthalene
10	120	C_3-benzene	49	144	1-Naphthol
11	94	Phenol	50	268	n-Nonadecane (n-C_{19})
12	118	Indane	51	266	1-Nonadecene
13	170	n-Dodecane (n-C_{12})	52	282	n-Eicosane (n-C_{20})
14	168	1-Dodecene	53	246	n-Dodecylbenzene
15	116	Indene	53*	246	Dodecylbenzene
16	108	o-Cresol	54	280	1-Eicosene
17	108	p- & m-Cresol	55	296	n-Heneicosane (n-C21)
18	184	n-Tridecane (n-C_{13})	56	294	1-Heneicosene
19	182	1-Tridecene	57	178	Phenanthrene
20	130	Methylindene	58	310	n-Docosane (n-C_{22})
21	122	Tetralin	59	308	1-Docosene
22	122	2,4-Dimethylphenol	60	324	n-Tricosane (n-C_{23})
23	122	1,2-Dihydronaphthalene	61	322	1-Tricosene
24	122	4-Ethylphenol	62	338	n-Tetracosane (n-C_{24})
25	128	Naphthalene	63	336	1-Tetracosene
26	146	Methyltetralin	64	352	n-Pentacosane (n-C_{25})
27	198	n-Tetradecane (n-C_{14})	65	350	1-Pentacosene
28	146	Methyltetralin	66	366	n-Hexacosane (n-C_{26})
29	196	1-Tetradecene	67	364	1-Hexacosene
30	110	Catechol (Pyrocatechol)	68	380	n-Heptacosane (n-C_{27})
31	136 + 144	C_3-phenol + C_2-indene	69	378	1-Heptacosene
32	124	3-Methylcatechol	70	394	n-Octacosane (n-C_{28})
33	212	n-Pentadecane (n-C_{15})	71	392	1-Octacosene
34	142	2-Methylnaphthalene	72	408	n-Nonacosane (n-C_{29})
35	210	1-Pentadecene	73	406	1-Nonacosene
36	124	4-Methylcatechol	74	422	n-Triacotane (n-C_{30})
37	142	1-Methylnaphthalene	75	420	1-Triacotene
38	226	n-Hexadecane (n-C_{16})	76	436	n-Hentriacotane (n-C_{31})
39	174 + 160	C_3-tetralin + C_2-tetralin	77	434	1-Hentriacotene

C. Song's sample S-915 / File: D:\Data\aq\Ajay\S915 / Py-GC-MS Run at 5°C/ms to 610°C for 10 s

Liquefaction of DECS-9 Montana Subbituminous Coal.

The temperature-programmed liquefaction (TPL) and non-programmed liquefaction (N-PL) of DECS-9 Montana subbituminous coal in various solvents were carried out at final temperatures ranging from 300 to 425°C. The selected temperature program consisted of rapid heat-up to a low temperature of 200°C, subsequent soaking at 200°C for 15 min, programmed heating at about 7°C/min to a final temperature, followed by a 30 min hold. The importance of controlling the heat-up step in coal liquefaction has been discussed in previous reports [Song et al., 1989, 1991; Song and Schobert, 1992]. For the sake of comparing the amount of organic materials in the THF-insoluble residues, Figure 4 shows the conversions of DECS-9 coal into THF-soluble products plus gas from duplicate runs of DECS-9 coal, as a function of final temperature of TPL or N-PL in tetralin and in WI-MD. It has been found that TPL gives higher conversion of low-rank coals in H-donor solvents such as tetralin and WI-MD than non-programmed liquefaction (N-PL). On the other hand, TPL in non-donor solvents such as naphthalene or methylnaphthalene gave only slightly higher or similar conversions as compared to N-PL runs. However, under comparable conditions (either TPL or N-PL), the coal conversions decreased as the solvent quality decreased: none < naphthalene < methylnaphthalene < WI-MD < tetralin. Detailed TPL results may be found elsewhere [Song and Schobert, 1992; Song et al., 1992b].

CPMAS ^{13}C NMR of Liquefaction Residues.

Figure 5 presents the NMR spectra of the THF-insoluble residues from TPL runs with tetralin. The spectrum of THF-extracted unreacted coal serves as a baseline. The THF-insoluble residue from TPL at final temperature of 300°C has a spectrum (Figure 5B) similar to that of the THF-extracted coal (Figure 5A). In this spectrum, an intense peak is present for aliphatic carbons (0-60 ppm) which may also include trace amounts of aliphatic ether (-C-O-X). This aliphatic peak becomes progressively smaller with increasing severity of liquefaction. The aromatic region has three peaks: an intense peak around 130 ppm (aromatic C), and two shoulders, one at about 142 ppm (possibly catechol-like C), and another at 152 ppm (phenolic or aromatic ether C). A peak at 181 ppm (carboxyl C), and a broad band around 212 ppm (ketone or aldehyde C) define the rest of the spectrum. The peaks at 142 and 212 ppm almost disappear after TPL at 350°C, and the peak at 181 also diminishes after TPL at 375°C. A decrease in intensity of the peak at 152 ppm is only observed after 375°C, and this is accompanied by further loss in aliphatic carbons. Concomitant with the decrease in total aliphatic carbons, the relative contribution from methyl carbons (0-25 ppm) increases. Figure 6 gives the NMR spectra of residues from TPL runs with a process solvent, WI-MD. The trends observed from Figures 5 and 6 are similar to each other. In general, the

intensity of the aliphatic region (0-60 ppm) decreases, and the aromaticity increases with an increase in severity of TPL. The half-width of the aromatic peak decreased and hence the peak became narrower and sharper with increasing temperature, indicating that the aromatic carbons in the residue from a run at higher temperature tend to become more similar to each other (or less diverse).

Pyrolysis-GC-MS of Liquefaction Residues.

Figure 7 shows the 0-32 min RT window of the Py-GC-MS profiles for the residue from TPL in tetralin at 300°C and THF-extracted raw coal, the major peaks of which are numbered and identified in Table 1. Phenol, alkylphenols, alkylbenzenes, catechols as well as alkanes and alkenes are formed from flash pyrolysis of the THF-extracted raw coal. Relative to this sample, there is apparent change in the Py-GC-MS profile of the residue from TPL at 300°C. The disappearance of catechol (peak No. 30) and methylcatechol (No.36) and appearance of a major peak for naphthalene (No.25) differentiate the latter from the former. This is especially interesting, since the NMR spectra of these two samples (Figure 5) and the corresponding yields of THF-solubles (7-9%) are very similar to each other [Song et al., 1991; Song and Schobert, 1992]. From these results, it is clear that the reaction at 300°C did cause some structural change. Repeated Py-GC-MS runs have confirmed the disappearance of catechol and methylcatechol peaks. The naphthalene peak in Figure 7 is due mainly to the use of tetralin as solvent, because this peak was found to be very small with other solvents or without solvent. Since the residue has been extracted by THF for over 24 h, washed by acetone and pentane (to remove THF completely) several times and then dried in a vacuum oven at 90-100°C for 6 h, the naphthalene/tetralin remained in the residue must be either chemically bound to other species or physically entrapped in solvent-inaccessible micropores or closed pores which can not be removed by solvent extraction. From these results, it appears that Py-GC-MS can detect some subtle differences in coal structure which are not easily detectable by CPMAS ^{13}C NMR.

Figure 8 presents the Py-GC-MS profiles of residues from TPL in tetralin at 375°C and 400°C. The numbers attached to the main peaks correspond to those shown in Table 1 for identification. It is clear that even after liquefaction at 375°C for 30 min, the residue still contains significant amounts of structures whose pyrolytic cleavage gives rise to phenol and cresols. The intensities of naphthalene and methylnaphthalene in the pyrolyzates became much higher as compared to the residue from run at 300°C shown in Figure 7. Although in this case part of the naphthalene peak also comes from the tetralin solvent as mentioned above, the ratio of methylnaphthalenes to phenols clearly increased significantly as TPL temperature rose from 300 to 375°C (Figures 7B and 8A). Even higher intensity of naphthalene and methylnaphthalene (relative to the phenols) is seen for the pyrolyzates of residue from TPL at 400°C (Figure 8B). We have

made several replicate Py-GC-MS runs of this sample as well as some other samples. In general the reproducibility was good and distribution patterns of major peaks remained unchanged, although considerable deviations occur sometime with the intensities of the very light C_4-C_6 molecules relative to the other major peaks, presumably due to differences in the amount of liquid nitrogen and time used for cooling capillary column to trap pyrolysis products. In any Py-GC-MS runs of this sample, naphthalene was the most predominant peak. These results indicate higher contents of naphthalene and alkylnaphthalene structures in the residues from runs at higher temperatures, being consistent with the aromaticity increase with increasing temperature as can be seen from Figures 5 and 6.

Quantitative CPMAS ^{13}C NMR for C-Distribution

The progressive changes observed in NMR spectra shown in Figures 5 and 6 prompted us to make quantitative evaluation of coal structural change during liquefaction by curve-fitting the NMR spectra of the residues. Figure 9 shows an example of peak separation of NMR spectrum by using the curve-fitting program in LAB CALC software. Table 2 gives the results of quantitative calculation for the raw and THF-extracted DECS-9 coal. The oxygen-containing peaks are grouped into oxygen-bound aromatic C-O and aliphatic C-O. The calculated carbon distribution shows that aromaticity of raw DECS-9 coal is about 63 % and this coal contains 18 oxygen-bound carbons per 100 carbon atoms. An interesting result is that most of the oxygen is bound to aromatic carbon: 15 aromatic C versus 3 aliphatic C per 100 C. This means that about 84% of all the oxygens are bound to aromatic rings and nearly 20% of the aromatic carbons are bound to oxygen, pointing to one O-bound C every 5-6 aromatic C. Table 2 also indicates that the total number of O/100 C from NMR data is very similar to that from independent, elemental analysis.

Figure 10 shows the change of aromaticity as well as coal conversion as a function of final temperature of TPL in tetralin. There appears to be a linear relation between aromaticity of the residue and the reaction temperature above 300°C. It is also clear from Figure 10 that higher coal conversion corresponds to higher aromaticity of the residue. A similar trend for aromaticity change with coal conversion was also observed by Fatemi-Badi et al. [1991]. Figure 11 shows the carbon distribution of THF-insoluble residues versus temperature of TPL in tetralin. Increasing temperature below 300°C had little impact but further increase up to 425°C resulted in almost linear decrease of aliphatic carbons and O-bound carbons and increase of aromatic carbons. In a previous work, the increased aromatics in residues from liquefaction of subbituminous coals with naphthalene solvent was attributed to naphthalene adduction [Solomon et al., 1991]. We have examined the residues from runs with different solvents (tetralin, naphthalene, methylnaphthalene, WI-MD) and without solvent by using solid state NMR and Py-GC-MS. Figures 12 and 13 shows the NMR spectra of

residues from TPL of DECS-9 coal with different solvents at 350°C and 400°C, respectively. For comparison, Figure 14 presents the NMR spectra of residues from TPL and N-PL runs with tetralin at temperatures ranging from 350-425°C. Taking the significant differences in coal conversion into account, the differences between the ^{13}C NMR spectra of residues from runs at the same final temperatures but using different solvents (Figures 12 and 13) or different heat-up program (Figure 14) are relatively small. Table 3 gives some results of quantitative calculation of NMR data. The data in Figures 5,6,11-14 and Table 3 show that aromaticity increase is mainly dependent on reaction temperature; the use of different solvents and different conditions did not cause substantial differences in the aromaticity of the residue, although the coal conversions can vary significantly in different solvents or under different conditions (Figure 4). These results reveal that the final reaction temperature is most important in determining carbon distribution and structural transformation.

Table 2. C-Distribution & O-Functionality of DECS-9 Subbituminous Coal

	Total Oxygen		Carbon Distribution (%)[a]			
Samples	O/100 C	O/100 C	Aromatic C	Aliphatic C	Aliphatic C-O	Aromatic C-O
	^{13}C NMR	Elemental	95-160 ppm	0-60 ppm	170-230	Shoulders[b]
Raw DECS-9	18	17.4	63	35	3	15
THF-extr. DECS-9	18		64	33	3	15

a) The absolute deviations for the carbon distribution calculations are about ± 2 %.

b) Include phenolic carbons around 156 ppm and catechol-like carbons around 145 ppm.

Table 3. C-Distribution of Liquefaction Residues from DECS-9 Subbituminous Coal

Conditions			Carbon Distribution (%)[a]		
Temperature	Solvent	Program	Aromatic C	Aliphatic C	O-bound C[b]
350	Tetralin	TPL	70	26	15
350	Tetralin	N-PL	70	25	16
350	Naphthalene	TPL	70	28	13
400	Tetralin	TPL	76	24	8
400	Tetralin	N-PL	74	26	7
400	WI-MD	TPL	74	26	7
400	WI-MD	N-PL	75	25	7
400	1-MN	N-PL	78	22	6
400	Naphthalene	N-PL	76	24	5
400	None	N-PL	75	24	6

a) The absolute deviations for the carbon distribution calculations are about ± 2 %.

b) Include phenolic carbons around 156 ppm and catechol-like carbons around 145 ppm.

Figure 15 indicates that both total and aromatic O-bound carbons decrease with increasing temperature from 300 up to 425°C. The progressive changes of O-containing compounds can be clearly seen from the gradual decrease of catechol-like and subsequently phenolic peaks in the expanded aromatic region of the NMR spectra of these residues, as shown in Figure 16. However, the peak shapes of Figures 16E and 16F indicate that there still exist O-bound aromatic carbons even after reaction at 400 and 425°C. This observation is also supported strongly by the observed phenolic components in the pyrolyzates as shown in the Py-GC-MS TIC in Figure 8. It also appears from the expanded region that increasing the temperature from 400 to 425°C caused a decrease in protonated aromatic-C (93-129 ppm) and an increase in bridgehead-C and substituted-C (130-150 ppm), indicating increased degree of condensation.

While the total aliphatic carbons decreased, Figure 17 shows that the percentage of methyl

carbons relative to total aliphatic carbons increased with increasing reaction temperature. This can be due either to the increase or formation of methyl carbons or the decrease in methylene carbons. However, the expanded aliphatic region of NMR spectra, as shown in Figure 18, unambiguously show that the trend observed from Figure 16 is due mainly to the decrease or removal of methylene carbons from the coal during the reaction. Selective ion monitoring using SIC at m/z 71 provided additional evidence from Py-GC-MS data. As shown in Figure 19, the contents of long-chain paraffins in the pyrolyzates decreased with increasing temperature above 300°C, and this is at least partially responsible for the decrease in aliphatic methylene carbon observed from ^{13}C NMR. The above results also demonstrate the potential and importance of combining CPMAS ^{13}C NMR and Py-GC-MS.

Mathematical Correlation of CPMAS ^{13}C NMR Data

On the basis of above-mentioned NMR data, there exist good correlations between carbon distribution in the residues and the reaction temperature above 300°C. This presents a unique opportunity for us to attempt mathematical correlation. Little or no work has been reported in literature on mathematical correlation of CPMAS ^{13}C NMR data with reaction temperature. We have found that the changes in distributions of aromatic, aliphatic, and oxygen-bound carbons in the residues can be correlated with reaction temperature by equations 1, 2 and 3, respectively,

$$C_{arm} = \alpha_1 f_{arm} + \beta_1 T \qquad \text{For aromatic carbon or aromaticity} \qquad 1)$$

$$C_{alip} = \alpha_2 f_{alip} + \beta_2 T \qquad \text{For aliphatic carbons} \qquad 2)$$

$$C_{O\text{-}C} = \alpha_3 f_{O\text{-}C} + \beta_3 T \qquad \text{For oxygen-bound carbons} \qquad 3)$$

where f_{arm}, f_{alip} and $f_{o\text{-}c}$ and C_{arm}, C_{alip}, and $C_{o\text{-}c}$ represent the contents of aromatic, aliphatic, and oxygen-bound carbons in the original coal and in the residues, respectively; T stands for reaction temperature in degree Celsius; α and β are constants whose values depend on the samples and reaction conditions. A general expression of these correlations can be written as equation 4.

$$C_i = \alpha f_i + \beta T \qquad \text{For specific carbon type i} \qquad 4)$$

Figure 20 presents the plots and the linear correlations for residues from TPL in tetralin. A least-squares analysis of the data in Figure 20 was made in order to obtain a best fit. Table 4 lists the values of α and β and correlation coefficients. As can be seen from Figure 20 and Table 4, the mathematical correlations provide a very good fit of the CPMAS ^{13}C NMR data.

Table 4. Mathematical Correlation of ^{13}C NMR Data of Residues with Reaction Temperature

Carbon Type		$C_i = \alpha f_i + \beta T$ $T \geq 300°C$		Correlation Coefficient
C_i in Residue	f_i of Orig. Coal	α	β	
For TPL in Tetralin				
Aromatic C	63	0.5204	0.10696	0.997
Aliphatic C	35	1.5429	-0.0762	0.946
O-bound C	18[a]	3.0111	-0.1155	0.959
For All the Runs[b]				
Aromatic C	63	0.5431	0.1026	0.961
Aliphatic C	35	1.4747	-0.0684	0.826
O-bound C	18[a]	3.038	-0.1191	0.900

a) Including both aromatic O-bound C and aliphatic O-bound C.

b) For all the TPL and N-PL runs using different solvents including H-donor tetralin, non-donor naphthalene and methylnaphthalene, and process solvent WI-MD as well as a solvent-free run at 400°C.

In fact, we have processed the NMR spectra of 24 residue samples from TPL and N-PL runs of the coal in different solvents including tetralin, WI-MD, 1-methylnaphthalene and naphthalene, and one residue from solvent-free run at 400°C. Figure 21 presents the NMR data and the mathematical correlation by a linear fit for all of the samples. In fact, the % C values for runs at the same final temperature but using different solvents or under different conditions, are so close that many of them overlapped in Figure 21. The correlation coefficient associated with a least-squares analysis for aromatic C is 0.961, indicating a good fit of the data by a straight line even though the samples were derived from considerably different conditions. These results revealed that the change of carbon distribution, especially aromaticity, is strongly dependent on the final reaction temperature and only slightly on the nature of the solvents and heat-up program, even though using different solvents and different heat-up programs caused significant differences in the coal conversions and remaining amounts of organic materials in the residues. There is also a good correlation of C distribution of residues with coal conversion in TPL in tetralin or WI-MD, because the coal conversion is dependent upon the reaction temperature. These results also show that

prediction of the changes of carbon distribution of coals versus reaction temperature is possible in practice by using the methodology developed here.

Structural Characteristics and Liquefaction Reactions of Low-Rank Coals

Combination of the NMR and Py-GC-MS data suggests that the original DECS-9 coal contains significant quantities of oxygen-containing structures, which include catechol, methylcatechols, phenols, alkylphenols, and carboxylic and carbonyl groups, chemically bound to its macromolecular network, corresponding to about 18 O-bound C per 100 C atoms (Figures 5 and 6, Table 2). It is very interesting to note that curve-fitting and subsequent calculation of CPMAS ^{13}C NMR spectra of both raw and THF-extracted coal point to the presence of approximately one O-bound carbon in every 5-6 aromatic carbon atoms. Py-GC-MS data revealed that phenol, cresols, C_2-phenols, catechol and methylcatechols are the major components in the pyrolyzates of these samples (Figures 2 and 7, Table 1), being in excellent agreement with the CPMAS ^{13}C NMR data.

Characterization of residues from TPL revealed that liquefaction of the coal involves the considerable changes of the oxygen-containing structures including catechol-like structures, which seem to disappear in the liquefaction residues above 300°C; carboxyl groups, which almost disappear after 350°C; and phenolic structures which are most abundant in the original coal but diminish in concentration with increasing temperature. The analytical results point to the progressive loss of oxygen functional groups (Figures 13 and 14) and aliphatic species (Figures 17 and 18) from the macromolecular network of the subbituminous coal during its liquefaction under TPL conditions. Relative to the conventional N-PL runs, the higher conversions from TPL runs in tetralin (Figure 4) suggest that the removal of carboxylic and catechol groups from the coal during the programmed heat-up ($\leq$ 350°C) in H-donor vehicle has contributed to minimizing the retrogressive crosslinking at higher temperatures. In other words, the reactive sites generated by the removal of carboxyl and catechol groups, which could happen at low temperatures, can be effectively stabilized by H-transfer from tetralin at lower temperatures during programmed heat-up.

Low-rank coals are characterized by low aromaticities and high oxygen functionalities, which can also be seen clearly from data in Figures 1 and 2 and Table 2. Recently there has been increasing interest in finding ways to improve conversion of low-rank coals, which are often less readily liquefied than bituminous coals [DOE COLIRN, 1989; Derbyshire et al., 1989; Song et al., 1989; Song and Schobert, 1992]. This is considered to relate to the propensity for low-rank coals to form crosslinks upon heating, which render the coal less amenable to liquefaction [DOE COLIRN, 1989; Derbyshire et al., 1989]. It is now recognized that low-rank coals are more reactive than had been thought previously, and their conversion in high-severity processes is accompanied by

significant retrogressive reactions [DOE COLIRN, 1989; Suuberg et al., 1987; McMillen et al., 1985; Derbyshire et al., 1989; Song et al., 1989; Solomon et al., 1990; Lynch et al., 1991; Song and Schobert, 1992]. For example, Suuberg et al. [1987] reported that a lignite start to cross-link at much lower pyrolysis temperature than bituminous coals. Solomon et al. [1990, 1991] and Lynch et al. [1991] have suggested that low-temperature cross-linking is related to decarboxylation. Manion et al. found that it is difficult to establish coupling reactions resulting from decarboxylation of monomeric benzoid acid compounds under homogeneous reaction conditions [Manion et al., 1992], while our preliminary data suggest that crosslinking could be caused by decarboxylation reactions involving "immobilized molecular fragments" in low-rank coals. In regard to retrogressive reactions of other functional groups, McMillen et al. [1985] and Tse et al. [1991] have provided some evidence on the condensation of polyhydroxy structures in model compound studies. The present work has revealed progressive and important changes in oxygen-functionalities of a low-rank coal during its liquefaction at different temperatures.

The term crosslinking used in this report refers to chemical linking of molecular fragments (e.g., reactive radicals from coal thermal decomposition, or thermally unstable compounds, etc) to coal through covalent bonds, which leads to increased crosslinks (usually with stronger bonding) in coal macromolecular network. It should be noted that the definition of the term used here is different from that used in polymer science, where crosslinking means the linking of polymer chains through covalent or ionic bonds to form a network.

Our ^{13}C NMR and Py-GC-MS in combination with liquefaction data suggest that if one removes the catechol and carboxyl groups from coal macromolecular network under hydrogen-transferring conditions (e.g., with H-donor) at low temperatures ($\leq$ 350°C), the reactive sites generated from their reactions (such as decarboxylation) can be effectively stabilized by H-donor. It has been indicated [Song et al., 1989] that, for low-rank coals, using very fast heat-up to high temperatures would lead to extremely rapid formation of reactive radicals that exceed the capacity or rate of H-donation, resulting in significant retrogressive reactions. Therefore, programmed heat-up in H-donor in low temperature regime could significantly reduce retrogressive crosslinking (at the reactive sites) at high temperatures.

Probably the reactions responsible for retrogressive crosslinking during initial stage of liquefaction of low-rank coals in conventional high-severity processes are associated with their oxygen functional groups, such as crosslinking caused by reactions of catechols and phenollic compounds and decomposition of carboxlic groups. Comparative examination of our coal conversion data and Py-GC-MS and NMR spectroscopic data suggests that the TPL conditions in H-donor vehicle facilitate the reduction of crosslinking reactions of the thermally sensitive groups such as oxygen-functional groups at low temperatures.

Py-GC-MS also revealed the incorporation of the reaction solvents such as tetralin into coal

structure during liquefaction at both low and high temperatures, but CPMAS ^{13}C NMR was not sensitive with respect to this. When tetralin was used as the solvent, naphthalene and small amounts of tetralin and dihydronaphthalene were also detected in the pyrolyzates of the residues from TPL at 300-400°C, as can be seen from Figures 7 and 8 and Table 1. Comparative examination of Py-GC-MS profiles indicated that for runs at low temperatures such as 300°C, most of the naphthalene in the pyrolyzates of the residue came from the reaction solvent, presumably by physical imbibition which could not be removed by THF extraction, and in part by chemical binding; but in the residue from TPL at higher temperatures such as 400°C, the naphthalene peak also came from pyrolysis of the residue, because even the residues from solvent-free runs at 400°C can produce considerable amounts of naphthalene and methylnaphthalenes. It is considered that the aromaticity increase in the residues with temperature is due mainly to structural transformation, rather than solvent incorporation.

CONCLUSIONS

This work has clearly demonstrated that, by the combined use of the CPMAS ^{13}C NMR and Py-GC-MS techniques on properly prepared samples, it is possible to characterize both the structural features and molecular/structural components in coal macromolecular network, and to follow changes in functionalities and carbon distribution during coal liquefaction [Song et al., 1992c]. The present results indicate that DECS-9 Montana subbituminous coal contains considerable quantities of oxygen-containing structures, corresponding to about 18 O-bound C per 100 C atoms and one O-bound C every 5 to 6 aromatic C. The oxygen-bearing components in the coal include phenolic structures, catechol-like structures, and carboxyl groups. Py-GC-MS in combination with ^{13}C NMR revealed that some dominant structures in the coal exist in a fashion such that they will produce phenol, alkylphenols, catechol, methylcatechols, toluene, and xylene upon flash pyrolysis.

The analytical results of liquefaction residues point to the progressive loss of oxygen functional groups and aliphatic species from the macromolecular network of the coal during its depolymerization in tetralin under TPL conditions. The progressive changes for the oxygen-bearing components are characterized by disappearance of the catechol-like structures from the liquefaction residues at ≥300°C, disappearance of carboxyl groups after 350°C, and gradual decrease of phenolic structures with increasing reaction temperature. The higher conversions in TPL runs (relative to the conventional non-programmed runs) in tetralin suggest that the removal of catechol and carboxylic groups from the coal macromolecular network and the stabilization of the reactive sites (generated from the reactions of catechols, carboxyl groups, etc.) by H-transfer from H-donor at ≤ 350°C have contributed to minimizing the retrogressive crosslinking at higher temperatures.

Quantitative calculation of NMR data and mathematical correlation were also attempted in

this work, and the results, though preliminary, appear to be very promising. For a relatively large number of experimental samples (24 residues) derived under significantly different conditions, quantitative and linear correlations between C-distribution and reaction temperature have been found, which can be expressed by a simple equation, $C_i = \alpha f_i + \beta T$, where f_i and C_i represent content of aromatic, aliphatic, or oxygen-bound carbons in the original coal and residue, respectively; T stands for the reaction temperature; α and β are constants.

2. Characterization of Raw and Pretreated Bituminous Coals

TGA

Experimental

Thermogravimetric analysis' were preformed on coals DECS-7, Adaville #1, DECS-6, Blind Canyon, and DECS-12, Pittsburgh #8. This thermal method of analysis measures percent weight loss of material (devolatilization) upon heating in an inert (N_2) atmosphere. The yields of volatile components, moisture, and reactivity of the coals can be determined with this technique. Prior to analysis the coals were dried in a vacuum oven at 45 ^oC for twenty four hours. Fifteen to nineteen milligrams of coal were weighted directly in a crucible in the furnace of a Perkin -Elmer TGA 7 thermogravimetric analyzer. The coal was heated from 30 ^oC to 750 ^oC-800 ^oC at a rate of 5 ^oC/min.

Results

Figures 22, 23, 24 show the weight loss curves vs time for each of the coal samples. All three coals show the same general trend. Initially there is an immediate weight loss which is due to water, carbon dioxide, and argon which still remains in the coal even after drying. The percent weight loss curve then levels off after 16 minutes (110^o C) and remains relatively flat until release of the volatile components of the coal. Devolatilization starts a few degrees above 320^o C for both the Adaville #1 and the Pittsburgh #8 coals but starts 40^o C lower, 280^o C for the Blind Canyon coal. This early weight loss in Blind Canyon is due to a devolatilization of resinite which constitutes a significant maceral component of the coal. This maceral volatilizes at a lower temperature than the other macerals. Pyrolysis GC/MS data discussed below confirms this conclusion. Between 500^o C and 525^o C the rate of weight loss slowly levels off until the end of the experiment. Table 5 shows the results of the TGA experiments.

Table 5 TGA analysis of selected coals

Coals	% MOISTURE	DEVOLATILIZATION TEMPERATURE	% VOLATILES	% RESIDUE
DECS-7	8.7	~317°	36.7	54.6
DECS-6	2.7	~280°	41.8	55.5
DECS-12	0.9	~315°	33.5	65.6

Pyrolysis/Gas Chromatography/Mass Spectrometry

Experimental

Flash Py/GC/Ms procedures are the same as those explained in Song et al., (1992d). A series of four Py/GC/MS experiments were preformed on the Adaville #1 and the Blind Canyon coals with pyrolysis temperatures starting at 310° C and increasing to 610° C at 100° C increments . Sample weights ranged from 0.5 mg to 1.0 mg.

Results

Figure 25 shows the chromatogram of DECS-7 run at 310° C. This temperature is insufficient to pyrolyze the sample, but the temperature is high enough to thermally desorb the coal. Duplicate experiments yielded between seven and nine percent desorbed material. The volatiles consisted of sulfur compounds, mostly SO_2 and a trace of COS, and high molecular weight biomarkers, pentacyclic triterpenoids and aromatized triterpenoids. Also released but not shown in Figure d was bound water, CO_2, and argon.

Figure 26 shows a series of chromatograms run at 310° C, 410° C, 510° C and 610° C. There is little difference between the 310° C and 410° C pyrograms except for a trace of the alkene Prist-1-ene. At 510° C an increase in volatile pyrolysis products is observed indicating that significant pyrolysis of the coal occurs at this temperature. An abundant amount of Prist-1-ene and some straight chain alkanes, C19 through C31, are released. Not until 610° C does major pyrolysis of the coal occur. Released at this temperature are the homologous series of alkanes/alkenes, C4 through C31, phenols and alkyl phenols (C1 through C3) and benzene and alkylbenzenes (C1 through C4). Single ion chromatograms for the alkane/alkenes (m/z 71, 69), benzene compounds (m/z 78, 92, 106, 120), and phenol compounds (m/z 94, 108, 122) are shown in Figures 27, 28, and 29, respectively. Figure 30 is a plot of the volatile yield vs pyrolysis temperature. This plot shows that as temperature increases the amount of volatile material released increases from 7 percent at 310° C to 33 percent at 610° C.

A similar set of experiments was run on the Blind Canyon coal with different results, Figure 31. At 310° C the major products released were the bicyclic sesquiterpenoids, C20 to C30 straight chain alkanes, and sesquiterpenoids and triterpenoids. Again little change occurs at 410°

C but also little change occurs at 510° C with only a slight increase of the high molecular weight alkanes. Just as in the DECS-7 experiments, pyrolysis of all the major compounds does not occur until 610° C. Figure 32 shows with increasing temperature the amount of volatile product also increases just as with the Adaville #1 coal.

Thermal Treatment

Experimental

The thermal pretreatments of the raw coals, DECS-7, DECS-6, and DECS-12 were carried out at 400° C. Four grams of coal were placed in a 25 ml microautoclave and pressurized with H_2 to 1000 psi. The coals were heated for 30 minutes. After the reaction, the products were separated by sequential extraction with hexane, toluene and THF. After the extraction the THF-insoluble residues were washed first in acetone and then in pentane in order to remove the THF, followed by drying at 110° C for 24 hours under vacuum (Song et al., 1992). The residue was then analyzed by PY/GC/MS.

Results

Figure 33 shows the chromatogram for the unreacted Adaville #1 coal and Figure 34 shows the chromatogram for the thermally treated Adaville #1 coal. A comparison of these two pyrograms shows a strikingly different pyrolyzates. Prist-1-ene, the alkane/alkenes series, and the high molecular weight biomarkers are completely missing from the reacted Adaville #1. Other changes that have occurred to the treated coal are the addition of naphthalene and alkyl naphthalenes in the pyrograms.and an increase in the phenol concentration relative to the C1 phenols. These differences indicate the macromolecular structure of the Adaville #1 coal has been altered due to severe heating (400° C) during the heating experiment.

Figure 35 shows the chromatogram for the unreacted Blind Canyon coal and Figure 36 shows the chromatogram for the thermally treated Blind Canyon coal. Again there is a significant difference between the unreacted and the reacted coal's. There is a complete loss of the alkane\alkene series, the bicyclic sesquiterpenoids, and the triterpenoids as compared to the unreacted coal. The addition of naphthalene and alkyl naphthalenes and the increase in the phenol concentration relative to the C1 phenols has also occurred.. Severe heating has caused the same changes to occur in the Blind Canyon coal as has occurred in the Adaville #1 coal.

Figure 37 and Figure 38 are pyrograms of the Pittsburgh #8 unreacted coal and heat treated coal, respectively. Here a comparison between the two coal shows that the differences in the

chromatograms are not as great as what has occurred in the previous two heating experiments. There is only a loss of the alkane/alkenes and an addition of anthracene and pyrene.

3. EFFECTS OF DRYING ON THE LOW TEMPERATURE LIQUEFACTION OF WYODAK SUBBITUMINOUS COAL

EXPERIMENTAL

Sample

The coal used was a Wyodak subbituminous coal obtained from the Penn State Coal Sample Bank (DECS-8, PSOC-1545). The characteristics of this coal is as follows: 32.38% volatile matter, 29.30% fixed carbon, 9.90% ash, 28.42% moisture on a raw coal basis; 75.84% C, 5.15% H, 1.02% N, 0.51% organic S and, 17.48% O on a dmmf basis.

Drying of Coal

None-oxidative drying of coal was done under vacuum at 100°C for 2h and the oxidative drying was done in air at 100°C for various intervals of time (2-100h).

Catalyst Loading

The catalyst precursor, ammonium tetrathiomolybdate (ATTM) (purchased from Aldrich, 99.97%), was dispersed on coal by incipient wetness impregnation method using water as solvent. The loading was 1% of molybdenum on the basis of dmmf coal. After loading of the catalyst precursor, the coal sample was dried in vacuum for 2h at 100°C, then removed and stored under a nitrogen atmosphere.

Preliquefaction Experiments

The preliquefaction experiments were carried out in a tubing bomb at temperatures 350°C, and hydrogen gas pressure of 1000 psi (7 MPa) cold. The solvents used were tetralin and 1-methylnaphthalene (1-MN). The catalyst selected for pretreatment was Ammonium tetrathiomolibedate (ATTM). The experiments were performed with and without solvents and catalyst. The reactor bombs containing samples were heated by immersion in fluidized sand bath for 30 minutes plus 3 minutes for reactor heat-up. After the reaction,the bombs were cooled by immersing quickly in water for a very short contact time, enough to bring the temperature of the reactor below 200 °C, followed by cooling to room temperature in air. The bombs were then vented to determined the gases evolved by volumetric measurement and gas chromatographic analysis. The liquid and solid products were separated by sequential extraction

with hexane, toluene and THF. The extracted products were worked up to obtain the yields of oils (hexane-solubles), asphaltenes (toluene-solubles) and preasphaltenes (THF-solubles). In these analysis it was assumed that the solvents are the part of the hexane solubles. The final residues (THF-insoluble) were first washed with acetone and then with pentane followed by drying under vacuum at 110 °C for six hours.

Analysis of Residue

The NMR spectra were recorded on a Chemagnetic M-100 NMR spectrometer by using the cross-polarization and magic-angle-spinning (CPMAS) technique. The infrared spectra were recorded on Digilab FTS60 FTIR system. The transmission spectra of the samples were recorded using finally ground samples (2.0 to 3.0 mg) were weighed in dry aluminum weighing dishes and added to a weighed amount (about 300mg determined to+0.1 mg) of KBr. The KBr and samples were mixed by grinding in stainless steel grinding capsules for 2 minutes and pressed into a 13 mm diameter pellet in an evacuated die. The pellets were then weighed and the sample weight per cm2 of pellet area was determined.

RESULTS

The products distribution for the liquefaction of the raw coal and coal dried under different conditions are given in Tables 6 and 7.

Liquefaction of undried fresh raw coal.

The presence of catalyst does not seems to have any effect on the total conversion of the coal except in the case when there is no solvent present in the reaction mixture. In presence of catalyst and no solvent experiment there is an increase in the conversion from 24.2 to 43.8%. In fact this conversion is same as that in the experiments with tetralin as solvent with or without catalyst.

The increase in the conversion of the solvent free experiment of the undried coal with catalyst is due to the increase in all the product yields compared to the catalyst free run. But in the presence of the solvents, although there is no appreciable change in the total conversion, there are differences in the oil+gas and asphaltenes yields without having any effect on the preasphaltenes yields. There is an increase in the asphaltenes and decrease in the oil+gas products.

Liquefaction of vacuum-dried coal.

The presence of catalyst seems to have an appreciable effect on the total conversion of the coal. There is an increase in the total yield from 12.5 to 29.8% in presence of catalyst and solvent free experiment. This increase in basically due to the increase in all yields of all type of solubles. With tetralin as solvent and catalyst the increase in the total conversion is from 25.9 to 36.4%. The increase in mainly due to the increase in the yields of oil+gas and asphaltenes. But with a non proton-donor solvent (1-methyl naphthalene) the increase in the total conversion from 18.3 to 31.1% is due to the increase in the yields of all the products.

Table 6. Products distribution for the liquefaction of DECS-8 coal at 350 °C without catalyst, raw and dried under different conditions.

Coal	Solvent	Gas+Oil (%)	Asphal. (%)	preasph. (%)	Total Conv.(%)
Raw	none	12.7	3.1	8.6	24.2
Vacuum dried		4.9	2.6	4.5	12.5
Air-dried for 2 h		8.3	0.7	5.8	14.8
Air-dried for 20 h		8.1	0.6	3.2	15.5
Air-dried for 100 h		9.7	0.7	3.3	12.7
Raw	Tetralin	20.8	8.1	12.6	41.6
Vacuum dried		8.7	7.6	10.0	25.9
Air-dried for 2 h		17.1	7.4	10.6	35.1
Air-dried for 20 h		17.0	6.5	8.9	32.4
Air-dried for 100 h		14.8	6.3	9.7	30.8
Raw	1-MN	18.4	7.0	11.9	37.3
Vacuum dried		6.0	5.8	7.4	18.3
Air-dried for 2 h		9.4	4.0	9.5	22.9
Air-dried for 20 h		14.2	5.6	4.7	24.5
Air-dried for 100 h		10.7	4.1	6.3	21.1

Table 7. Products distribution for the liquefaction of DECS-8 coal at 350 °C in the presence of catalyst, raw and dried under different conditions.

Coal	Solvent	Gas+Oil (%)	Asphal. (%)	preasph. (%)	Total Conv.(%)
Raw	none	19.1	11.2	13.5	43.8
Vacuum dried		12.7	5.4	11.4	29.8
Air-dried for 2 h		12.2	3.2	10.1	29.2
Air-dried for 20 h		12.9	3.1	8.7	31.2
Air-dried for 100 h		15.6	2.4	5.1	28.4
Raw	Tetralin	18.5	12.0	11.7	42.2
Vacuum dried		12.9	12.9	10.6	36.4
Air-dried for 2 h		19.7	11.1	14.9	45.7
Air-dried for 20 h		24.2	8.6	10.7	43.5
Air-dried for 100 h		23.2	10.8	11.0	45.0
Raw	1-MN	13.4	10.3	11.9	35.6
Vacuum dried		8.7	10.1	12.3	31.1
Air-dried for 2 h		13.3	8.1	16.0	37.5
Air-dried for 20 h		20.3	8.7	10.5	39.7
Air-dried for 100 h		19.6	8.7	11.1	39.4

Products distribution for liquefaction of air-dried coal

The coal was dried for 2, 20 and 100 hours in an oven heated to 100°C and then subjected to liquefaction at 350°C. Basically the drying of coal in air for different intervals of time does not show any appreciable difference in the products distribution. In presence of the catalyst (ATTM) there is an increase in the total conversion compared to that without catalyst.

Comparison of the liquefaction products of raw-undried, vacuum dried and air dried coal

The undried and dried coal show clear differences in their total conversions and the

products distributions. On comparing the total conversions of the liquefaction experiments without catalyst, the undried coal shows the maximum conversion. The vacuum drying seems to have the worst effect on the total conversions. In solvent free experiments undried coal seems to produce more of oil+gas and preasphaltenes with a very small effect on asphaltenes. In presence of tetralin or 1-methyl naphthalene as solvents the increase in the total conversion of the undried coal is essentially due to the increase in the yields of all the products but the major increase is in the oil+gas yield.

The presence of catalyst increases the total conversion in all the experiment but the effect in the total conversion of the undried coal is rather unusual. There is no effect on the total conversion of the liquefaction experiments with tetralin and 1-methyl naphthalene as compared to that of the catalyst free experiments, but it shows a drastic increase in the total conversion in the solvent free run. The increase is so much that it supersedes the total conversion in the experiments with tetralin or 1-methyl naphthalene. In the liquefaction experiments of the air dried coal the total conversion is maximum in the experiments with catalyst and tetralin as solvents as compared to that of the vacuum dried coal. But the total conversion of the solvent free experiment of the undried coal is quite comparable with that in the air dried coal.

Compared to the products distributions of the liquefaction experiments of the vacuum dried coal in presence of catalyst, the total conversion is more in the experiments with undried coal with or without solvents. The difference is mainly due to the increase in the oil+gas products except in the solvent free run.

The total conversion in the air dried experiments with solvents and catalyst show a slight increase compared to that of the undried coal. This increase is mainly due to the increase in the preasphaltenes yield.

FT-IR Analysis of Residue and Raw Coal

Dried Raw Coal

In Figure 39 the spectrum of the 'as-received' DECS-8 raw coal is compared to the spectra of samples dried in air at 100 °C for 2, 20 and 100h and at 125 and 150 °C for 20h. The oxidation of coal is apparent by the increase in the intensity of the peak near 1700 cm^{-1} as compared to that in the undried coal. The broad band between the region 3000 -3500 cm-1 has decreased due to the loss of water upon drying. The extent of oxidation at different intervals of time at 100 °C is not

apparent but drying at 125 and 150 °C for 20h show a slight increase in the 1700 cm-1 band as compared to that at 100 °C. If there are differences in the FT-IR spectra as a function of extent of drying at 100 °C they are not immediately apparent from Figure 39.

Subtle spectroscopic changes can often be detected through the use of difference methods. Figure 40 shows the difference spectra of the dried coal. The difference spectra were obtained by subtracting the spectrum of the 'as-received' sample from that of the air-dried coal. The criteria used to determine the correct degree of subtraction was the elimination of the kaolonite bands at 1035 and 1010 cm-1. The positive bands in the difference spectra represent functional groups that have appeared or increased and the negative bands show the removal of the functional groups. The difference spectra has prominent bands at 1720 and 1580 cm-1 which can be assigned to carbonyl (probably COOH) and carboxyl (COO-) groups respectively. Furthermore, a broad absorption near 1150 cm-1 is also apparent. This band is characteristic of C-O groups, although it is not easy to distinguish between the presence of this group in alcohols and ethers. From the difference spectra the relative extent of oxidation is clear from the intensity of the 1720 cm-1.

It is generally thought the first step in the oxidation of coal is the formation of peroxides by the oxidation of the aliphatic and olefinic structures present in coal. For a saturated hydrocarbon the basic mechanism is believed to be as follows:

$$R\text{-}H \longrightarrow R$$
$$R + O_2 \longrightarrow R\text{-}O\text{-}O$$
$$R\text{-}O\text{-}O + R\text{-}H \longrightarrow R\text{-}O\text{-}O\text{-}H + R$$

where R is aliphatic or aromatic. If R is aromatic, the oxidation probably occurs at the carbon alpha to the aromatic ring. The decomposition of the peroxide R-O-O-H can produce various oxygen-containing compounds such as acids, peracids, alcohols, ketones, aldehydes esters and ethers.

Residue from the Liquefactions

Figures 41, 42 and 43 show the FT-IR spectra of the THF-insolubles after the liquefactions of the air-dried coal at 100 °C for different intervals of time (2, 20 and 100h). The FT-IR spectra of the residues from the raw coal were also recorded. The FT-IR spectra of the residues after liquefaction show appreciable differences in the coal structure as compared to the raw coal. There is a noticeable reduction in the relative intensities of almost all the peaks. The presence of the catalyst produces further reduction in the intensities of the aliphatic and ether bands. Relatively the ether region seems to be more reduced than the other regions as compared to the catalyst free runs.

The drying of coal at 100 °C for different intervals of time seems to have no appreciable

effect on the coal structure after liquefaction at 350 °C.

CPMAS ^{13}C NMR Analysis

Figures 44,45,46, and 47 show the comparison of the CPMAS 13C NMR of the raw coal and the residues from the preliquefaction of the coal dried in air at 100 °C for 2, 20 and 100 h, respectively, with that of the unextracted and extracted raw coal. The NMR spectrum of the raw coal show two major broad bands between 0-60 ppm (aliphatic region) and 80-200 ppm (aromatic region). The aromatic region has three peaks: an intense peak around 130 ppm (aromatic C0, and two shoulders, one at about 142 ppm (possibly catechol like C), and another at 152 ppm (ketone or aldehyde C) define rest of the spectrum. The NMR spectra of the air-dried raw coal (Figure 6) show only a slight decrease in the intensity of the aliphatic region (0-600 ppm) as an extent of drying. The aromatic region (80-200 ppm) does not show any appreciable differences.

There are several structural differences which are apparent as a result of preliquefaction of air-dried coal. The NMR of the residues have been compared with that of the extracted raw coal. The most prominent difference is the reduced intensity of the aliphatic region (0-60 ppm). In the aromatic region (80-200 ppm) there is an apparent decrease in the intensities of the shoulders on the low energy side. The shoulder at 142 ppm seems to have disappeared, or it is very weak. The other bands at 182 and 212 ppm are also very weak compared to those of the raw coal. The presence of solvents also seems to have slight effect on the structure of the coal. The aliphatic region seems to be reduced relatively increasing the aromaticity of the coal. The type solvent used does not seem to produce any apparent effect on the NMR spectra of the residues.

The pretreatment in presence of catalyst (ATTM) has shown more severe effect on the coal structure. The aromatic region seems to be more effected than the aliphatic region. The aliphatic region seems to be affected in a similar fashion as in the catalyst free runs. The effect on the aromatic band is much sever in presence of solvents. The shoulder on the aromatic band at 142 ppm has disappeared along with the band at 212 ppm. The shoulder at 152 ppm is weaker in the experiment with tetralin but in the solvent free and with 1-methylnaphthalene runs this shoulder is quite comparable to the shoulder in the NMR of the raw coal.

4. Temperature-Programmed Liquefaction of Three Low-Rank Coals

PREPARATION OF CATALYTIC COAL SAMPLES

In catalytic coal liquefaction, one of the most determining factors of high conversion and optimum product distribution is the catalyst or catalyst precursor dispersion on the surface of a

coal. Ideally, the catalyst must be present at all the reaction sites when thermal cracking of the macromolecular structure of coal begins [Hawk and Hiteshue, 1965]. In another word, the catalyst must be distributed uniformly on both external and internal surface of the coal. The objective of the research is to find the best method for the impregnation of a catalyst on the coal. Three methods are proposed to be tested. The first is slurrying a coal sample with aqueous solution of the catalyst precursor. The second is incipient wetness. The third is to impregnate the precursor with a swelling solvent. So for, the last two method have been tested and details will be explained in this section.

Before the precursor was dispersed onto the coal, all coal samples were dried. The drying temperature in all cases was 95°C. The drying period depended on the rank of the coal and the moisture content. Table 1 shows the percentage of remained moisture as a function of drying time. For DECS-9 coal sample, it takes about 2.5 hours to remove all the moisture without losing any low boiling point matter in the coal. For DECS-1 sample, it takes about 4 to 5 hours to dry. While for DECS-11 sample, which contains the highest amount of moisture, it takes about 6.5 to 7 hours to dry.

Table 8 Moisture remained in Coal as a Function of Drying Time

Coal Sample	Rank	H_2O% before	Drying Time (h)	H_2O% after
DECS-9	Sub	24.68	2	4.6
			2	3.44
			3	-1.49
			4.5	-1.8
DECS-1	Sub	30	2.5	4.84
			3	2.67
			4	---
DECS-11	Lig	33.38	2.5	5.29
			5	3.78
			6	1.99

Impregnation of Catalyst Precursor by Incipient Wetness

The catalyst precursor, ammonium tetrathiomolybdate (ATTM, Aldrich, 99.97%), was dissolved in deionized water. The catalyst loading was 1% of molybdenum on the dry mineral matter free (dmmf) basis. Tetrahydrofuran (THF, Fisher Scientific, HPLC Grade) was then added to the solution to make the ratio of H_2O to THF equal to 44:56. This is the ratio that the least amount of H_2O is used for dissolving ATTM. This solution was then added to the dried coal sample dropwise while the coal sample being constantly stirred. The critical point of this technique is to cover the surface of the particles uniformly without excess solution between particles, so the amount of solution should be just enough. After all the solution was added to the coal, the coal sample, now wetted by the solution of catalyst precursor, was dried in a vacuum oven at 105°C for two hours, then stored under nitrogen atmosphere.

Impregnation of the Catalyst Precursor by Preswelling

It has been demonstrated that impregnating precursor with swelling solvent could significantly improve the total conversion as well as the product distribution [Joseph, 1991]. The three dried coal samples were first tested for swelling ratios. The swelling solvent was a mixture of deionized water and THF with ratio of 44/56. The reason of using this mixture is first for comparison with the incipient wetness method, and second, though THF is a good swelling solvent it does not dissolve ATTM, therefore, water is used in order to make a solution of ATTM. The procedure of swelling is described as following:

1) About 1 gram of dried coal sample (-60 mesh) was weighed, loaded into a 15 ml conical graduated screw-top centrifuge tube.

2) The sample was centrifuged at 2000 rpm for 40 minutes, then the height was recorded as H_1.

3) About four times swelling solvent (H_2O/THF) of that of coal volume was placed into the tube. The tube was capped and well shaken to make sure that all the coal particles were wetted. The coal sample was then allowed to soaked at room temperature for 3 or 24 hours.

4) The sample was centrifuged again at 2000 rpm for 40 minutes, then the height was recorded as H_2.

5) The swelling ratio was calculated by $S = H_2/H_1$.

Table 9 and 10 show the swelling ratios of the three coal samples after soaking for three and twenty-four hours respectively. The data show that the swelling ratios of three hours soaking are the same as those of twenty-four hours soaking. This indicates that within three hours, the structure can be swollen to the maximum point.

Table 9 Swelling Ratio after Three Hours of Soaking in THF-H_2O

Coal Sample	Weight	H_1(ml)	Sol (ml)	H_2 (ml)	S
DECS-1	1.0053	1.6	6.4	3	1.9
	1.0264	1.8	7.2	3.2	1.8
DECS-9	1.0254	1.8	7.2	3.5	1.9
	1.0053	1.8	7.2	3.4	1.9
DECS-11	1.0125	1.7	6.8	3.3	1.9
	1.031	1.6	6.4	3.2	2

For a maximum contact between the catalyst and the coal, and also for the convenience in the practice, twenty-four hours of soaking was allowed. The procedure of swelling-impregnation was bit different from that of swelling:

1) Dried coal sample (about 30 gram) was weighed and load into a 500 ml flat-bottom flask.

2) The approximate volume of the coal was calculated with the data in Tables 9 and 10. The volume of the swelling solvent (H_2O/THF) was about four times of that of coal. The desired amount of ATTM (1% of Mo based on dmmf) was first dissolved in the water and then THF was added to the solution.

3) The solution was mixed with the coal sample and the flask was connected with a cooling system. The system was under nitrogen to prevent any oxidation in the air. The cooling system was for condensing any THF vaporized from the solution. The mixture was constantly stirred by a magnetic stir-bar at room temperature for maximizing the coal-ATTM contact. This process was allowed for twenty-four hours.

4) The flask was disconnected from the system and first dried in a vacuum oven at room

temperature for 48 hours to remove the THF, and at 105°C for 24 hours to remove the water. The sample was then stored under nitrogen atmosphere.

Table 10 Swelling Ratio After 24 h Soaking in THF-H_2O

Coal Sample	Weight	H_1	Sol. Added	H_2	S
DECS-1	1.0162	1.6	6.4	3	1.9
	1.068	1.8	7.2	3.3	1.8
DECS-9	1.0292	1.7	6.8	3.5	2
	1.0885	1.7	6.8	3.6	2.1
DECS-11	1.013	1.6	6.4	3.2	2
	1.0368	1.7	6.8	3.2	1.9

TEMPERATURE-PROGRAMMED LIQUEFACTION

Liquefaction experiments were conducted in microautoclave reactors (tubing bombs) in a preheated fluidized sandbath. For each reaction, about 4 grams of coal (So far, only the samples prepared by incipient wetness method have been used, while the samples prepared by preswelling will be tested in the future.) and 4 grams of Wilsonville Middle Distillate (WIMD) as reaction solvent were added to the reactor, following which hydrogen was purged three times, with a final pressure of 7 MPa at room temperature. The reactor was then plunged into the sandbath and agitated at 200 cycles per minute.

After the reaction, the gaseous product was vented into a gas sample bag and later analyzed by gas chromatography. The liquid and solid products and residue were washed into a tared ceramic thimble using hexane. Then the products were separated under a nitrogen atmosphere by Soxhlet-extraction using hexane, toluene and THF as solvents. After extractions, solvents were removed by rotary evaporation and the products were dried in vacuum at 110°C for about 12 hours, except for the hexane solubles. The solid residue was washed first by acetone and then by pentane several times and dried in the same procedure as the reaction products. The asphaltene, preasphaltene and residue were then weighed, and conversion and product distributions were calculated based on dmmf coal.

For a temperature-programmed liquefaction (TPL), the tubing bomb was rapidly (in about 3 minutes) heated-up to a relatively low temperature (200°C) and soaked in the sandbath at that temperature for 15 minutes. The temperature was then gradually increased to a higher temperature level (400°C) and held for 30 minutes, followed by rapid quench. The heat-up period was about 30 minutes, and the total reaction time was about 75 minutes.

Table 11 shows the results of temperature-programmed liquefaction with and without catalyst. For DECS-1 sample, the catalyst significantly improves the total conversion from 73.94% to 92.71%. This increase is due to the 119.4% increase (calculated by (62.42-28.45)/28.45) in gas and oil yield. The asphaltene yield keeps almost the same. While the preasphaltene yield drops almost 50%. For DECS-9 sample, total conversion is also increased when the catalyst is applied. This increase is due to a 70% increase in gas and oil yield and 38.5% and 40% increase in asphaltene and preasphaltene respectively. Though the yields of all three products increase, the yield of gas and oil increases the most. For DECS-11 sample, the total conversion increases from 67.08% to 84.96% using the catalyst. This increase is contributed by 28.1%, 28.8%, and 19.8% increase in gas and oil, asphaltene and preasphaltene, respectively.

As is well-known, in liquefaction process, the macromolecular structure will thermally or catalytically crack down to many fragment radicals, followed by either hydrogenation or retrogressive reaction, in which the fragment radicals recombine to form , again, large molecules, such as those in preasphaltene. This explains the behavior of DECS-1 liquefaction with and without catalyst. When there is no catalyst present, the rate of thermal cracking is much faster than the rate of hydrogenation. Many fragments recombine with one another, thus the yield of preasphaltene is very high and dominates. When the catalyst is used, the rate of hydrogenation is promoted and most of the fragment radicals are stabilized, thus the yield of oil is increased and the yield of preasphaltene is dropped remarkably.

SEM ANALYSIS OF CATALYST-LOADED COAL SURFACE

To obtain some basic information concerning the dispersion of catalyst/catalyst precursor on coal surface, scanning electron microscopy (SEM) has been applied. The coal samples, impregnated by ATTM was prepared by the methods described in previous section. So far, the dried DECS-9, ATTM impregnated by H_2O solution, and ATTM impregnated by H_2O/THF solution have been investigated.

Table 11 Temperature-Programmed Liquefaction With and Without Catalyst

Coal Sample	Tol. Conv.	Gas + Oil	Asphaltene	Preasphaltene
Non-Catalytic				
DECS-1	73.94	28.45	13.89	31.6
DECS-9	58.57	30.27	17.24	11.06
DECS-11	67.08	38.58	15.42	13.08
Catalytic				
DECS-1	92.71	62.42	14.36	15.93
DECS-9	91	51.49	23.93	15.5
DECS-11	84.96	49.43	19.86	15.67

A very small amount of particulate sample (-60 mesh) was dispersed on a brass sample holder. The sample and sample holder was then coated by gold to prevent heat damage by the electron beam and to eliminate the buildup of surface charge which can interfere with imaging. After coating, the sample was placed into the SEM chamber, ready to be examined.

Figure 48 shows the surface of the dried DECS-9 under SEM. At the bottom of each SEM micrograph the number indicates the electron operating voltage, magnification, number of microns represented by the white bar, the photograph number and the sample name. Figure 48(a) shows several coal particles and Figure 48(b) is part of the particle with an arrow under a higher magnification. The microgram indicates that the surface is very uneven, with many pores and fractures enclosing large surface area. The objective of the research is to identify the method by which the catalyst can be impregnation inside the pores.

Figure 49 shows the sample prepared by incipient wetness method using aqueous solution. In Figure 49 (a), the catalyst particles are less than one micron, randomly dispersed on the surface. The one pointed by the arrow sits on the edges of a fracture but does not penetrate. Figure 49 (b) shows the other coal particulate. there are two small particles located beside a relatively large pore and no particles observed inside the pores. Energy dispersed spectroscope (EDS) was planned to identify the chemical composition of the particles on the coal. Unfortunately, instrument was

temporarily out of order, the identification could not be shown in this report.

Figure 50 is the micrograph of the sample prepared by incipient wetness method using H_2O/THF solution. Similar as that in Figure 49, the catalyst particles disperse randomly on the surface. The difference is that several particles, indicated by arrows, are "mounted" in the pores.

In the first quarterly report [Song et al., 1992d], we compared the liquefaction results of samples impregnated by H_2O solution (named sample I) and H_2O/THF solution (named sample II). Sample II showed a significant increase in total conversion and much better product distribution than sample I. It was predicted that THF had a higher affinity to coal surface than water. The solution containing THF was able to impregnate the catalyst onto the internal surface of coal particles, and this improved the liquefaction. From the scanning electron micrographs shown above, though very preliminary, sample I has catalyst particles on its external surface, while sample II has catalyst particles inside, or partially inside the pores, thus proves the above prediction. This work has been just started, more information will be reported in the future.

REFERENCES CITED

Alemany, L.B.; Grant, D.M.; Pugmire, R.J.; Alger, T.D.; Zilm, K.W., 1983. J. Am. Chem. Soc., 105: 2142.

Andrew, E. R., 1977. Progress in NMR Spectroscopy, Vol 8, Part 1.

Botto, R.E.; Wilson, R.; Winans, R.E., 1987. Energy & Fuels, 1: 173.

Burgess, C. and Schobert H.H., ACS Fuel Chem. Prepr., 1990, 35, 31.

Burgess, C.; Artok, L.; Schobert H.H., ACS Fuel Chem. Prepr., 1991, 36 (2), 462-469.

Davidson, R.M., 1980. Molecular Structure of Coal, ICTIS/TR08, IEA Coal Research, London, 86 pp.

Davidson, R.M., 1986. Nuclear Resonance Studies of Coal, ICTIS/TR32, IEA Coal Research, London.

Davis, A., Derbyshire, F.J., Finseth, D.H., Lin, R., Stansberry, P.G. and Terrer, M-T., Fuel, 1986, 65, 500.

Davis, A., Derbyshire, F.J., Mitchell, G.D. and Schobert, H.H., "Enhanced Coal Liquefaction by Low-Severity Catalytic Reactions", U.S. Department of Energy, Final Report DOE-PC-90910-F1, July, 1989, 175 p.

Davis, A., Schobert, H.H., Mitchell, G.D. and Artok, L., "Catalyst Dispersion and Activity under Conditions of Temperature-Staged Liquefaction", Progress Report DOE-AC-22-89PC89877, January, 1990.

Dennis, L.W.; Maciel, G.E.; Hatcher, P.G., 1982. Geochimica et Cosmochimica Acta, 46, 901-907

Derbyshire, F.J., Davis, A., Epstein, M. and Stansberry, P., Fuel, 1986a, 65, 1233.

Derbyshire, F.J., Davis, A., Lin, R., Stansberry, P. and Terrer M-T., Fuel Proc. Technol., 1986b, 12, 127.

Derbyshire, F.J. and Stansberry, P., Fuel, 1987, 66a, 1741.

Derbyshire, F.J., Catalysis in Coal Liquefaction: New Directions for Research, IEA Report, IEACR/08, June, 1988, 69p.

Derbyshire, F.J., Energy & Fuels, 1989, 3, 273.

Derbyshire, F.; Davis, A.; Lin, R., 1989. Energy & Fuels, 3: 431-437.

DOE COLIRN Panel, 1989. "Coal Liquefaction", Final Report, DOE-ER-0400.

Fatemi-Badi, S.M., Swanson, A.J., Sethi, N.K. and Roginski, R.T., 1991. Am. Chem. Soc. Div. Fuel Chem. Prepr., 36 (2) : 470-480.

Franco, D.V., Gelan, J.M., Martens, H.J. and Vanderzande, D. J.-M., 1991. Fuel, 70: 811-817.

Gallegos, E.J., 1979. "Pyrolysis Gas Chromatography", in "Chromatography in Petroleum Analysis", K.H. Altgelt and T.H. Gouw Eds., Marcel Dekker, New York, pp.163-184.

Gollakota, S.V., Davies, O.L., Vimalchand, P., Lee, J.M. and Cantrell, C.E., 1990. Proceedings of U.S. DOE Direct Liquefaction Contractors' Review Meeting, Sept. 24-26, Pittsburgh, pp.129-158.

Hatcher, P.G.; Lerch, H.E.; Kotra, R.K.; Verheyen, T.V., 1988. Fuel, 67: 1069-1075.

Hatcher, P.G., Wilson, M.A., Vassallo, A.M. and Lerch III, H.E., 1989. Int. J. Coal Geol., 13, 99.

Hawk, C., O., and Hiteshue, R., W., 1965. Hydrogenation of Coal in the Batch Autoclave, U. S. Bur. Mines Bull. 1965, No. 622

Joseph, J. T., 1991. Fuel, 70, 139

Lai, W.-C., Song, C. and Schobert, H.H., 1992. Am. Chem. Soc. Div. Fuel Chem. Prepr., 37 (4): 1671-1680.

Lynch, L.J.; Sakurovs, 1991. Proc. 1991 Int. Cof. Coal Sci., Newcastle upon Tyne, Sept. 16-20, 1991, pp. 592-595.

Manion, J.A., McMillen, D.F. and Malhotra, R., 1992. Am. Chem. Soc. Div. Fuel Chem. Prepr., 37 (4): 1720-1726.

Maswadeh, W.S., Fu, Y., Dubow, J., Meuzelar, H.L.C., 1992. Am. Chem. Soc. Div. Fuel Chem. Prepr., 37 (2) : 699-706.

McMillen, D.F.; Chang, S.; Nigenda, S.E.; Malhotra, R., 1985. Am. Chem. Soc. Div. Fuel Chem. Prepr., 30 (4): 414-426.

Meiler, W. and Meusinger, R. 1990. NMR of Coals and Coal Products, Annual Reports of NMR Spectroscopy, Vol.23, Academic Press, New York, pp.375-410.

Meuzelaar, H.L.C.; Haverkamp, J.; Hileman, F.D., 1982. "Pyrolysis Mass Spectrometry of Recent and Fossil Biomaterials", Elsevier, Amsterdam, 287pp.

Neavel, R.C., in "Coal Sciencae" Vol. 1, Academic Press, New York, 1982, pp. 1-19.

Nip, N.; de Leeuw, J.W.; Schenck, P.H.; Meuzelaar, H.L.; Stout, S.A.; Given, P.H.; Boon, J.J., 1985. J. Anal. Appl. Pyrol., 8: 221-240.

Nomura, M., Ida, T., Miyake, M., Kikukawa, T. and Shimono, T., 1989. Chem. Lett., 1989: 645-648.

Philp, R.P., 1985. Fossil Fuel Biomarkers, Elsevier, Amsterdam, 294 pp.

Pines, A.; Gibby, M.G.; Waugh, J.S., 1972. J. Chem. Phys., 56: 1776.

Pines, A.; Gibby, M.G.; Waugh, J.S., 1973. J. Chem. Phys., 59: 569.

Saini, A.K., Song, C., Schobert, H.H., Hatcher, P.G., 1992. Am. Chem. Soc. Div. Fuel Chem. Prepr., 37 (3) : 1235-1242.

Saiz-Jimenez, C.; De Leeuw, J.E., 1986. J. Anal. Appl. Pyrol., 9: 99-119.

Schaefer, J.; Stejskal, E.O., 1976. J. Am. Chem. Soc., 98:1031

Schobert, H.H., 1990. Resources, Conservation and Recycling, 3: 111-123.

Snape, C.E., Axelson, D.E., Botto, R.E., Delpuech, J.J., Tekely, P., Gerstein, B.C., Pruski, M., Maciel, G.E. and Wilson, M.A., 1989. Fuel, 68: 547.

Solomon, P.R.; Serio, M.A.; Despande, G.V.; Kroo, E., 1990. Energy & Fuels, 4: 42-54.

Solomon, P.R.; Serio, M.A.; Despande, G.V.; Kroo, E., Schobert, H.H., Burgess, C., 1991. Am. Chem. Soc. Sym. Ser., 461: 193-212.

Solum, M.S.; Pugmire, R.J.; Grant, D.M., 1989. Energy & Fuels, 3: 187-193.

Song, C., Hanaoka, K. and Nomura, M., 1989. Fuel, 68: 287-292.

Song, C.; Nomura, M.; Ono, T., Am. Chem. Soc. Div. Fuel Chem. Prepr., 1991a, 36 (2), 586-596.

Song, C.; Schobert, H.H.; Hatcher, P.G., 1991b. Proc. 1991 Int. Conf. Coal Sci. U.K., 1991, pp.664-667.

Song, C.; Schobert, H.H.; Hatcher, P.G., 1992a. Am. Chem. Soc. Div. Fuel Chem. Prepr., 37 (2) : 638-645.

Song, C.; Schobert, H.H., 1992. Am. Chem. Soc. Div. Fuel Chem. Prepr., 37 (2) : 976-983.

Song, C.; Schobert, H.H.; Hatcher, P.G., 1992b. Energy & Fuels, 6: 326-328.

Song, C.; Hatcher, P.G., 1992. Am. Chem. Soc. Div. Petrol. Chem. Prepr., 37 (2) : 529-539.

Song, C.; Hou, L., Saini, A.K., Hatcher, P.G., Schobert, H.H., 1992c. Fuel Processing Technology, submitted.

Song, C.; Saini, A.K., Huang, L., Wenzel, K., Hatcher, P.G., Schobert, H.H., 1992d. "Effects of Low-Temperature Catalytic Pretreatments on Coal Structure and Reactivity in Liquefaction", Technical progress report to U.S. DOE Pittsburgh Energy Technology Center, DE-AC22-91PC91042-TPR-1, January 1992, 90 pp.

Supaluknari, S.; Larkins, F.P.; Redlich, P.; Jackson, W.R., 1989. Fuel Processing Technology 23: 47-61.

Suuberg, E.M.; Unger, P.E.; Larsen, J.W., 1987. Energy & Fuels, 1: 305-308.

Tse, D.S., Hirschon, A.S., Malhotra, R., McMillen, D.F. and Ross, D.S., 1991. Am. Chem. Soc. Div. Fuel Chem. Prepr., 36 (1): 23-28.

van Bergen, P.F., Collinson, M.E., Damste, S.S. and de Leeuw J. W., 1991. Am. Chem. Soc. Div. Fuel Chem. Prepr., 36 (2): 698-701.

VanderHart, D.L.; Retcofsky, H.L., 1976. Fuel, 55: 202

Whitehurst, D.D., "Coal Liquefaction Fundamentals", Am. Chem. Soc. Sym. Ser. 1980a, 139, 132.

Whitehurst, D.D., Mitchell, T.O. and Farcasiu, M., "Coal Liquefaction", Academic Press, New York, 1980b.

Wilson, M.A.; Pugmire, R.J.; Karas, J.; Alemany, L.B.; Woolfenden, W.R.; Grant, D.M., 1984. Anal. Chem., 56: 933-943.

Winans, R.E. , Melnikov, P.E. and McBeth, R.L., 1992. Am. Chem. Soc. Div. Fuel Chem. Prepr., 37 (2) : 693-698.

Yannoni, C.S., 1982. Acc. Chem. Res., 15: 201

Yoshida, T.; Maekawa, Y., 1987. Fuel Processing Technol., 15, 385-395.

Yoshida, T., 1992. Sekiyu Gakkaishi, 35 (1): 1-13.

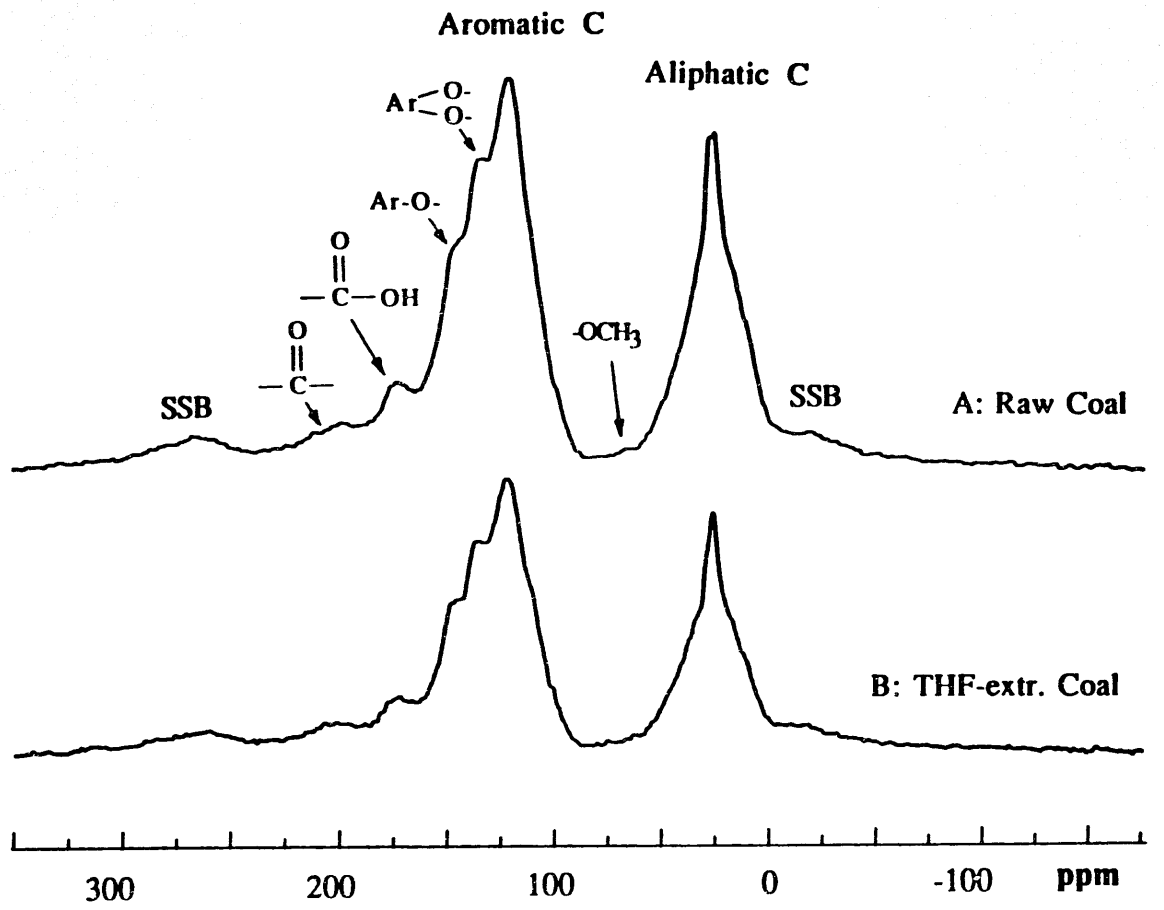

Figure 1. CPMAS ^{13}C NMR spectra of DECS-9 Montana subbituminous coal (A) and the THF-extracted coal (B).

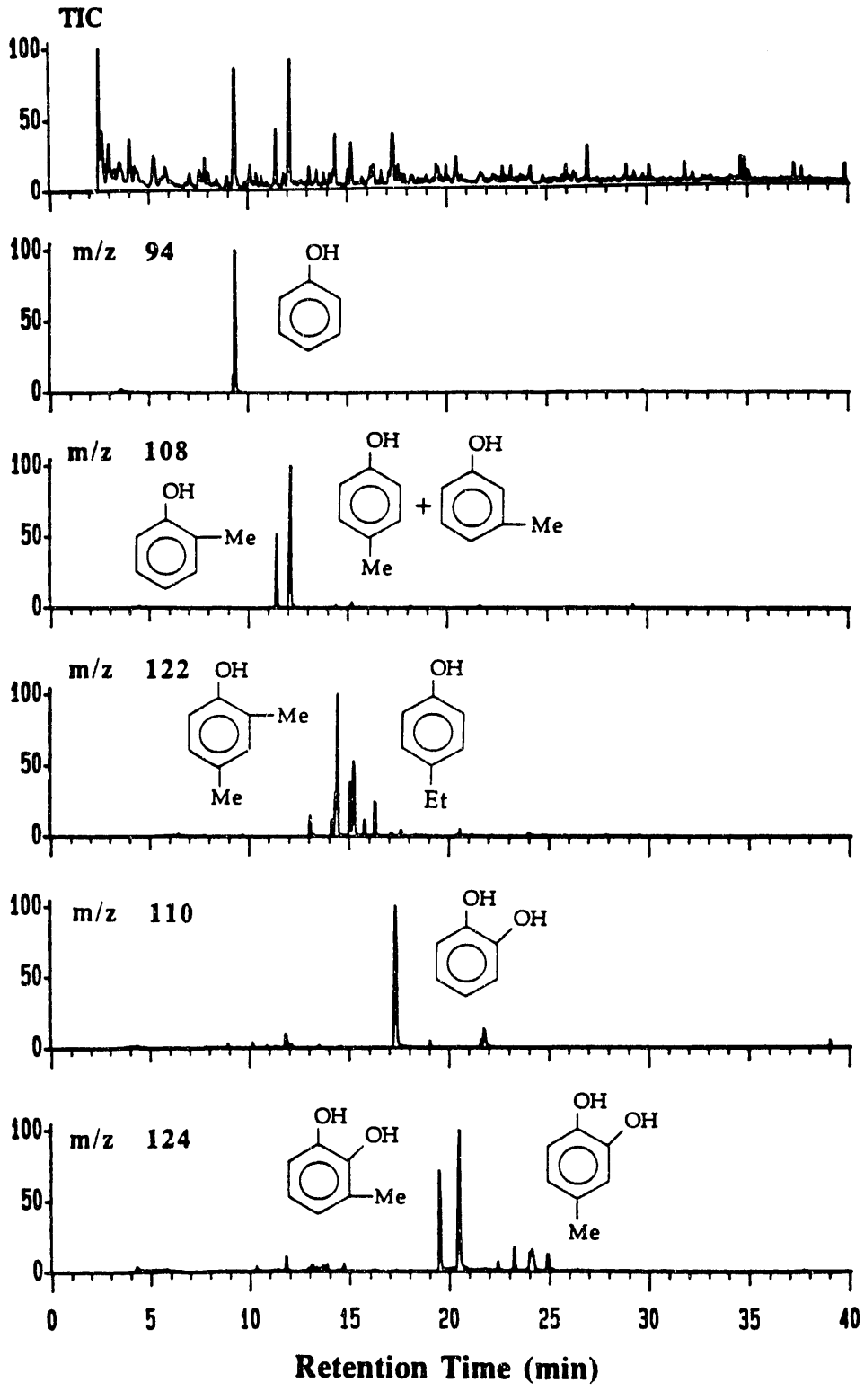

Figure 2. Retention time window (0-40 min) of totoal ion chromatogram (TIC) from pyrolysis-GC-MS of THF-extracted DECS-9 coal, and specific ion chromatograms (SIC) at ion masses characteristic of O-containing compounds.

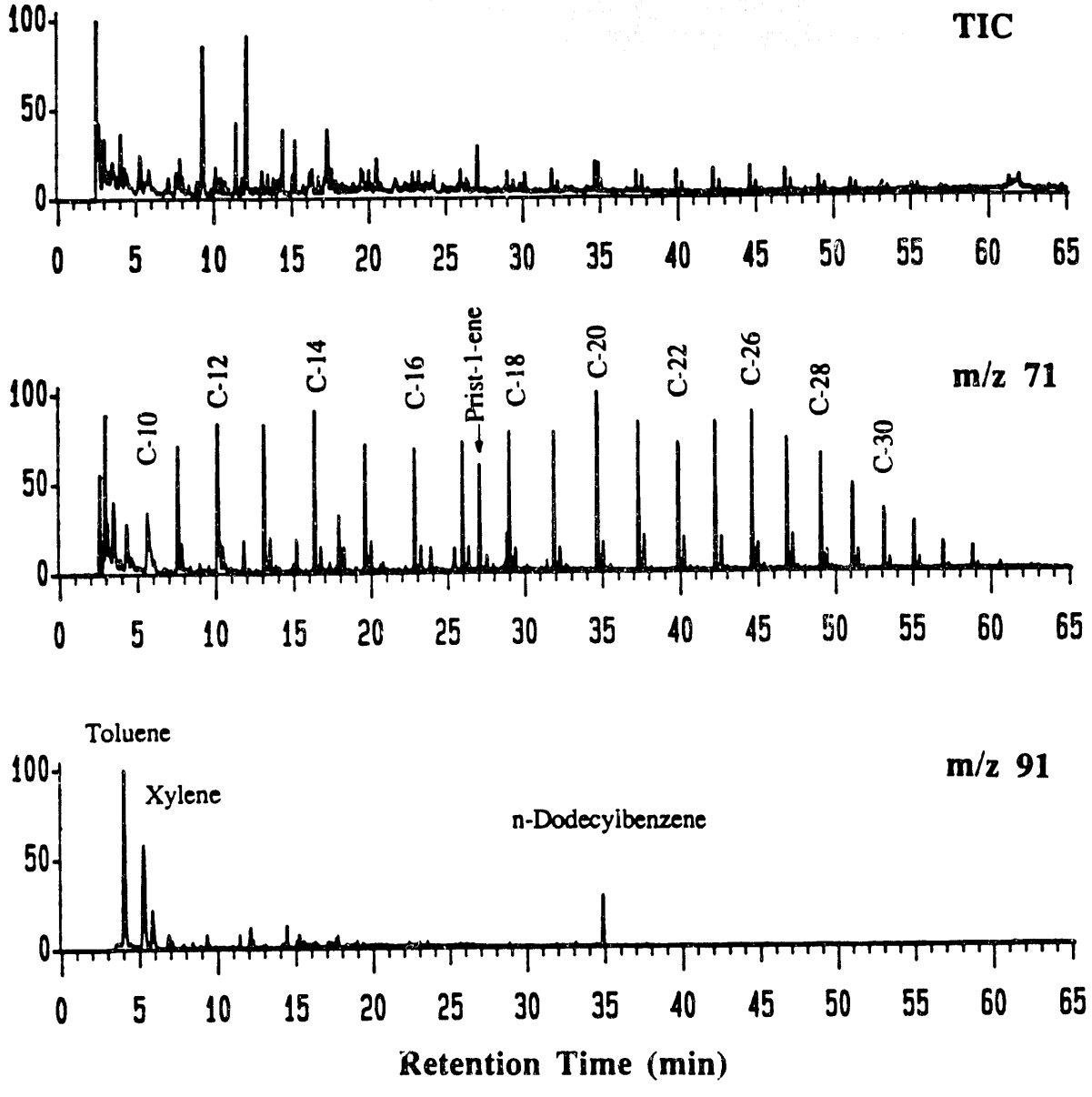

Figure 3. Py-GC-MS TIC of THF-extracted DECS-9 coal, and SIC at ions characteristic of long-chain paraffins (m/z 71) and alkylbenzenes (m/z 91).

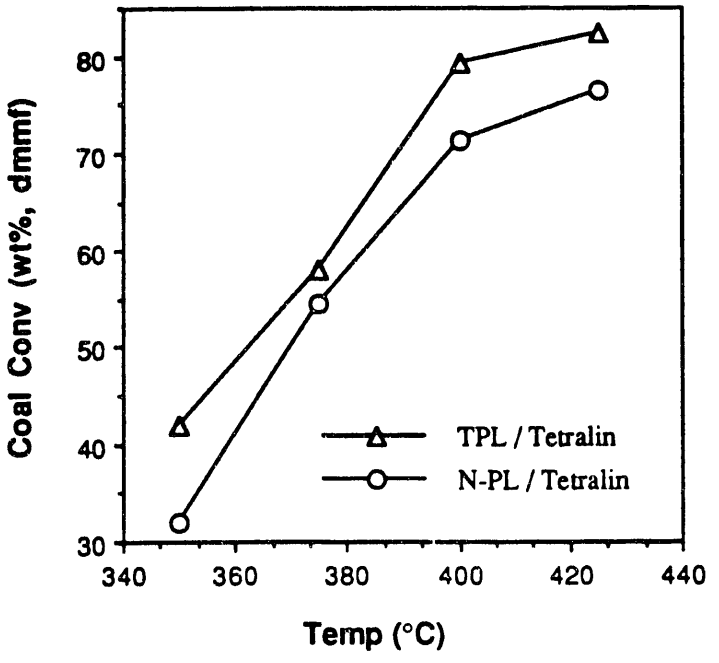

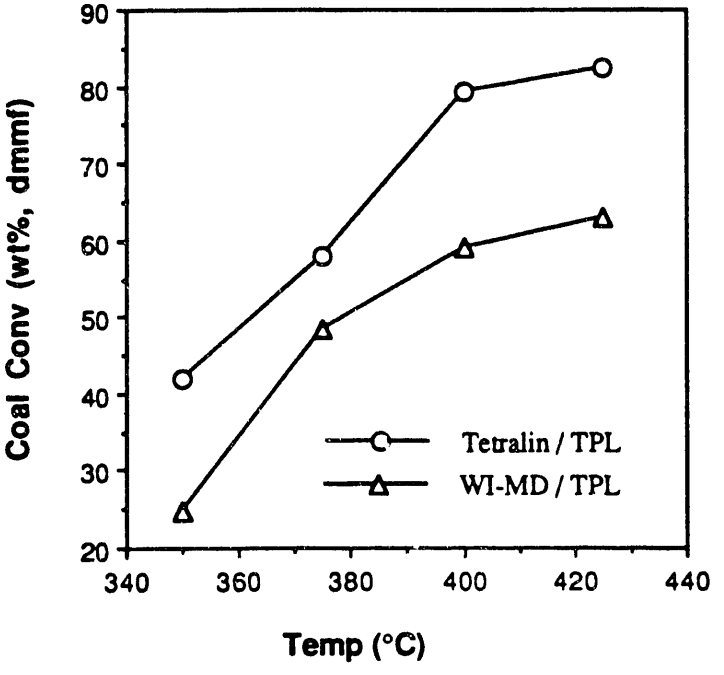

Figure 4. Conversion of DECS-9 coal to THF-solubles versus liquefaction temperature for TPL and N-PL in tetralin and for TPL in WI-MD.

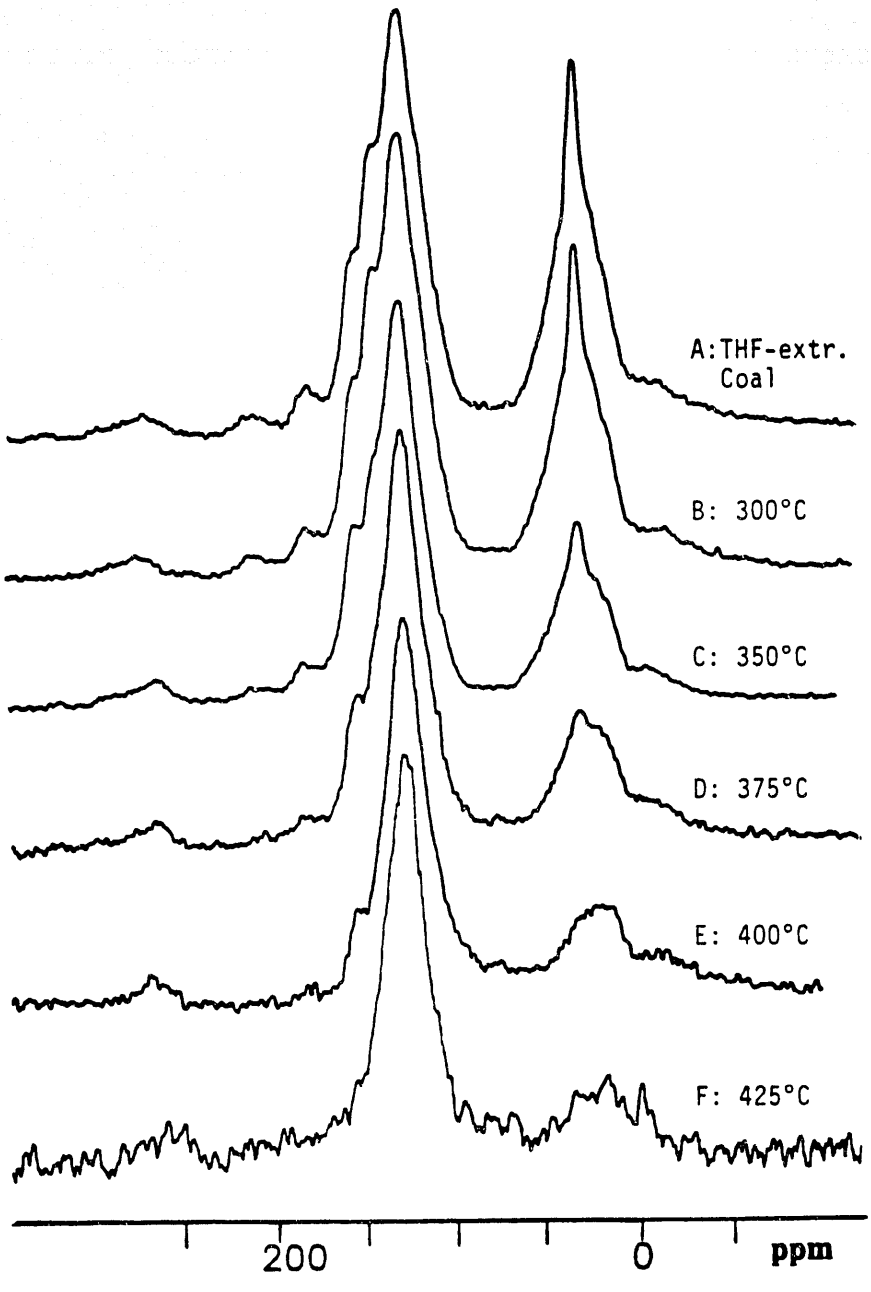

Figure 5. CPMAS ^{13}C NMR spectra of THF-insoluble residues from TPL of DECS-9 coal in tetralin at different final temperatures from 300 to 425°C.

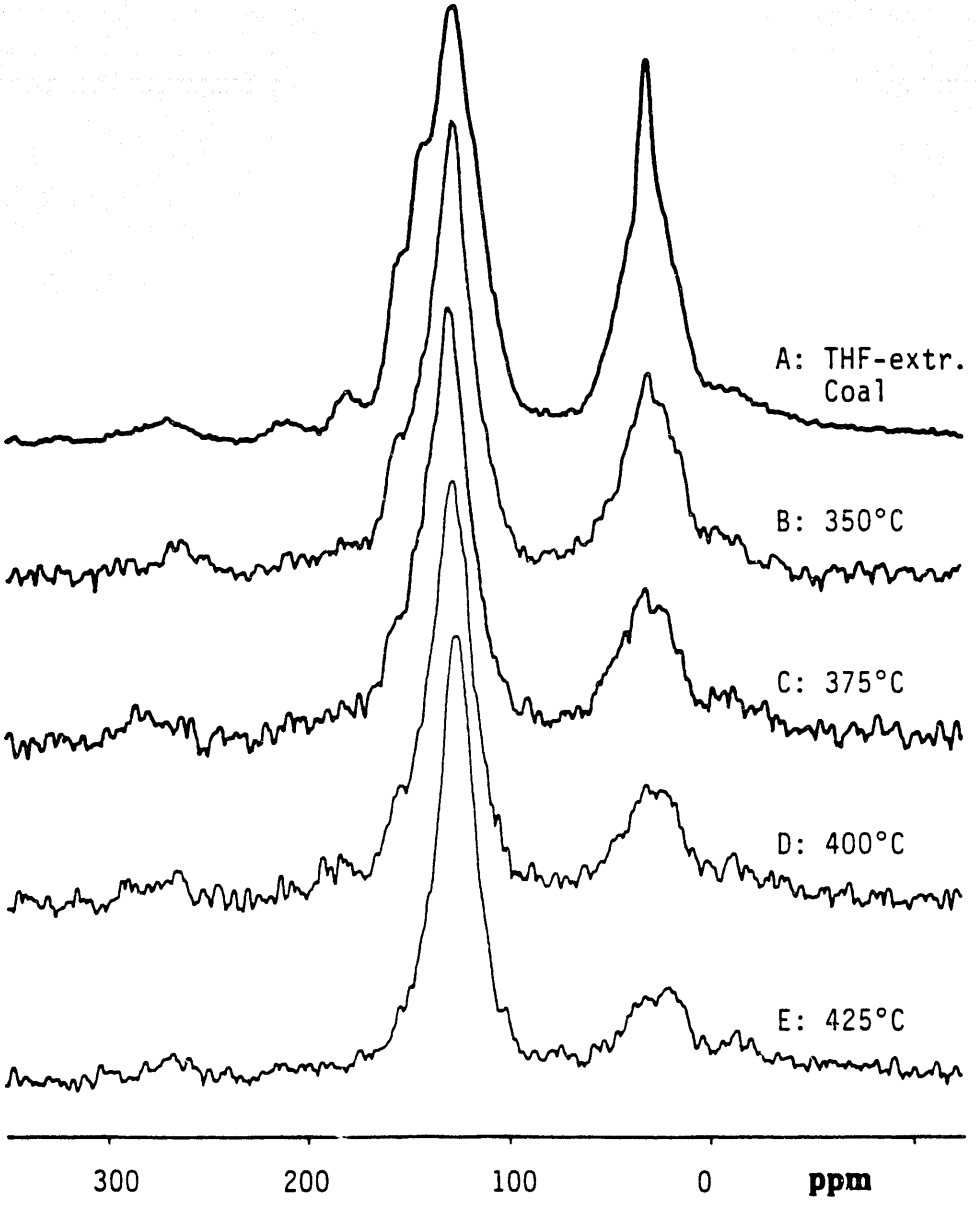

Figure 6. CPMAS ^{13}C NMR spectra of THF-insoluble residues from TPL of DECS-9 coal in WI-MD at different final temperatures from 350 to 425°C.

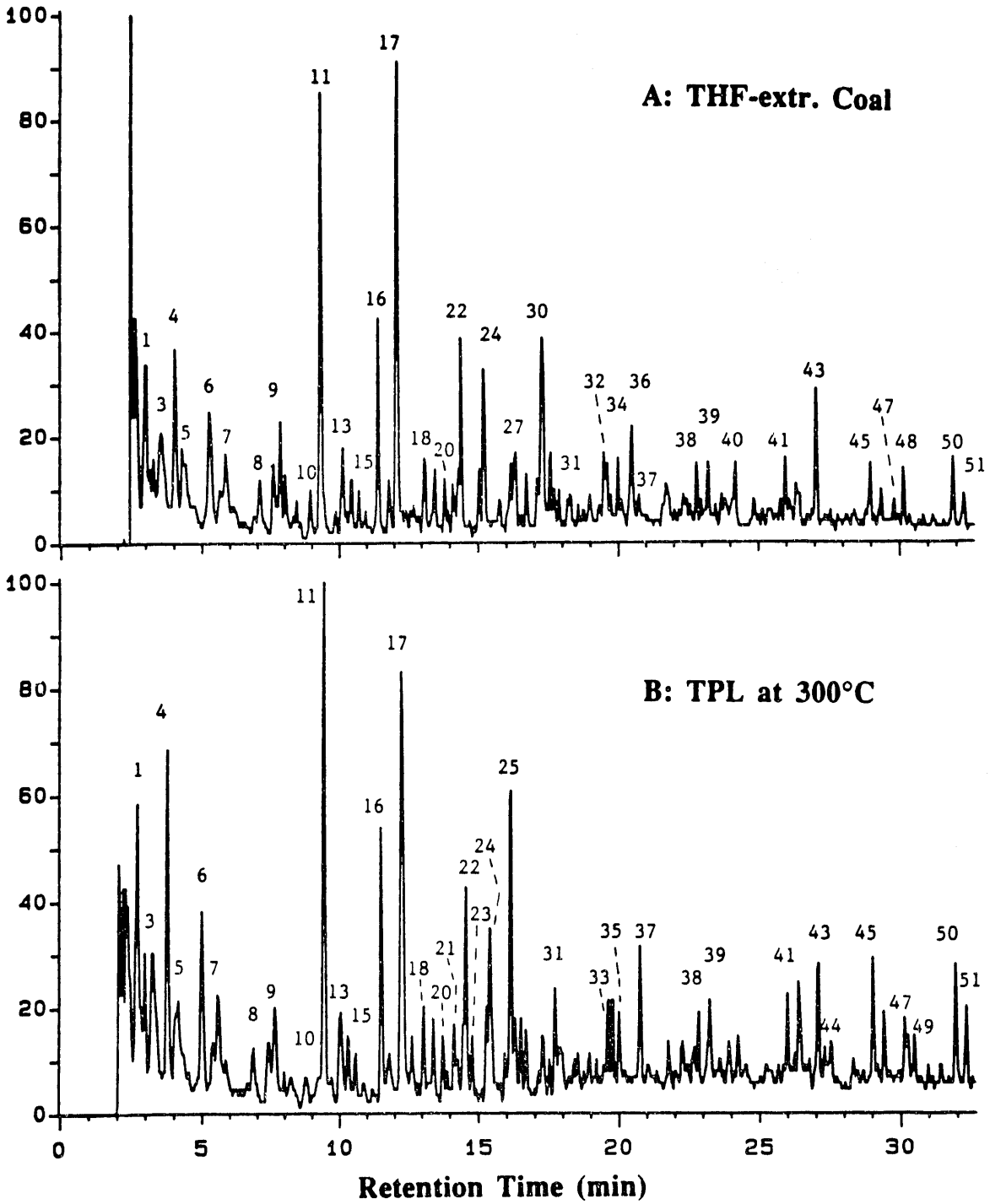

Figure 7. Py-GC-MS profiles of THF-extracted unreacted DECS-9 coal (A) and the residue (B) from TPL in tetralin at 300°C.

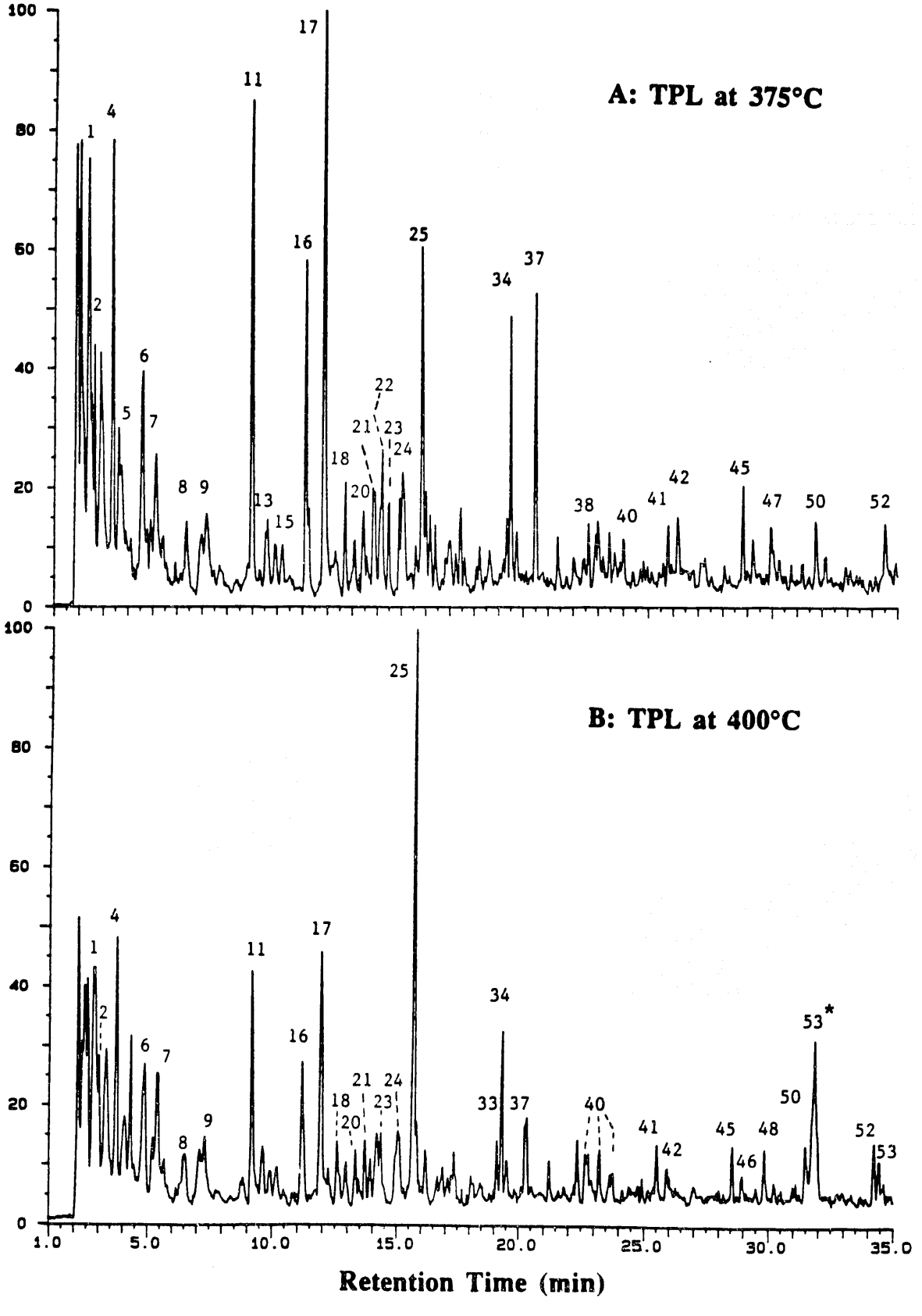

Figure 8. Py-GC-MS profiles of the residues from TPL in tetralin at 375°C (A) and 400°C (B).

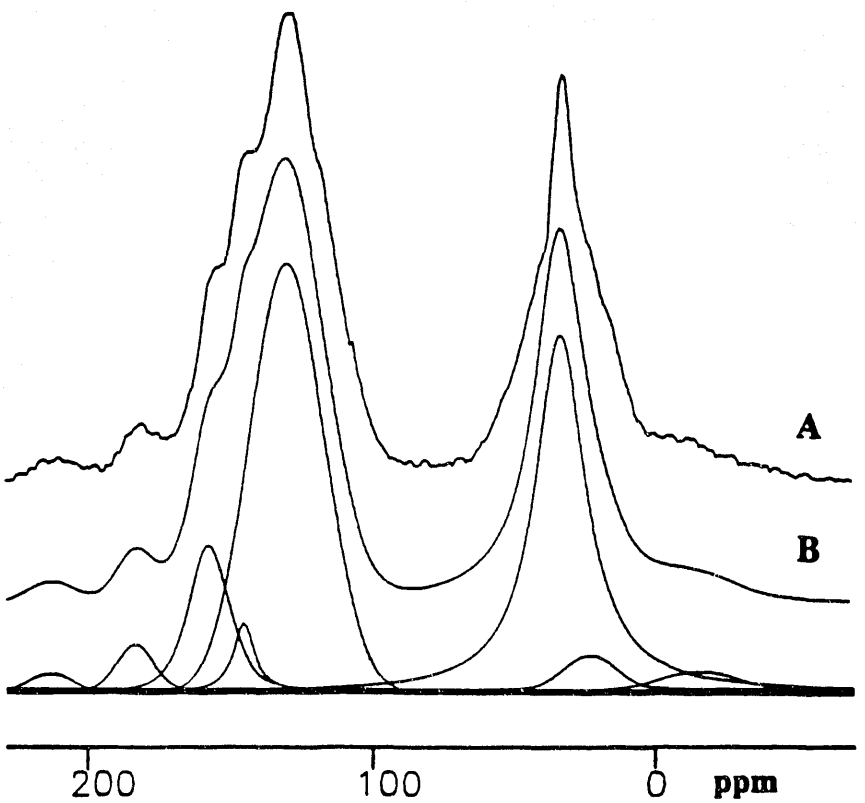

Figure 9A. Peak separation of NMR bands of THF-extracted raw DECS-9 coal using curve-fitting program. A: real spectrum, B: simulated spectrum.

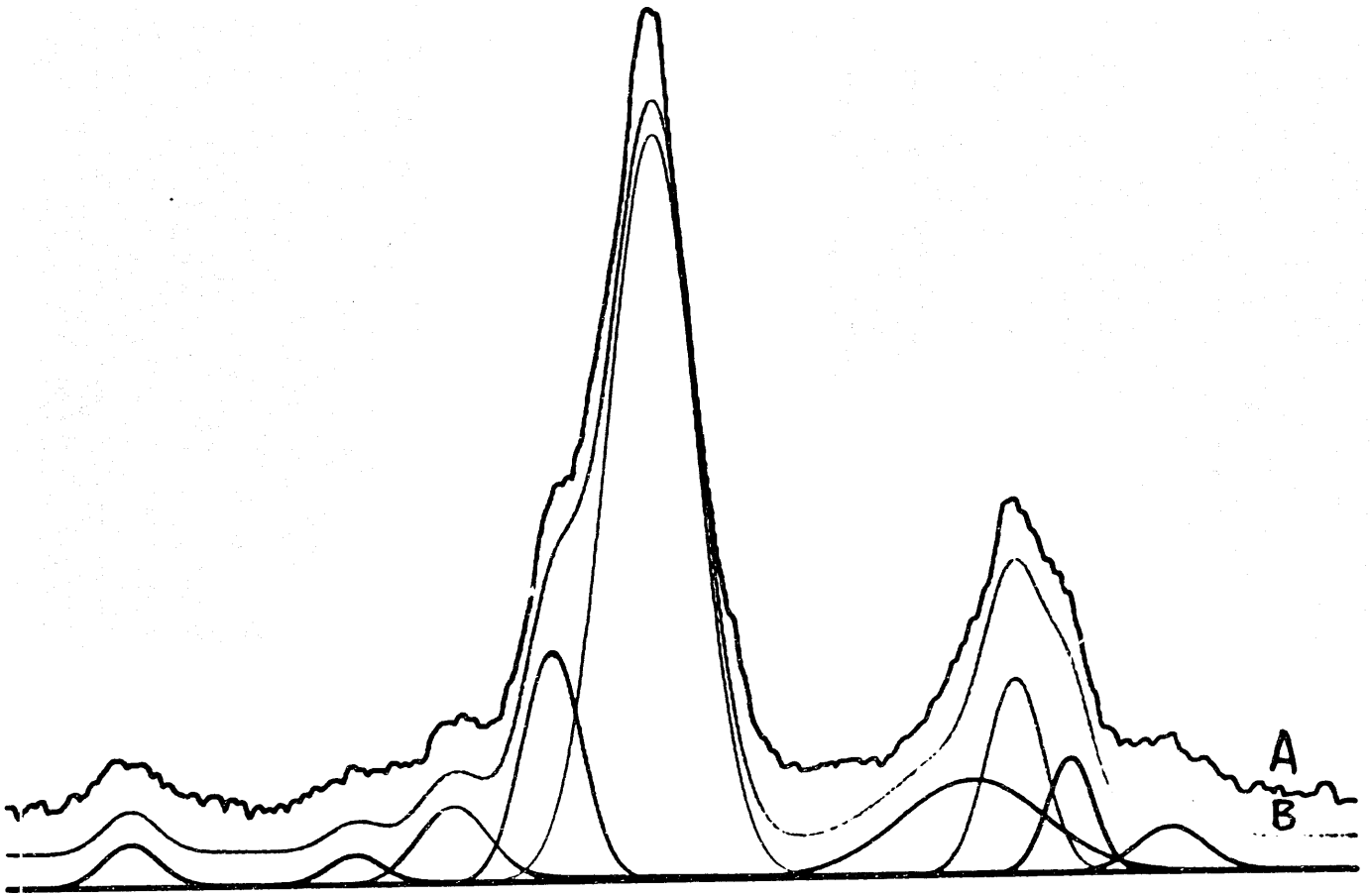

Curve Fitting on NMR Spectrum of Residue from TPL-350°C

Figure 9B. Peak separation of NMR bands of residue from TPL of DECS-9 coal in tetralin at 375°C using curve-fitting program. A: real spectrum, B: simulated spectrum.

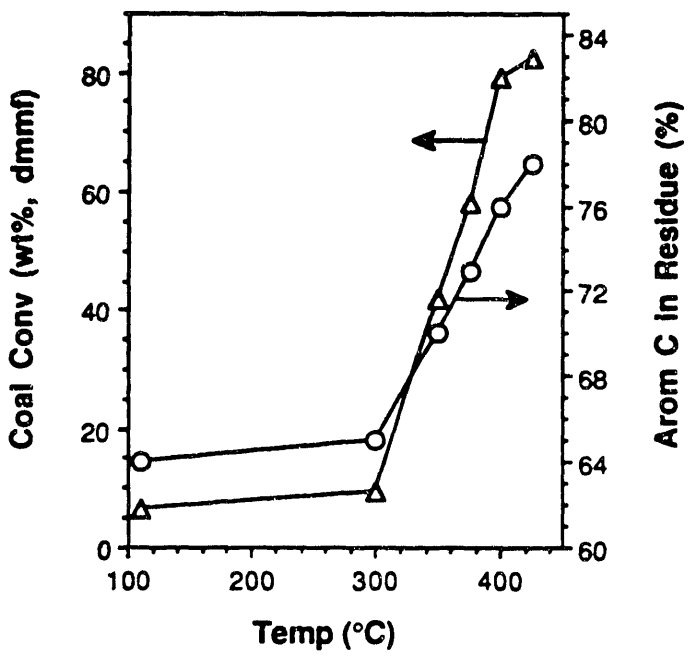

Figure 10. Changes of aromaticity of the residues and the coal conversion versus final temperature of TPL in tetralin.

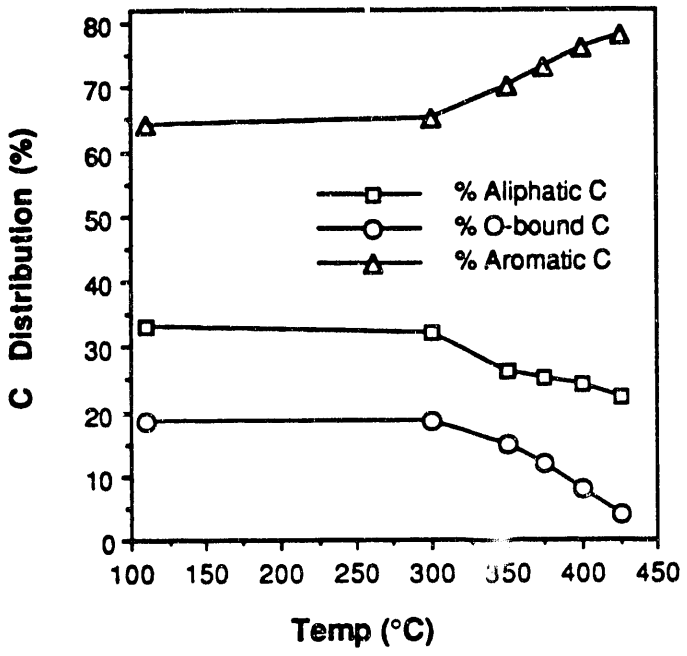

Figure 11. Changes of carbon distribution in the residues versus temperature of TPL in tetralin.

Effect of Solvent on NMR of Residues from TPL at 350°C

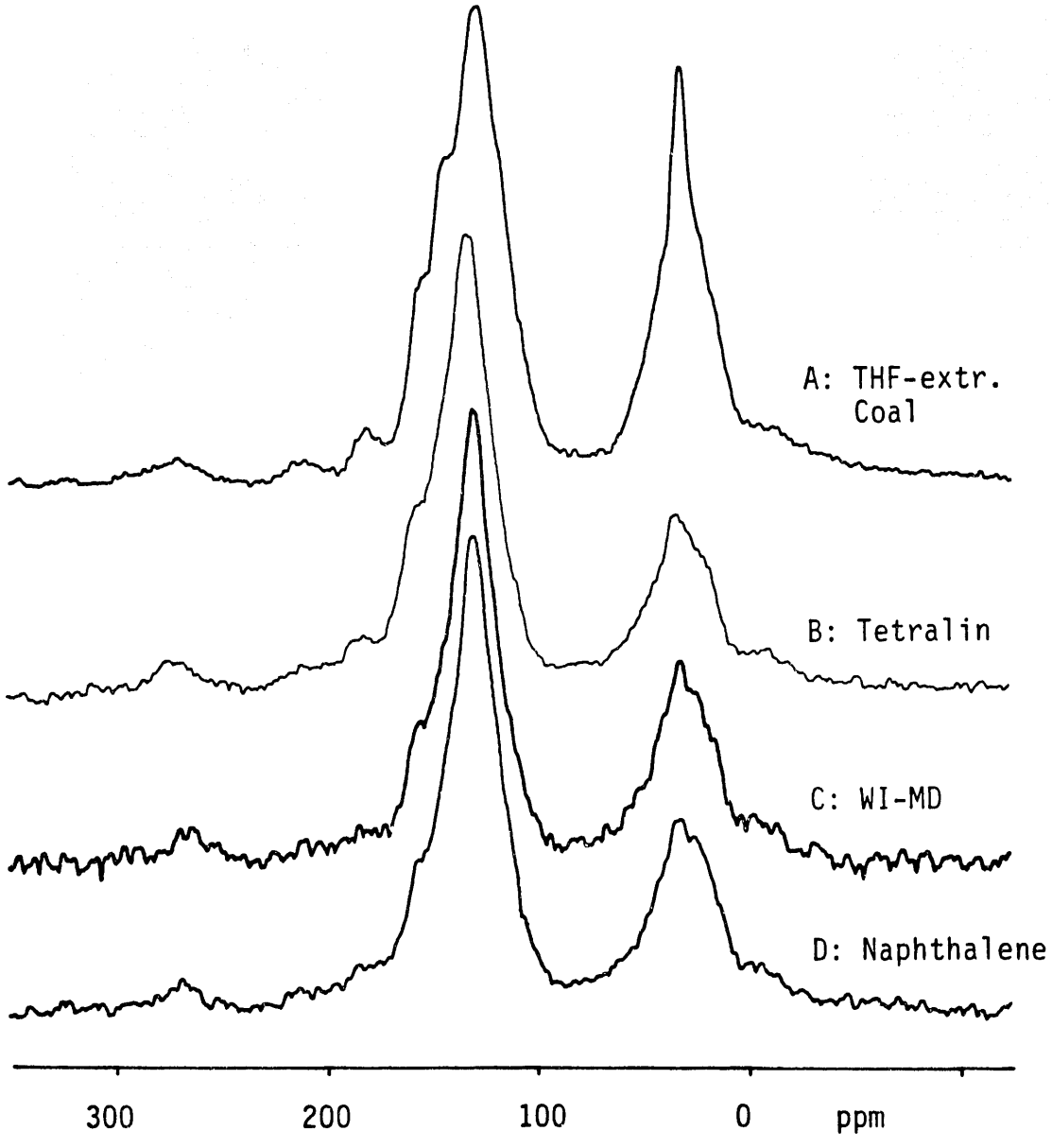

Figure 12. CPMAS ^{13}C NMR spectra of residues from TPL of DECS-9 coal at final temperature of 350°C (A, THF-extracted raw coal; B, tetralin; C, WI-MD; D, naphthalene).

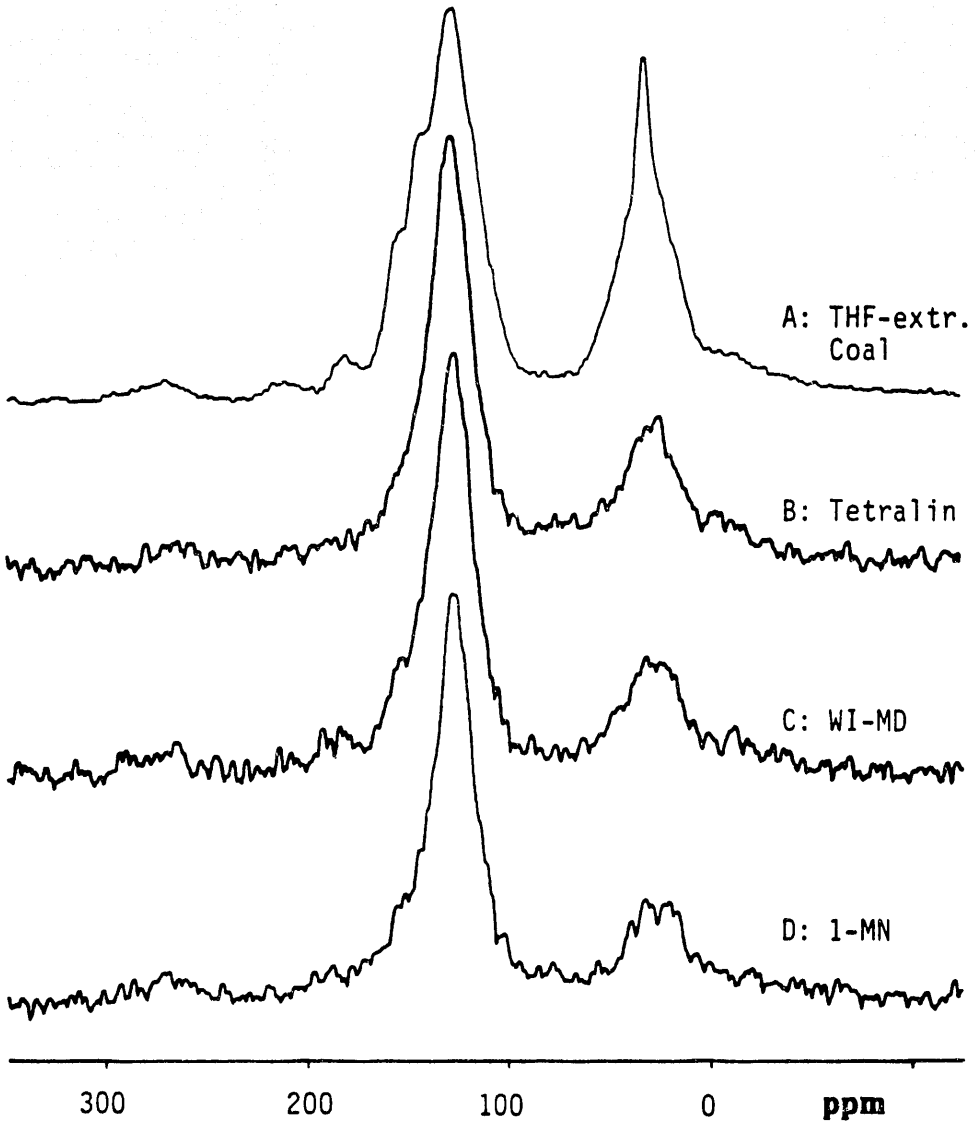

Figure 13. CPMAS ^{13}C NMR spectra of residues from TPL of DECS-9 coal at final temperature of 400°C (A, THF-extracted raw coal; B, tetralin; C, WI-MD; D, 1-methylnaphthalene).

CPMAS ^{13}C NMR of Residues from TPL & N-PL with H-donor Tetralin

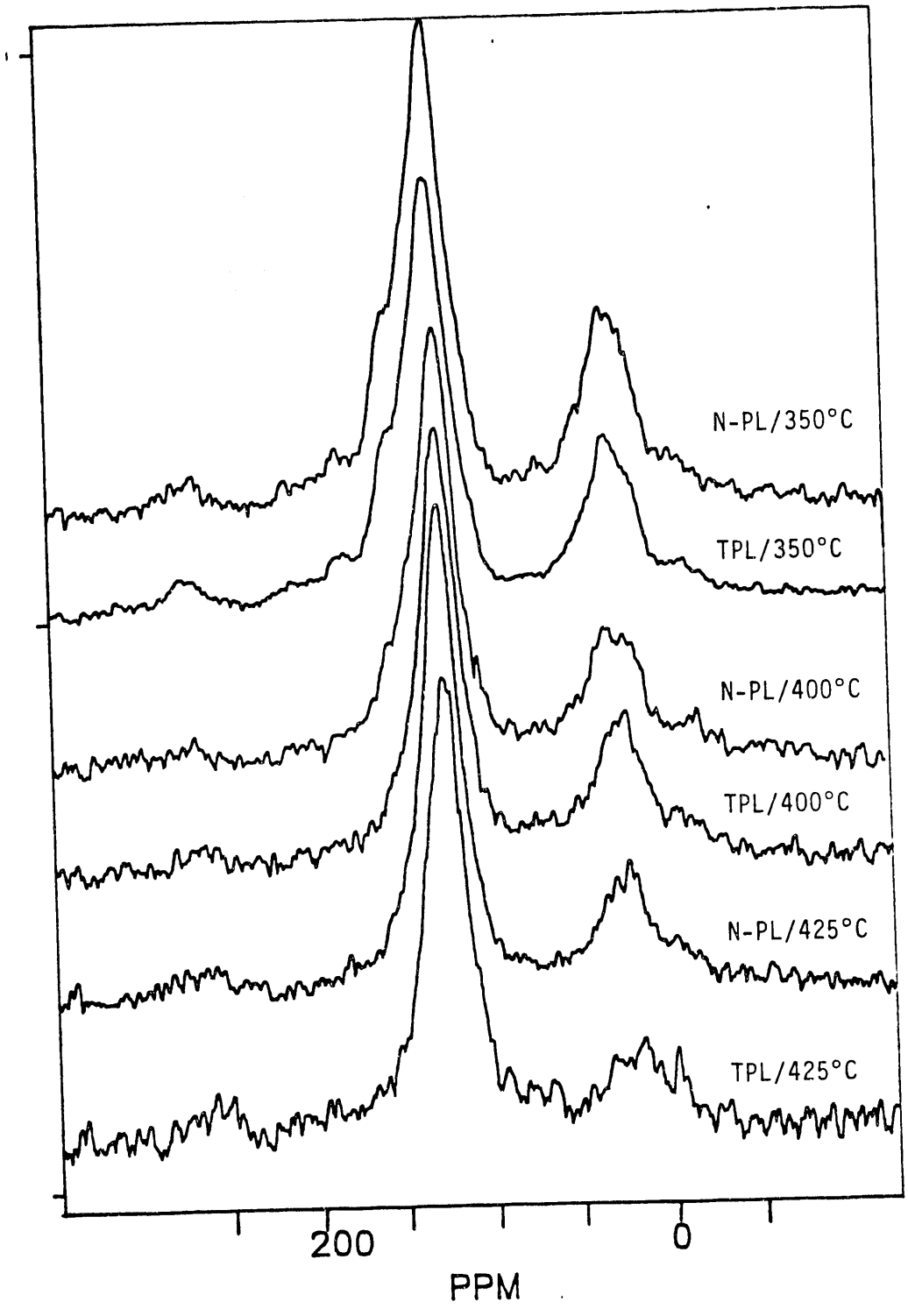

Figure 14. CPMAS ^{13}C NMR spectra of residues from TPL and N-PL of DECS-9 coal with tetralin at final temperatures ranging from 350 to 425°C.

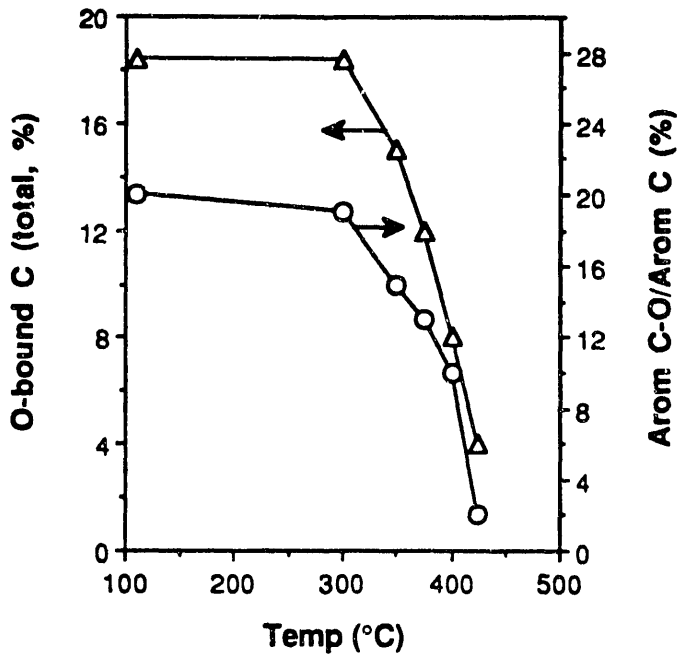

Figure 15. Changes of total oxygen-bound C and aromatic O-bound C versus final temperature of TPL in tetralin.

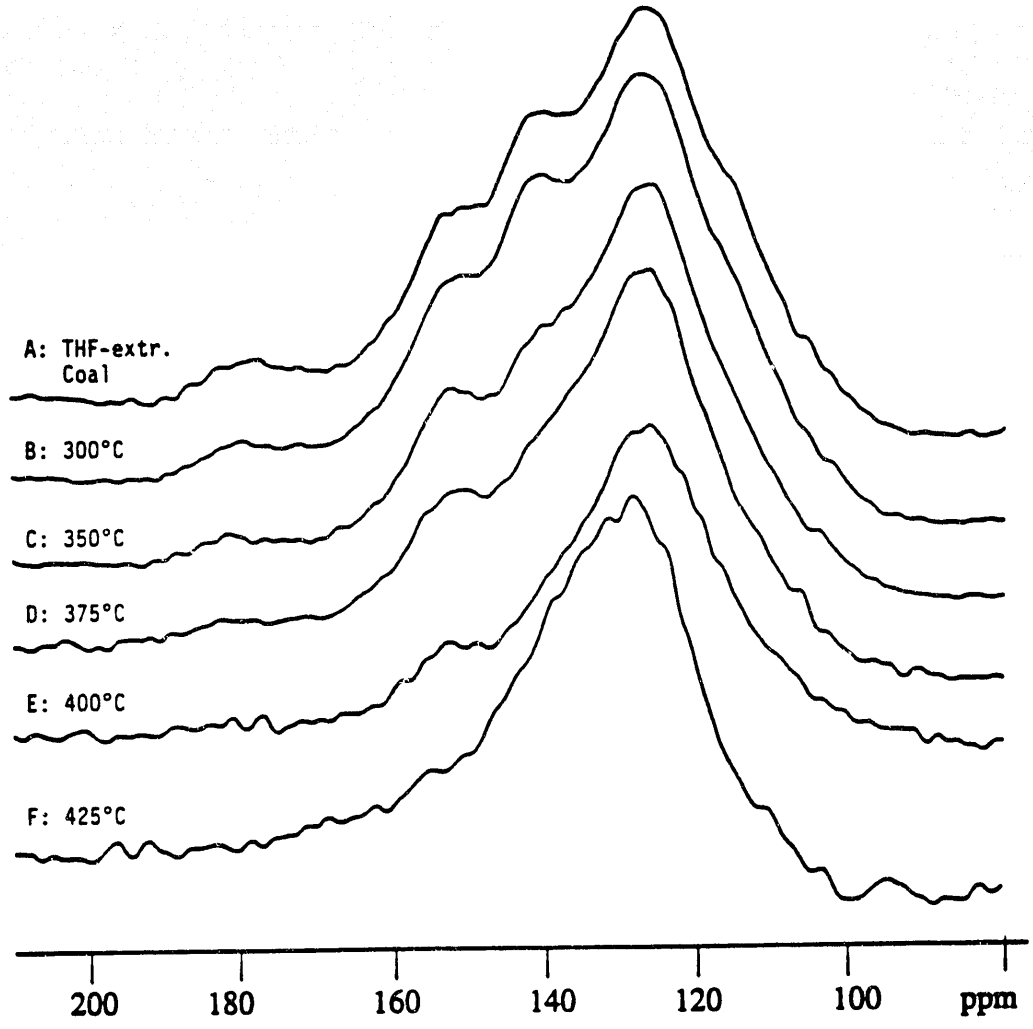

Figure 16. Expanded aromatic region of ^{13}C NMR spectra of residues from TPL in tetralin.

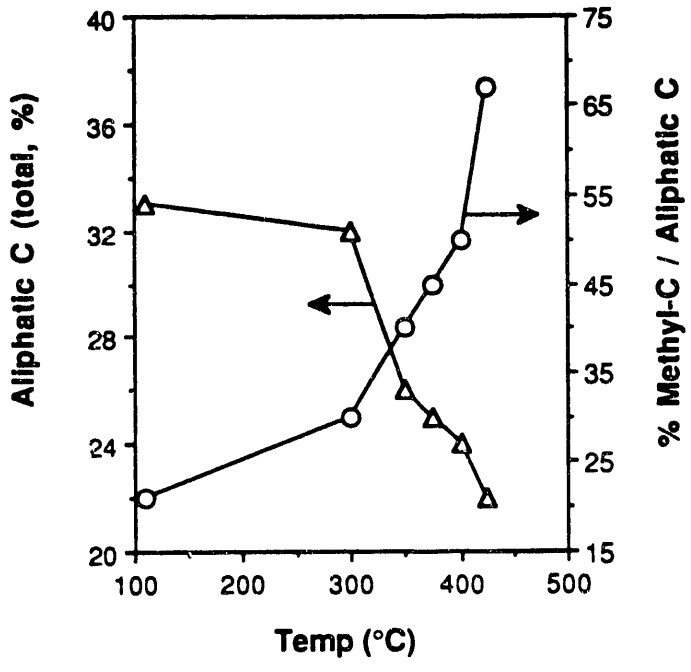

Figure 17. Changes of total aliphatic carbons and methyl carbons in the residues versus final temperature of TPL in tetralin.

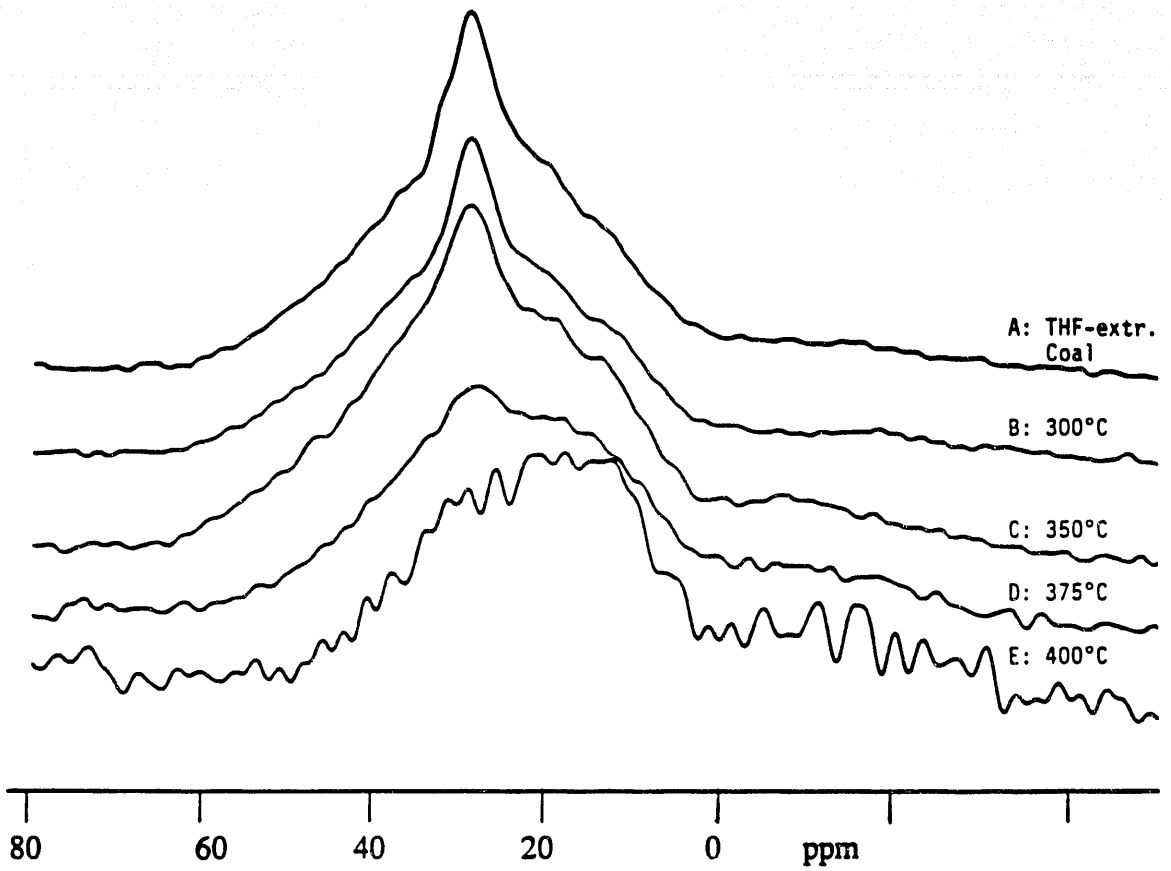

Figure 18. Expanded aliphatic region of ^{13}C NMR spectra of residues from TPL in tetralin.

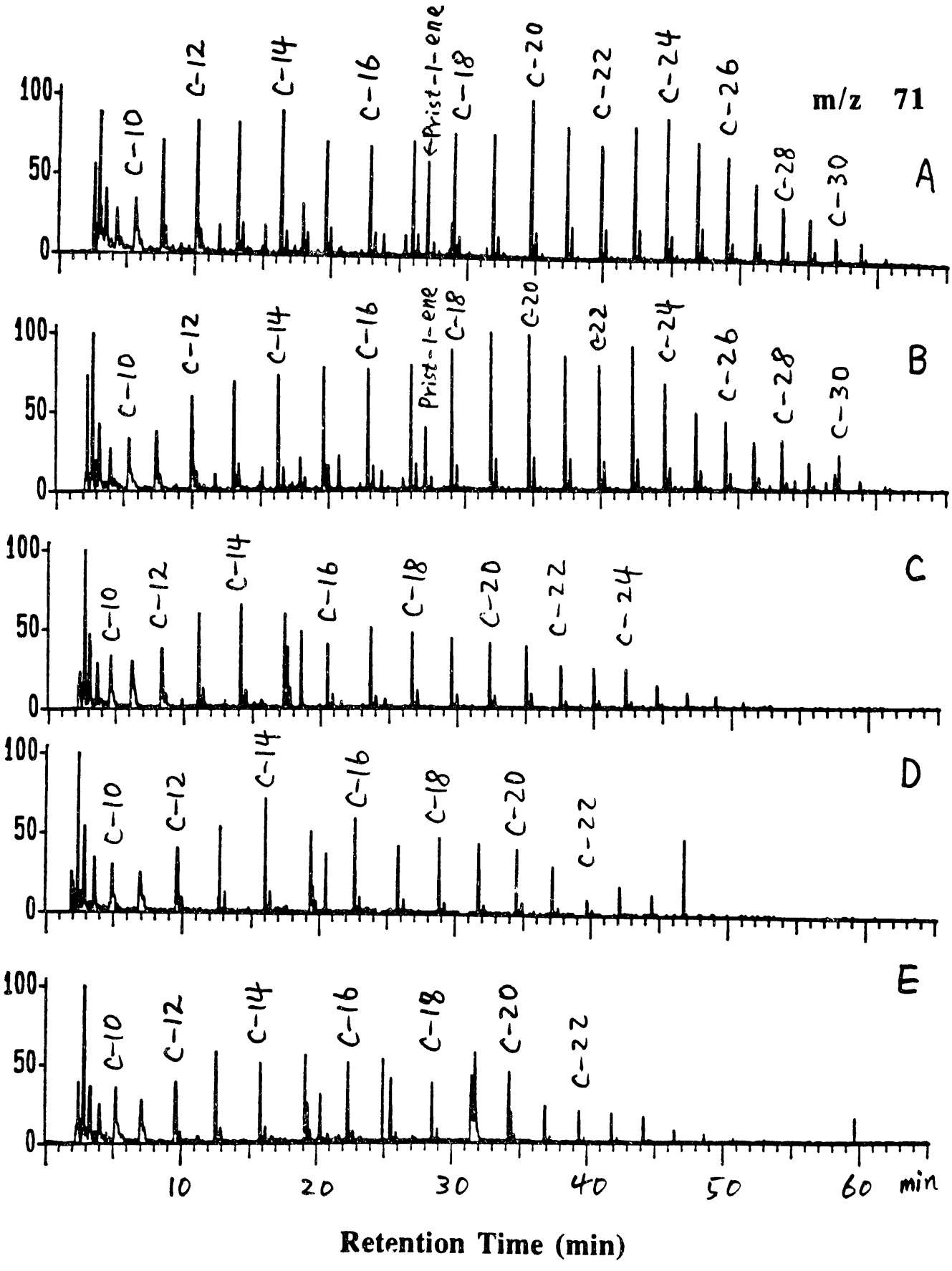

Figure 19. Selective ion monitoring of long-chain paraffins at m/z 71 from Py-GC-MS profiles of residues from TPL in tetralin at 300 °C (A), 375°C (B) and 400°C (C).

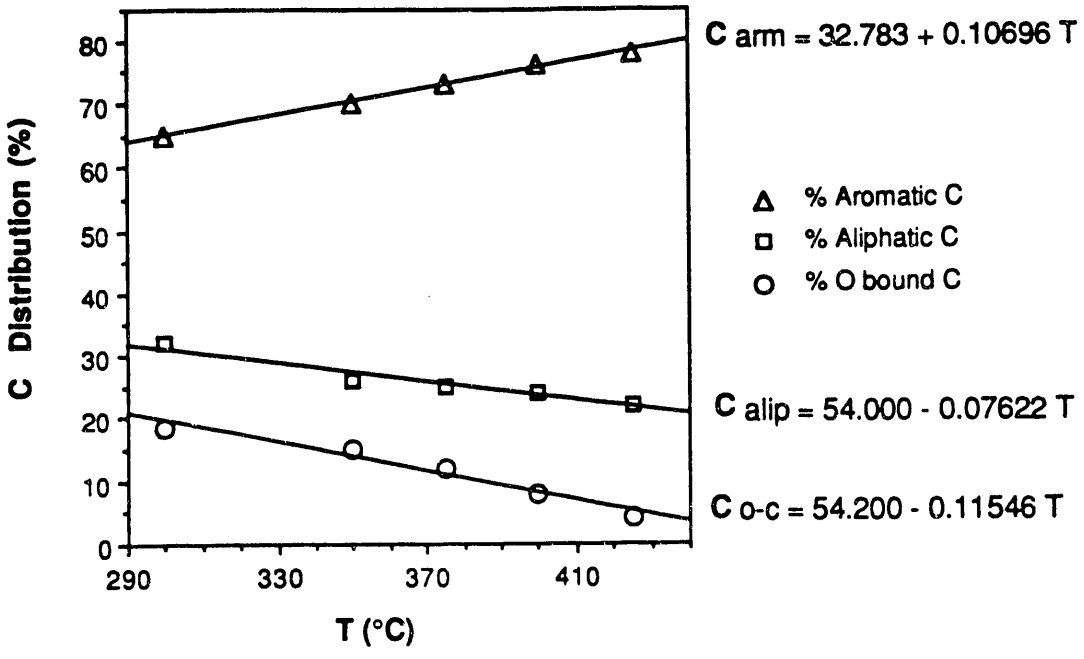

Figure 20. Correlation of C-distribution of residues with TPL temperature in tetralin (T≥ 300°C).

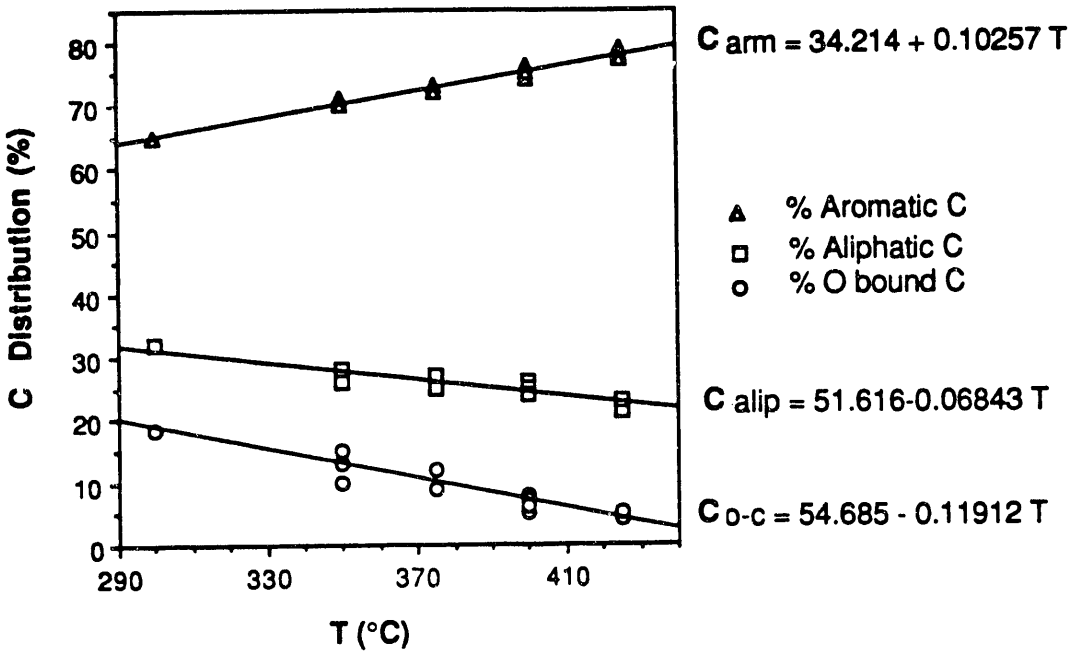

Figure 21. Linear correlation of C-distribution with final temperature for residues from TPL and N-PL runs using different solvents including tetralin, WI-MD, naphthalene and methylnaphthalene ($T \geq 300°C$).

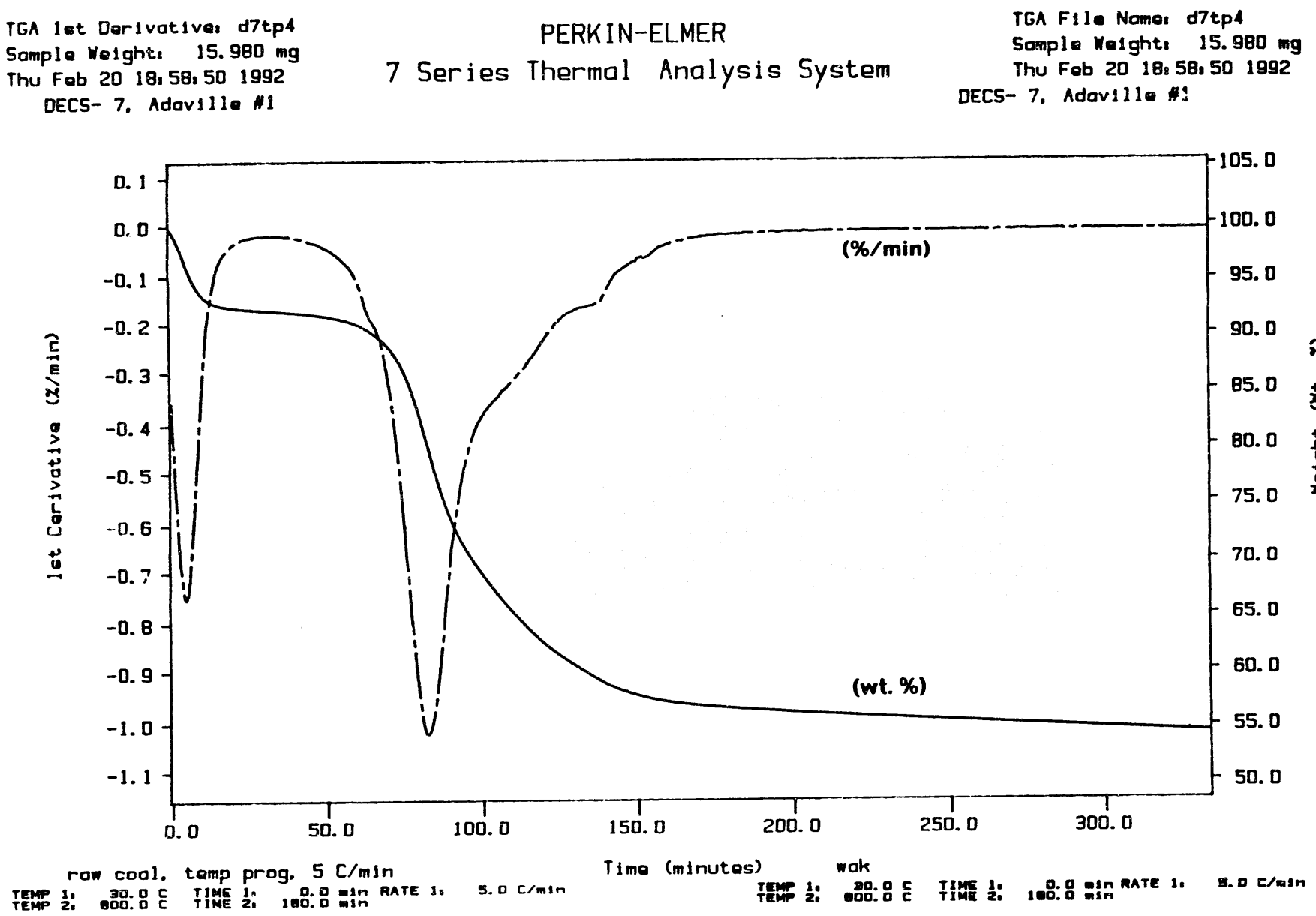

Figure 22. TGA and DTG plots of the Adaville #1 coal.

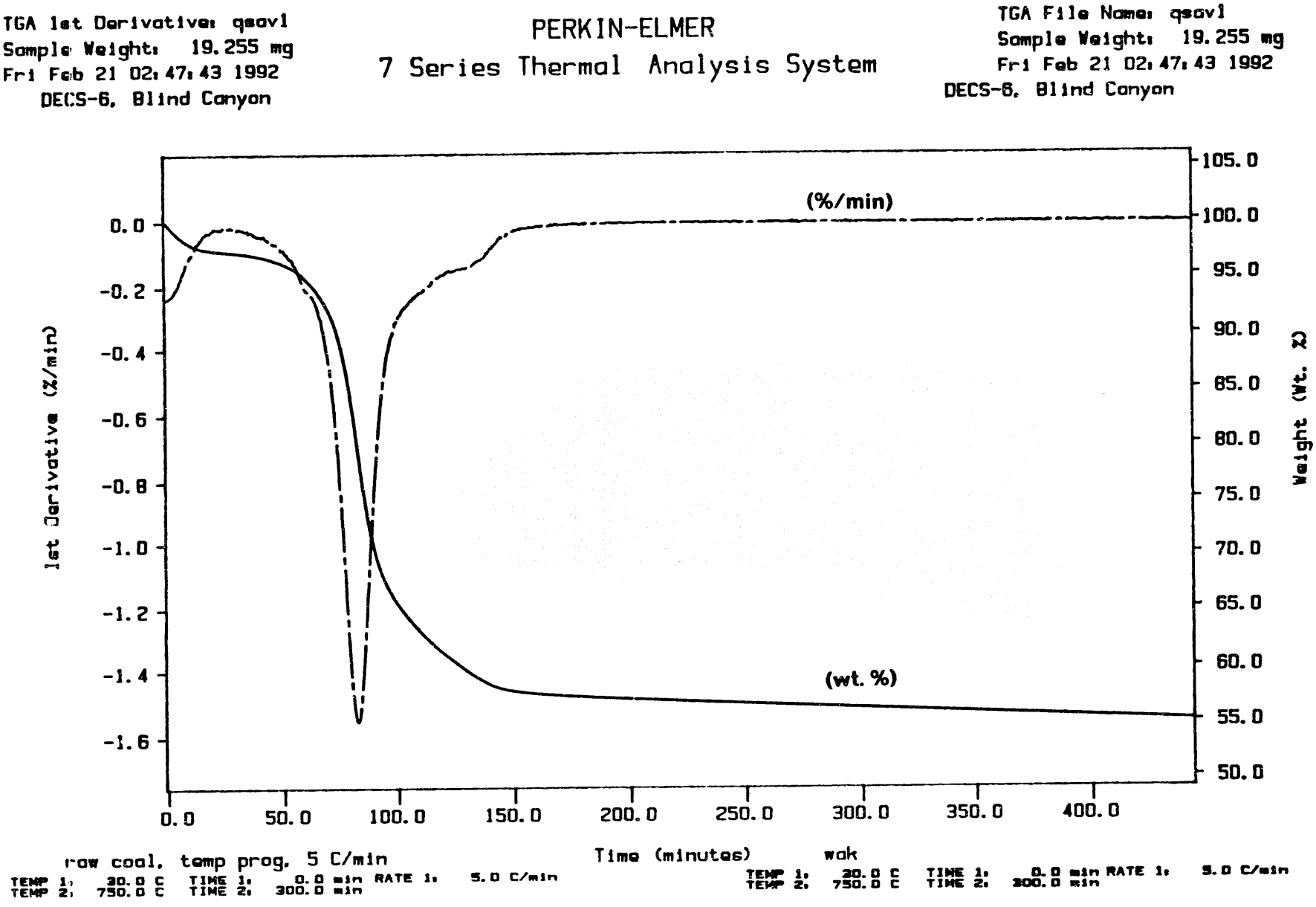

Figure 23. TGA and DTG plots of the Blind Canyon coal.

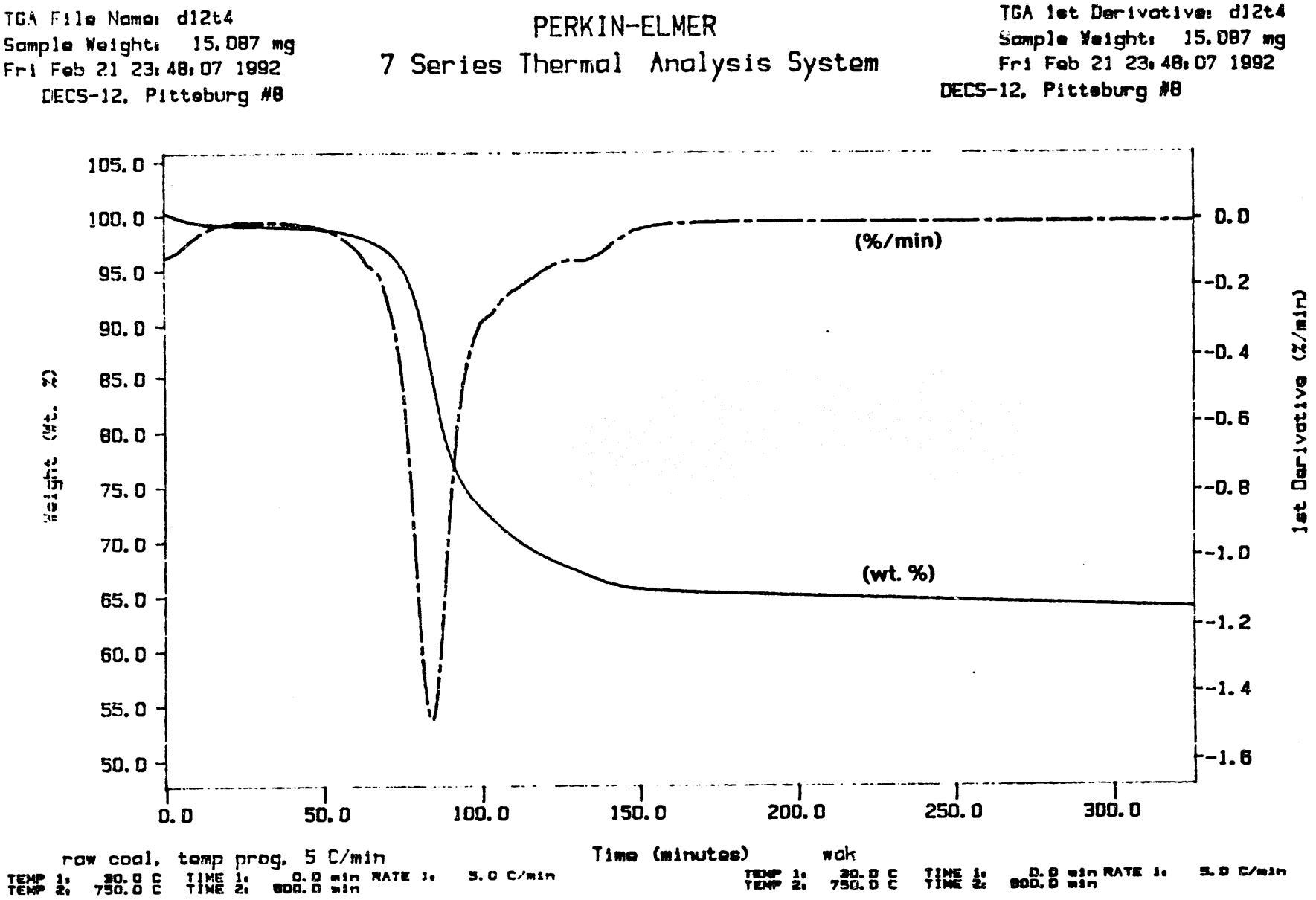

Figure 24. TGA and DTG plots of the Pittsburgh #8 coal.

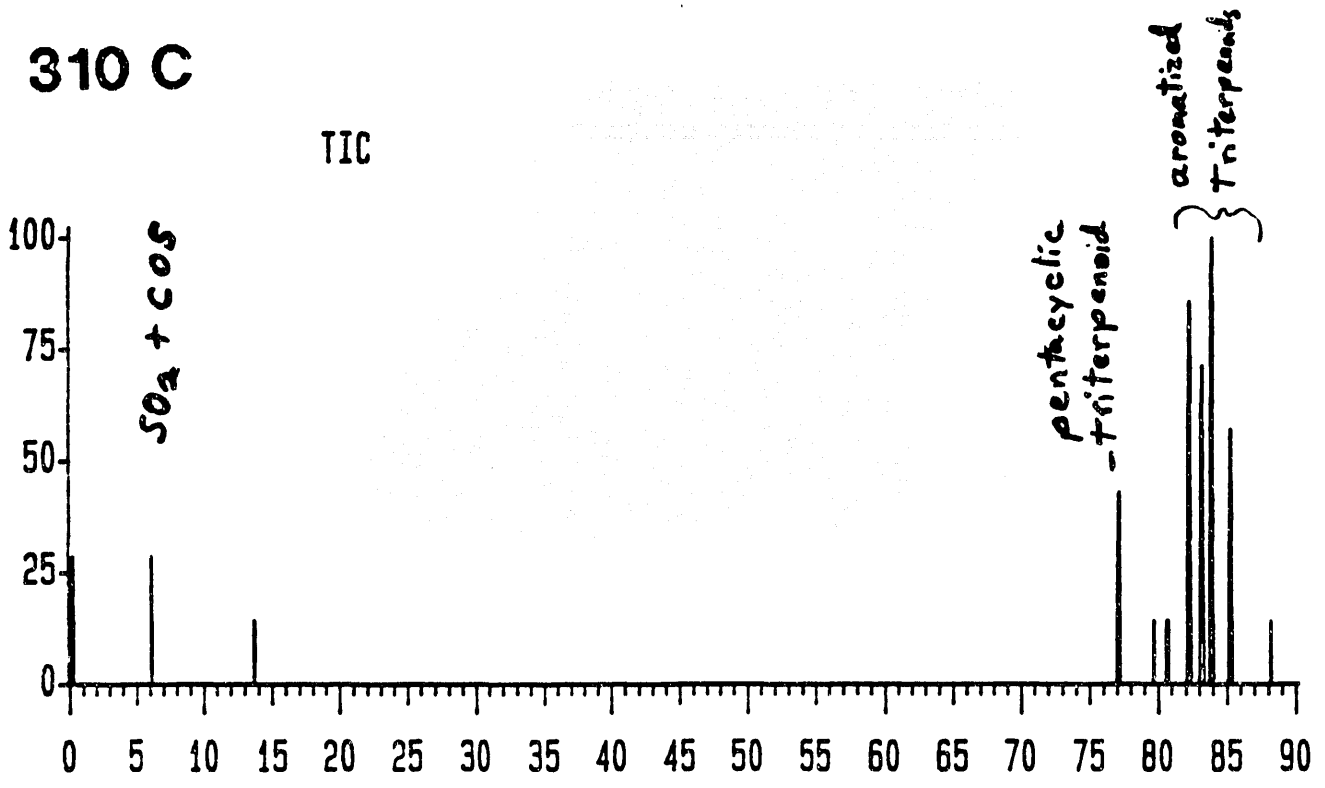

Figure 25. Pyrolysis-GC-MS chromatogram of DECS-7 Adaville #1 coal (pyrolysis at 310°C, representing thermally desorbed materials)

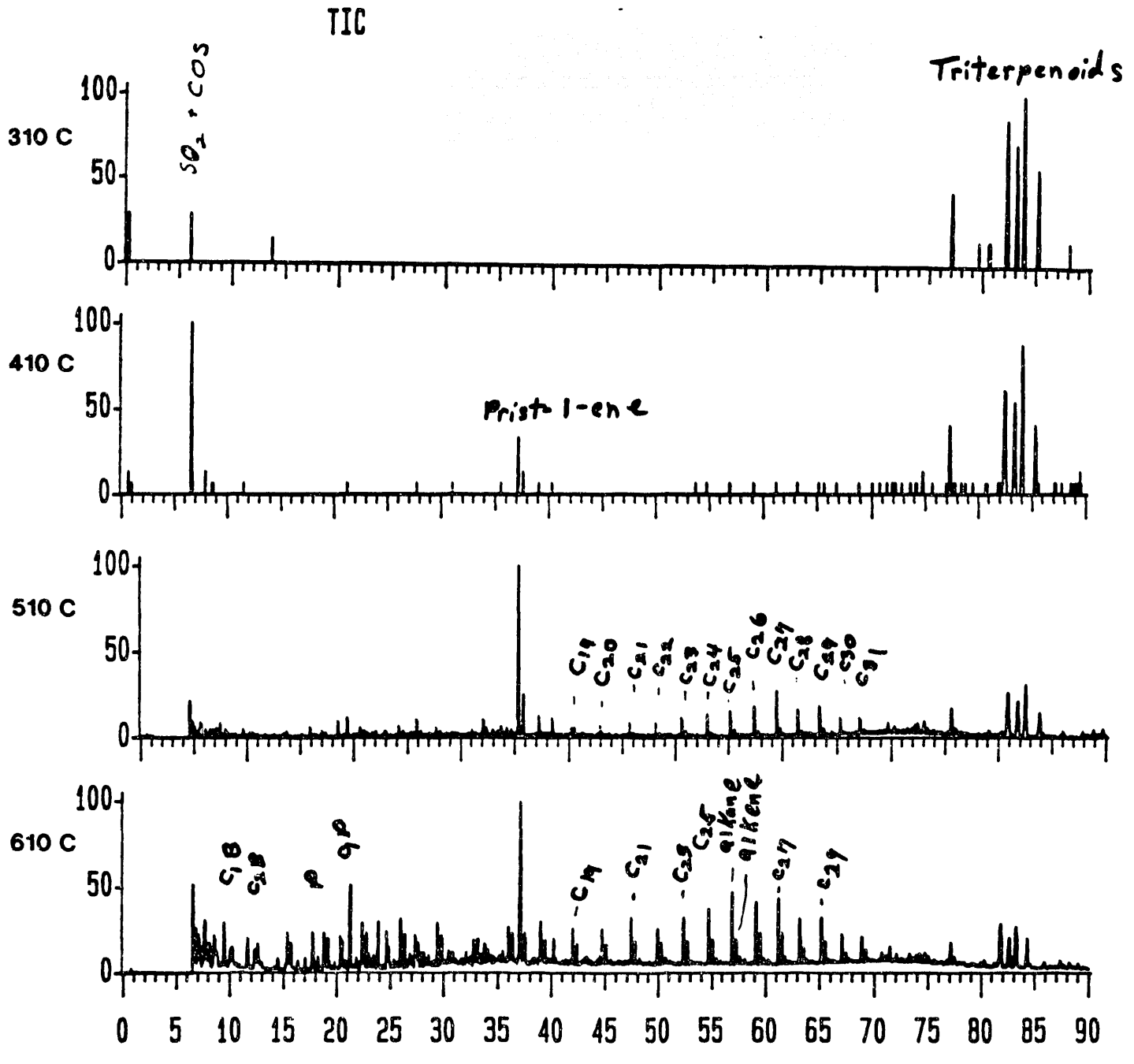

Figure 26. Pyrolysis-GC-MS chromatogram of DECS-7 Adaville #1 coal (pyrolysis at 310°C, 410°C, 510°C and 610°C).

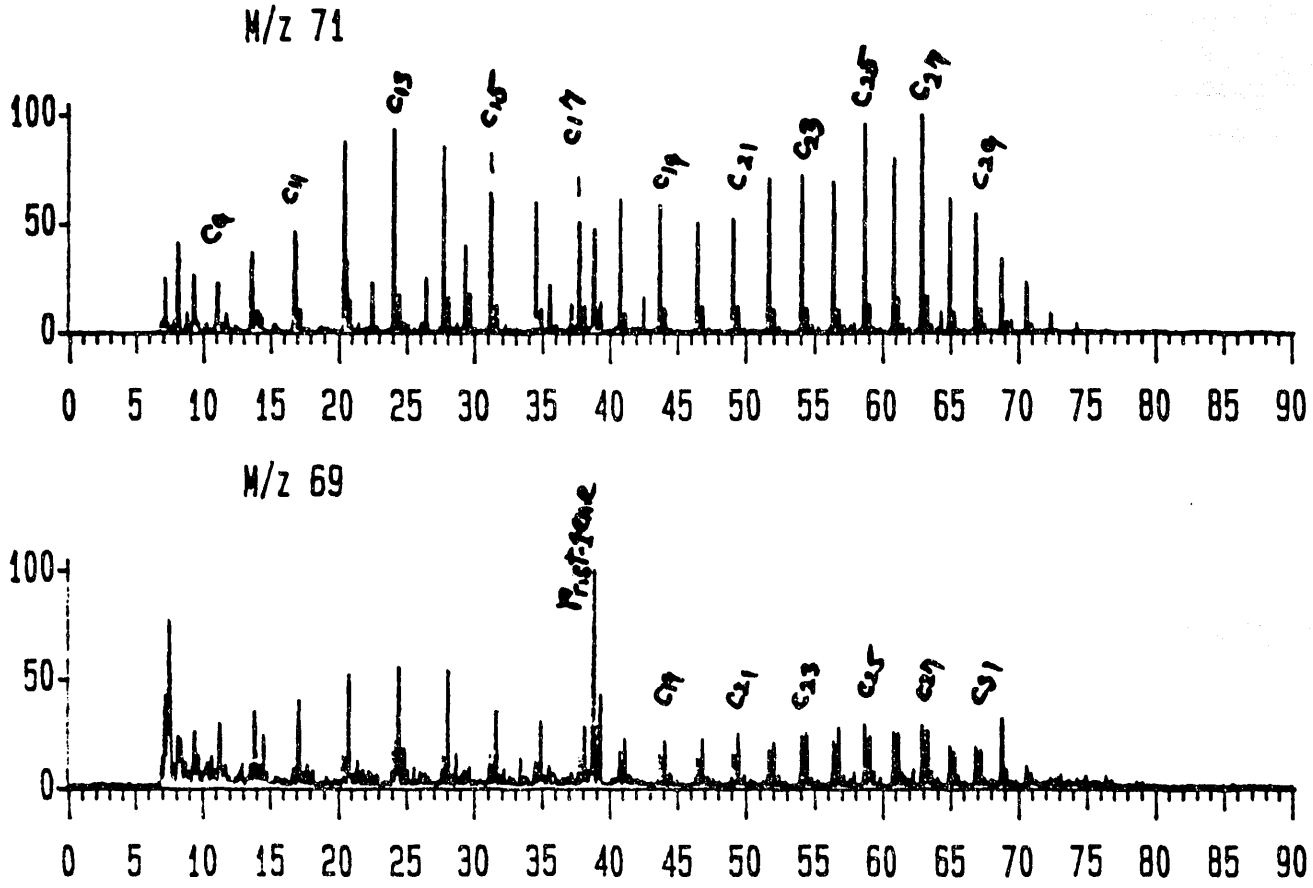

Figure 27. Single ion chromatograms from pyrolysis-GC-MS of DECS-7 Adaville #1 coal (representing the homologous series of alkanes (m/z 71) and alkenes (m/z 69).

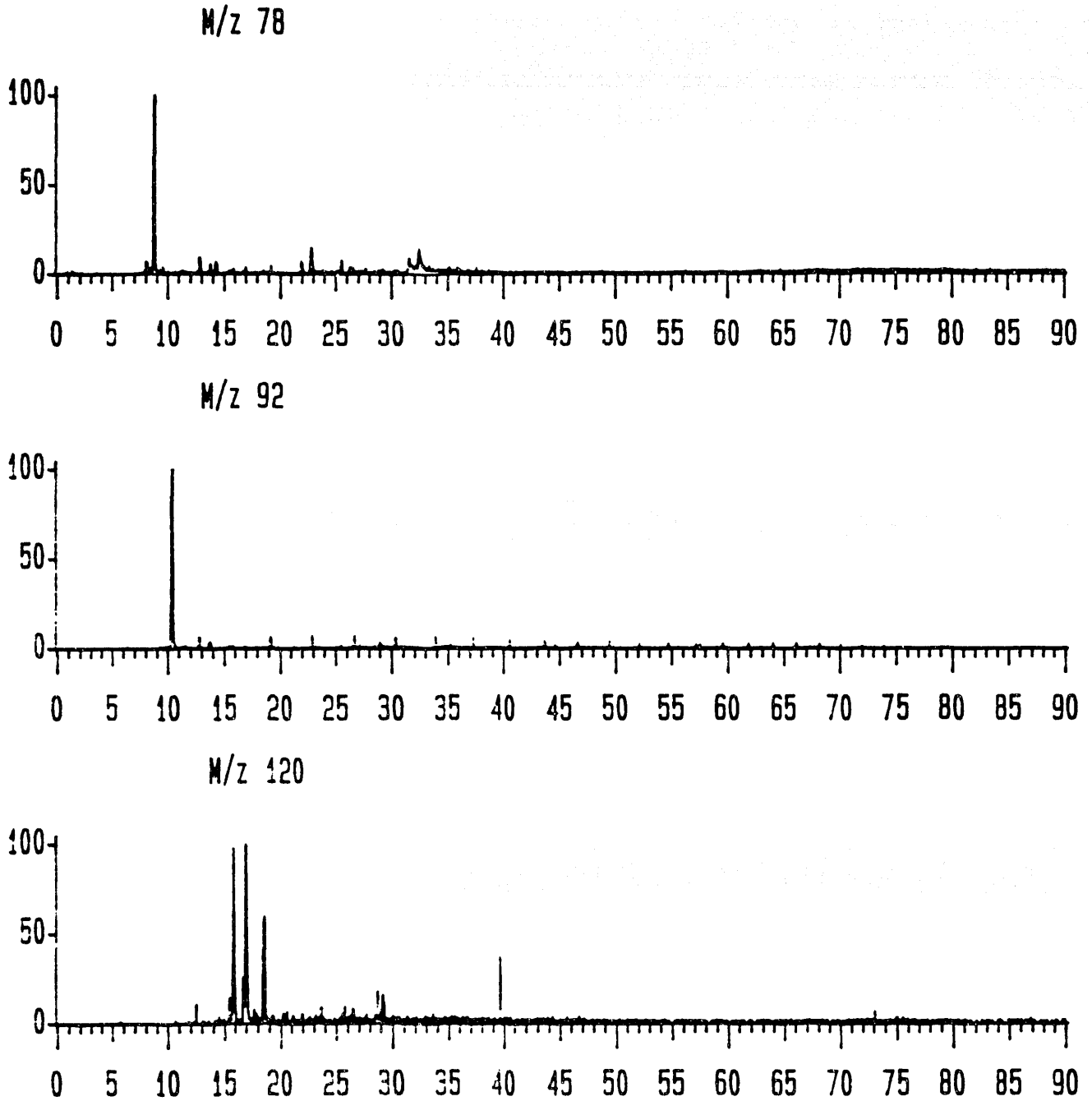

Figure 28. Single ion chromatograms from pyrolysis-GC-MS of DECS-7 Adaville #1 coal (representing benzene (m/z 78), toluene (m/z 92) and C_3-benzenes (m/z 120).

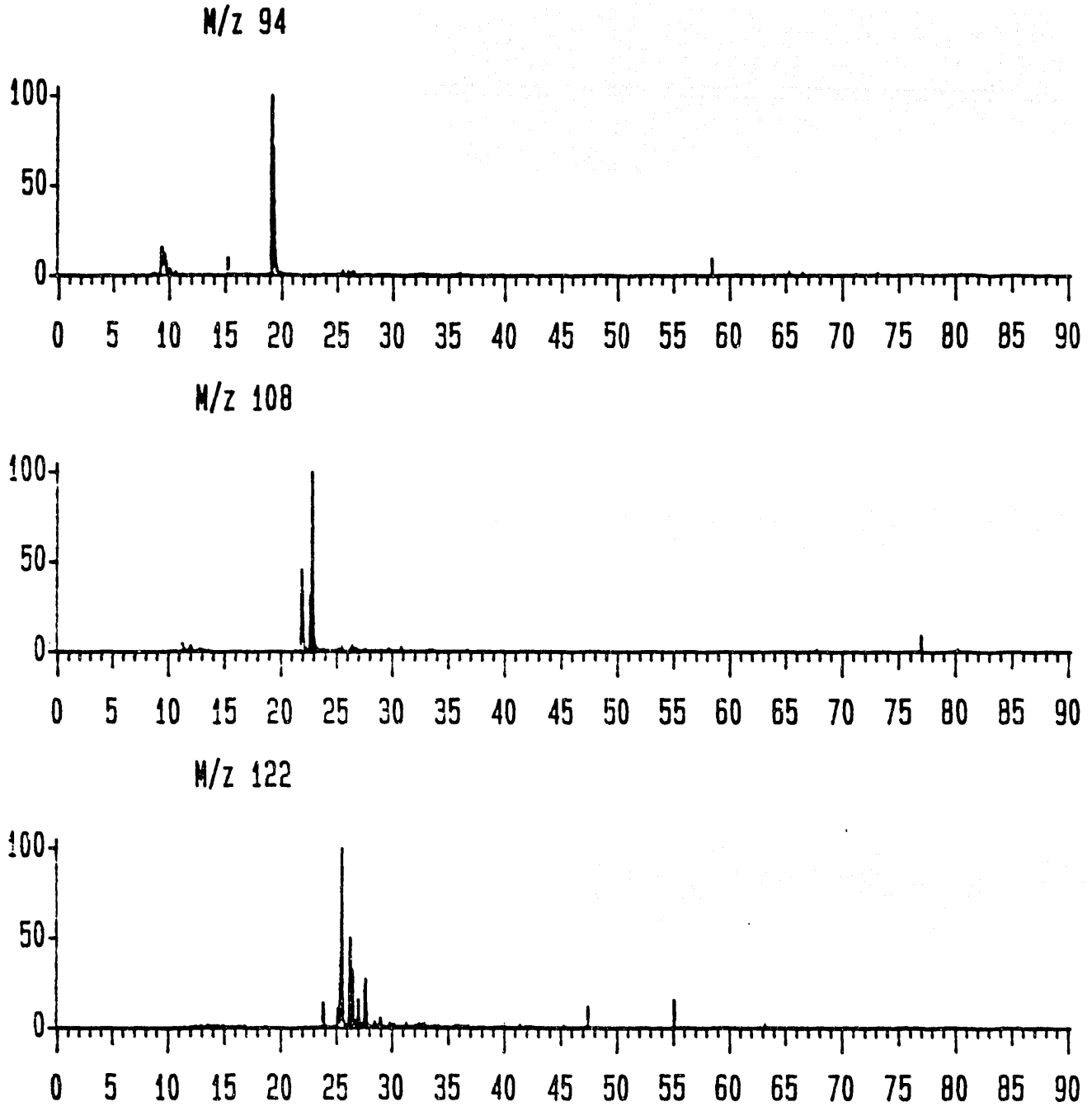

Figure 29. Single ion chromatograms from pyrolysis-GC-MS of DECS-7 Adaville #1 coal (representing phenol and alkylphenol).

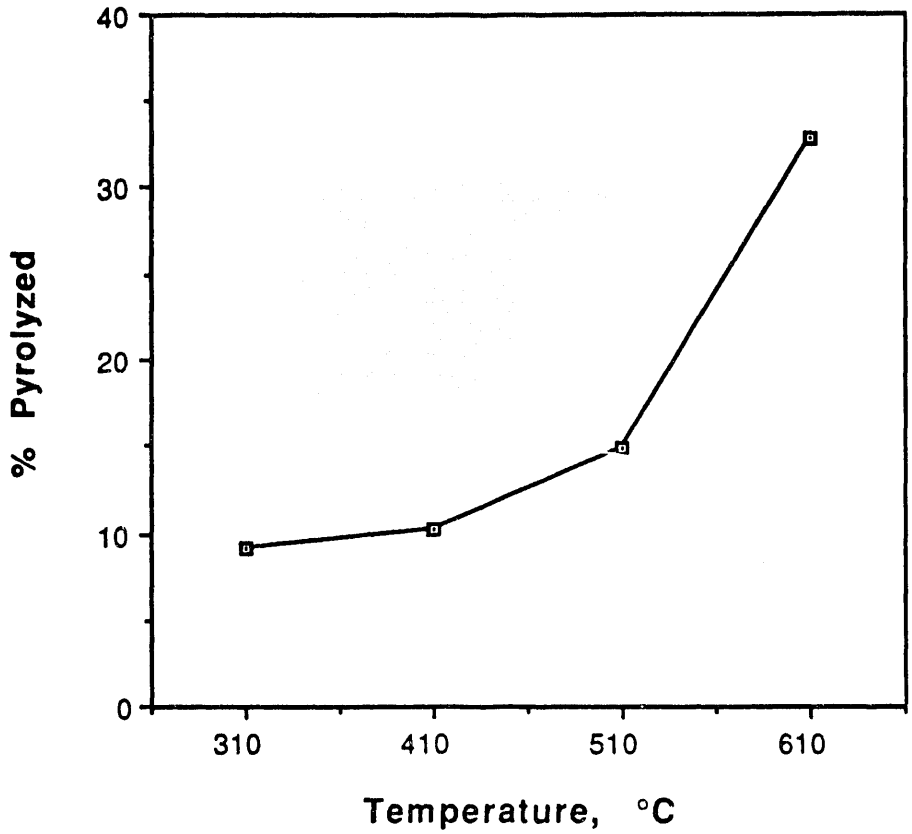

Figure 30. Percentage of the Adaville #1 coal pyrolyzed vs pyrolysis temperature.

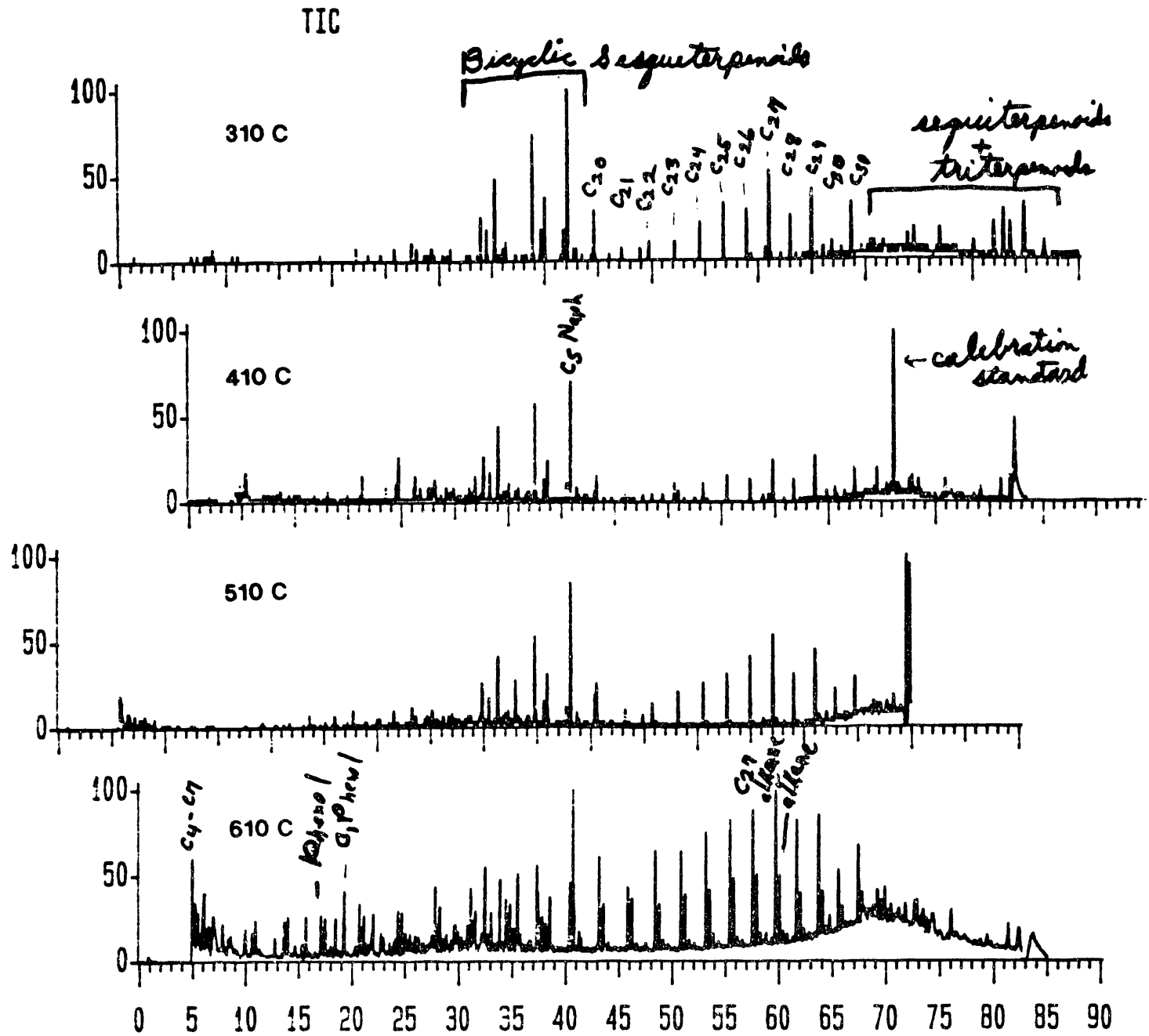

Figure 31. Pyrolysis-GC-MS chromatogram of the Blind Canyon coal (pyrolysis at 310°C, 410°C, 510°C and 610°C).

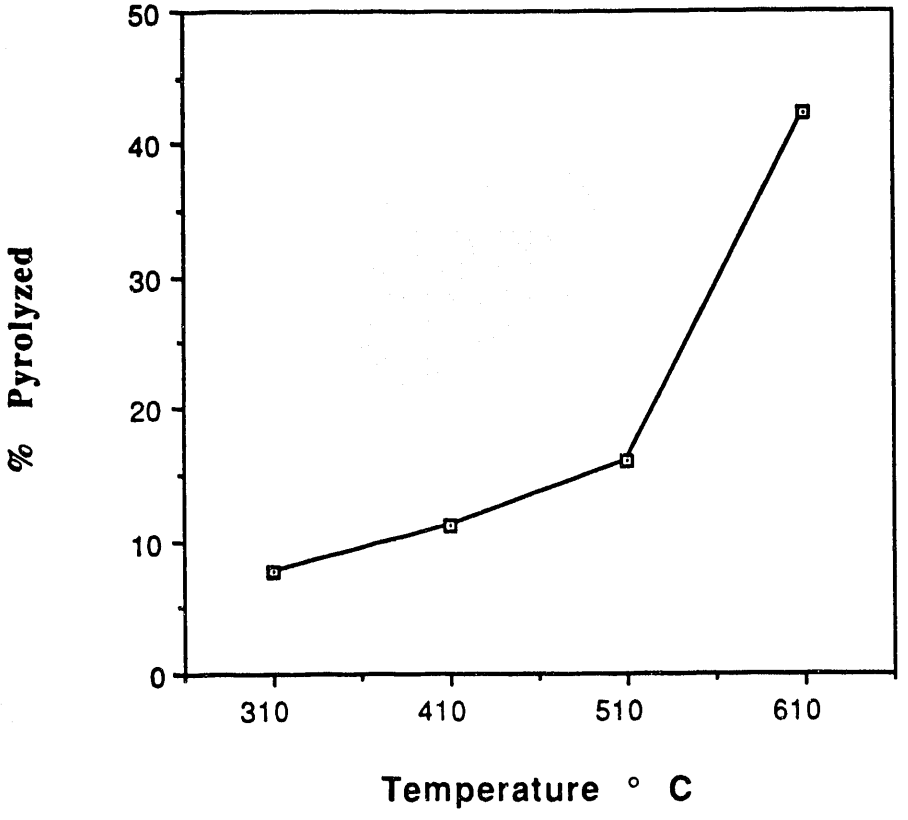

Figure 32. Percentage of the Blind Canyon coal pyrolyzed vs pyrolysis temperature.

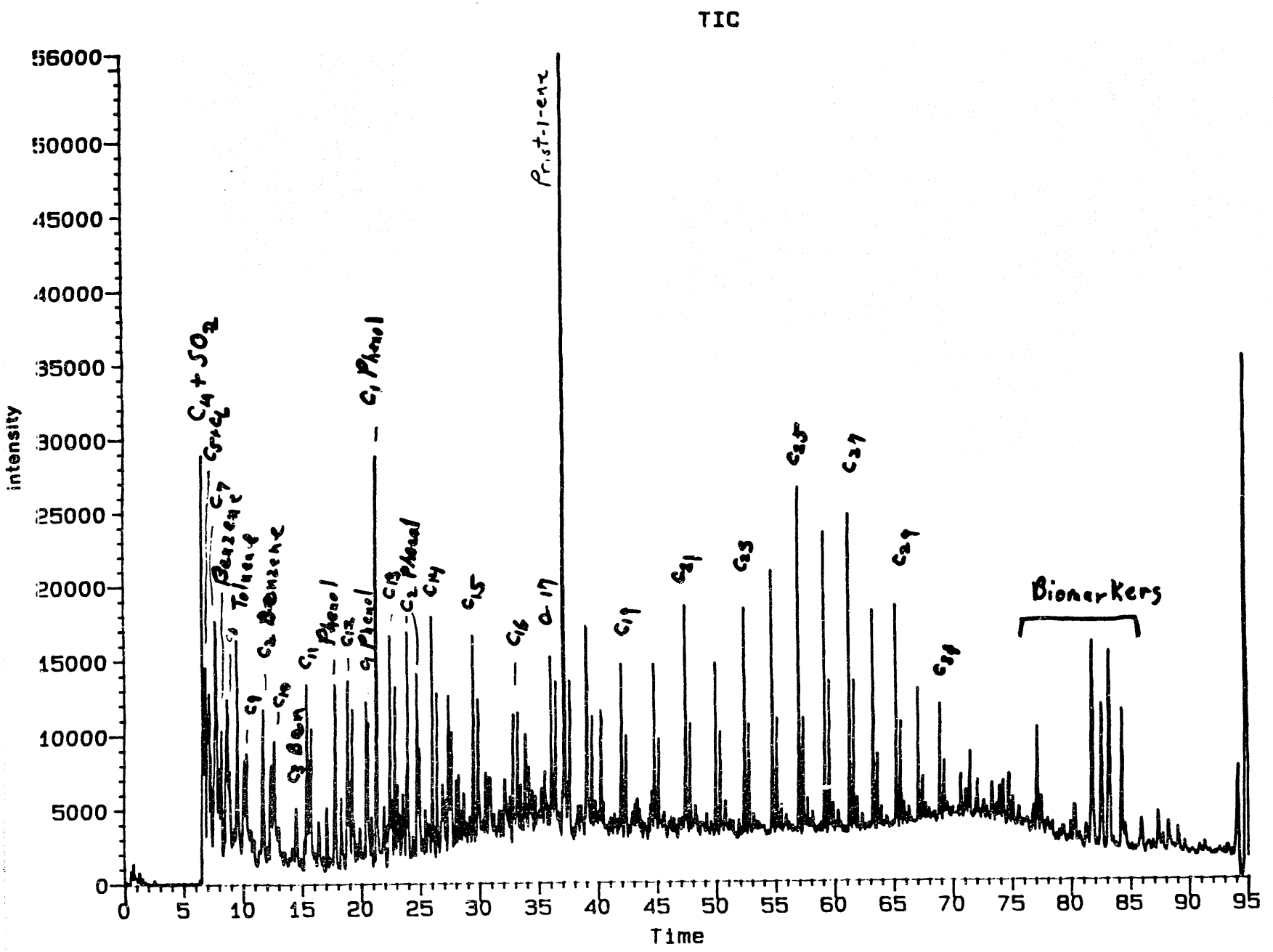

Figure 33. Pyrolysis-GC-MS chromatogram of the Adaville #1 coal.

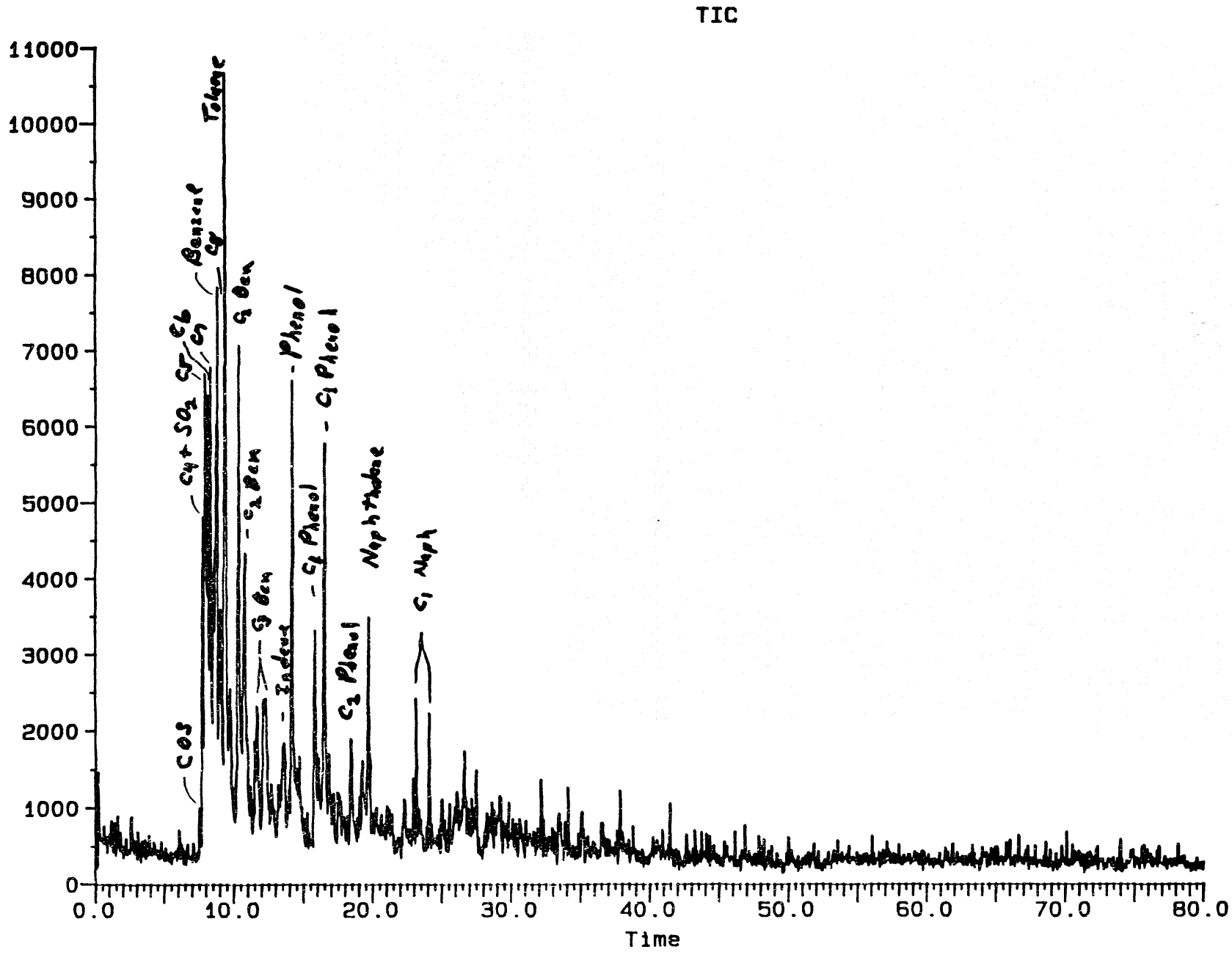

Figure 34. Pyrolysis-GC-MS chromatogram of the residue from Adaville #1 coal (after thermal pretreatment and extraction).

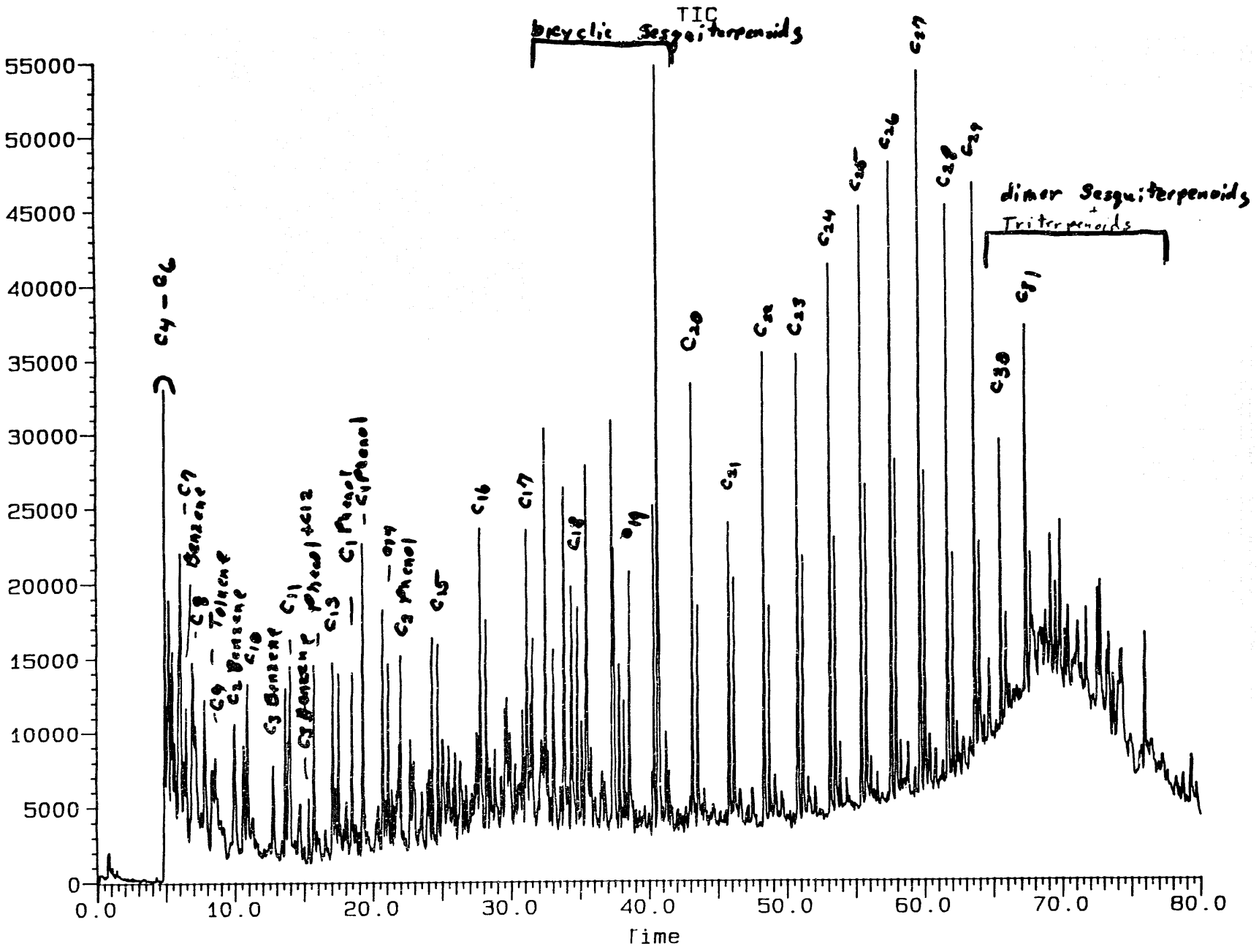

Figure 35. Pyrolysis-GC-MS chromatogram of the Blind Canyon coal.

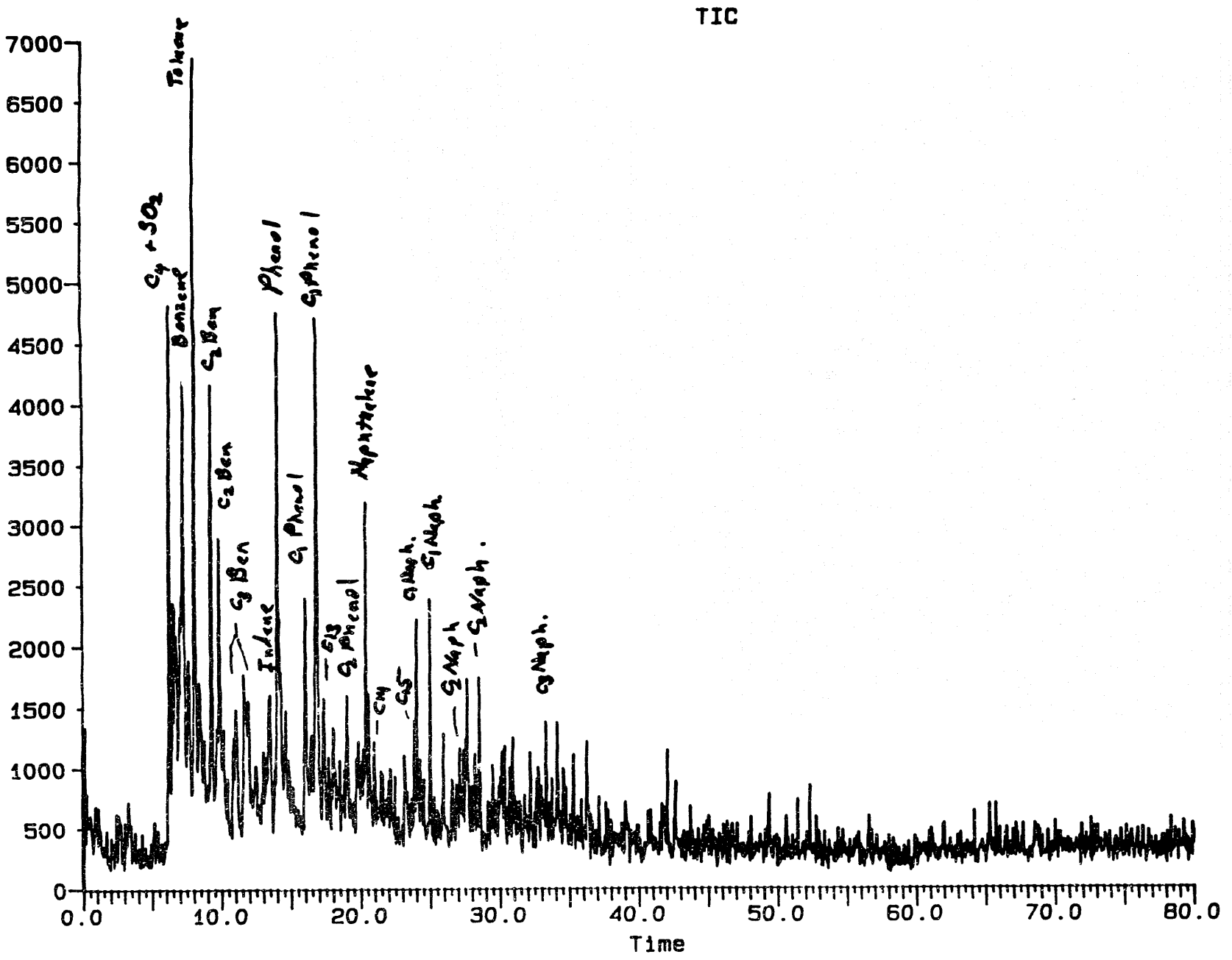

Figure 36. Pyrolysis-GC-MS chromatogram of the residue from Blind Canyon coal (after thermal pretreatment and extraction).

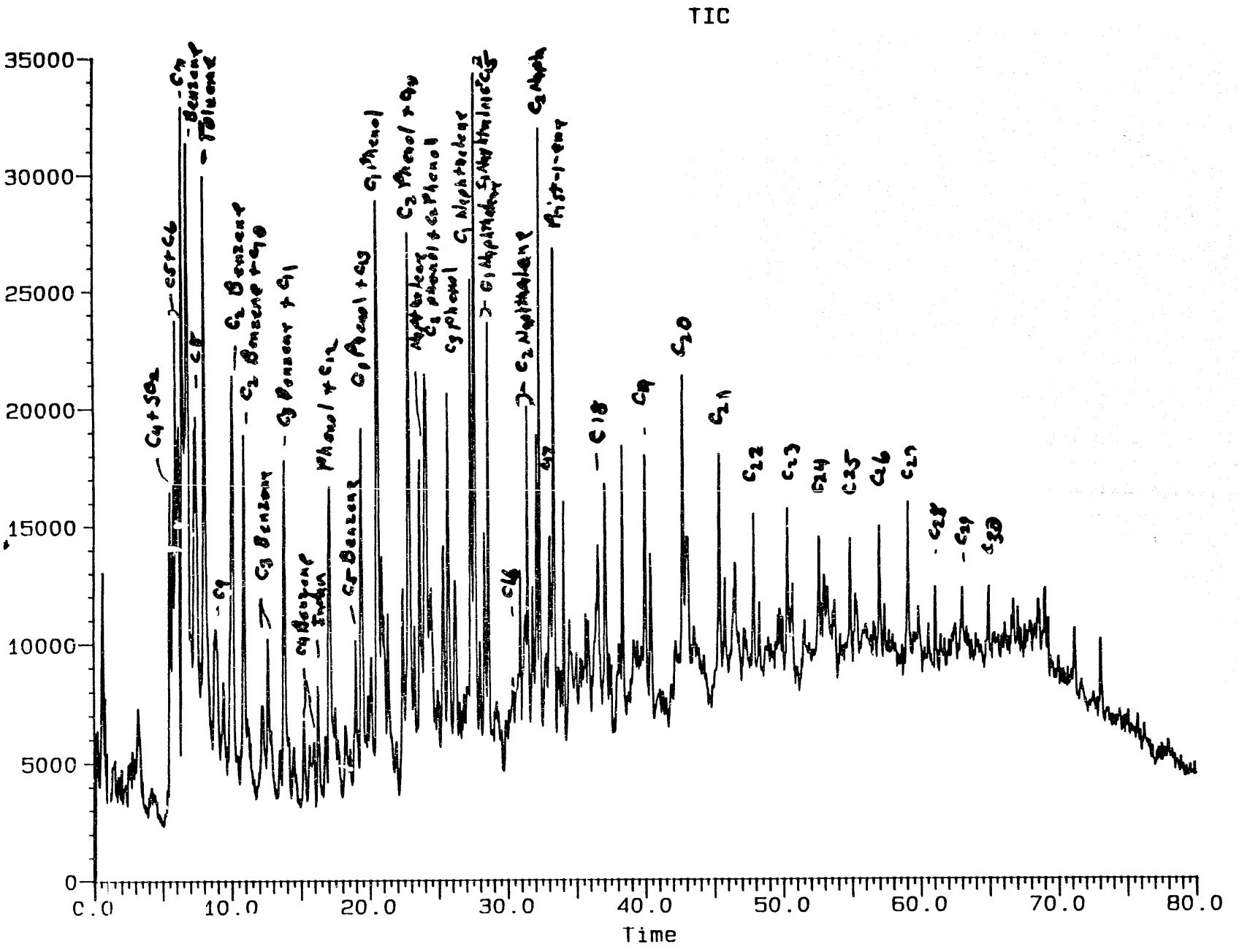

Figure 37. Pyrolysis-GC-MS chromatogram of the Pittsburgh #8 coal.

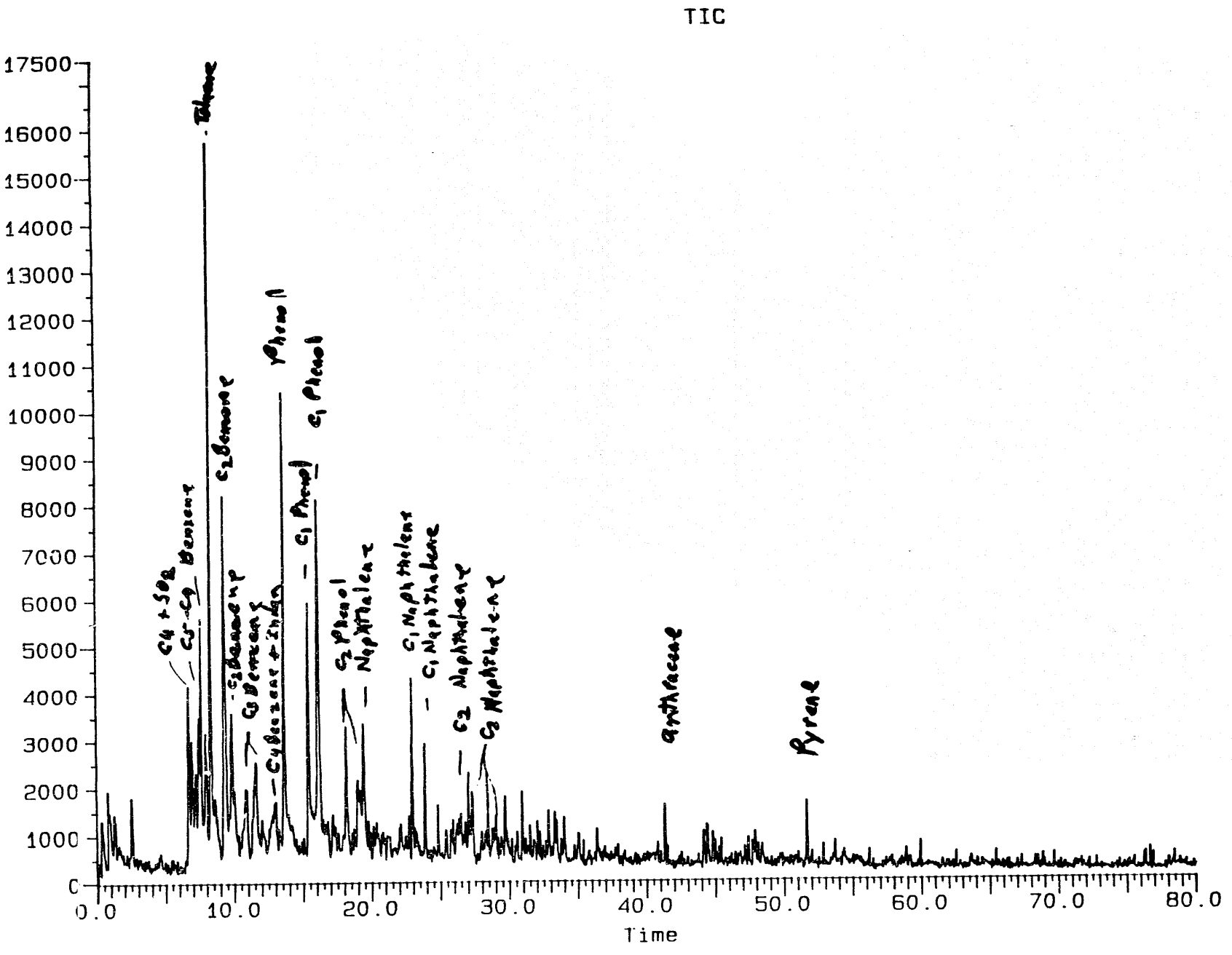

Figure 38. Pyrolysis-GC-MS chromatogram of the residue from Pittsburgh #8 coal (after thermal pretreatment and extraction).

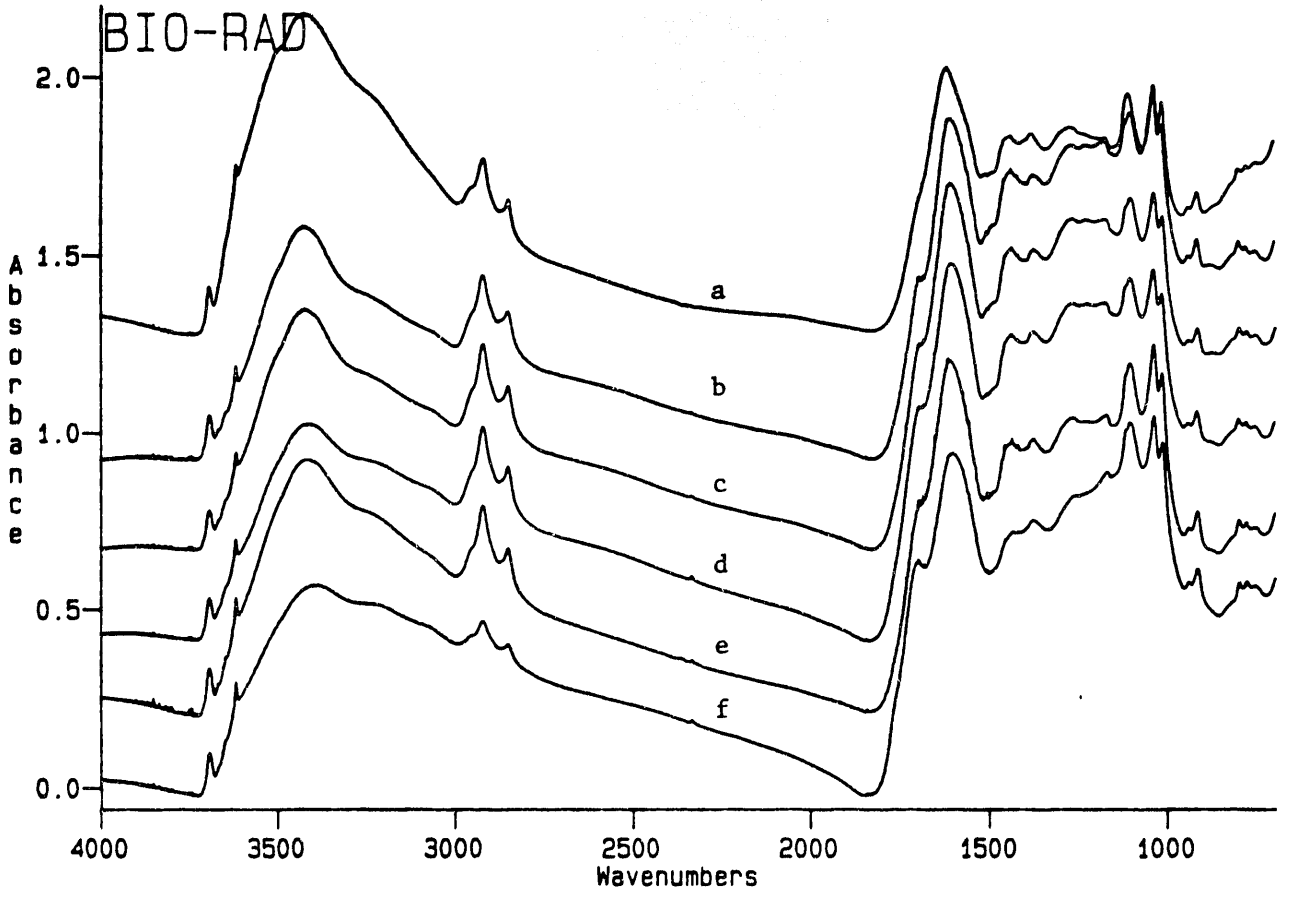

Figure 39. FTIR spectra of the DECS-8 raw coal a) as-received; dried in air at 100 °C for b) 2 h; c) 20 h; d) 100 h; e) dried at 125 °C for 20 h; and f) at 150 °C for 20 h.

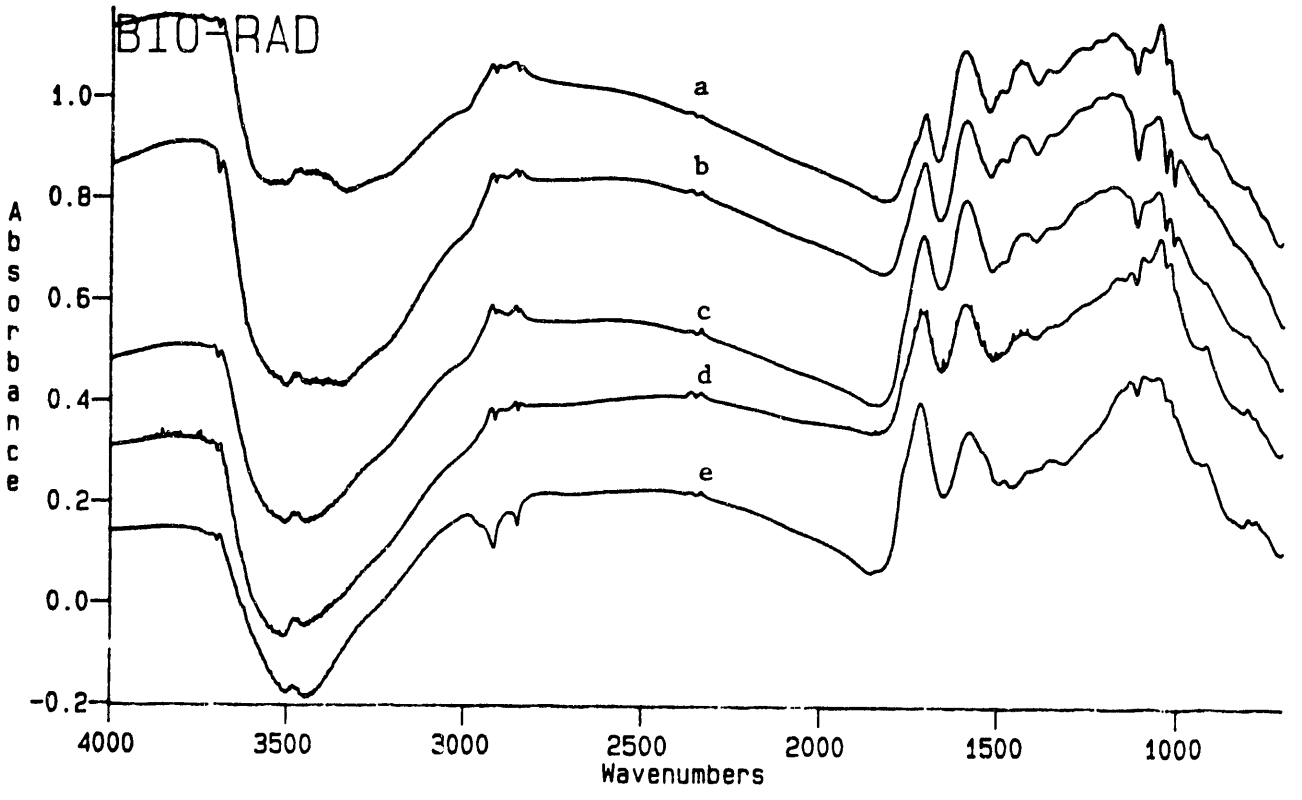

Figure 40. FTIR difference spectra after subtracting the FTIR spectrum of the raw coal 'as received' from the FTIR spectra of the coal dried in air at100 °C for a)2 h; b) 20 h; c) 100 h; d) coal dried at 125 °C for 20 h and e) at 150 °C for 20 h.

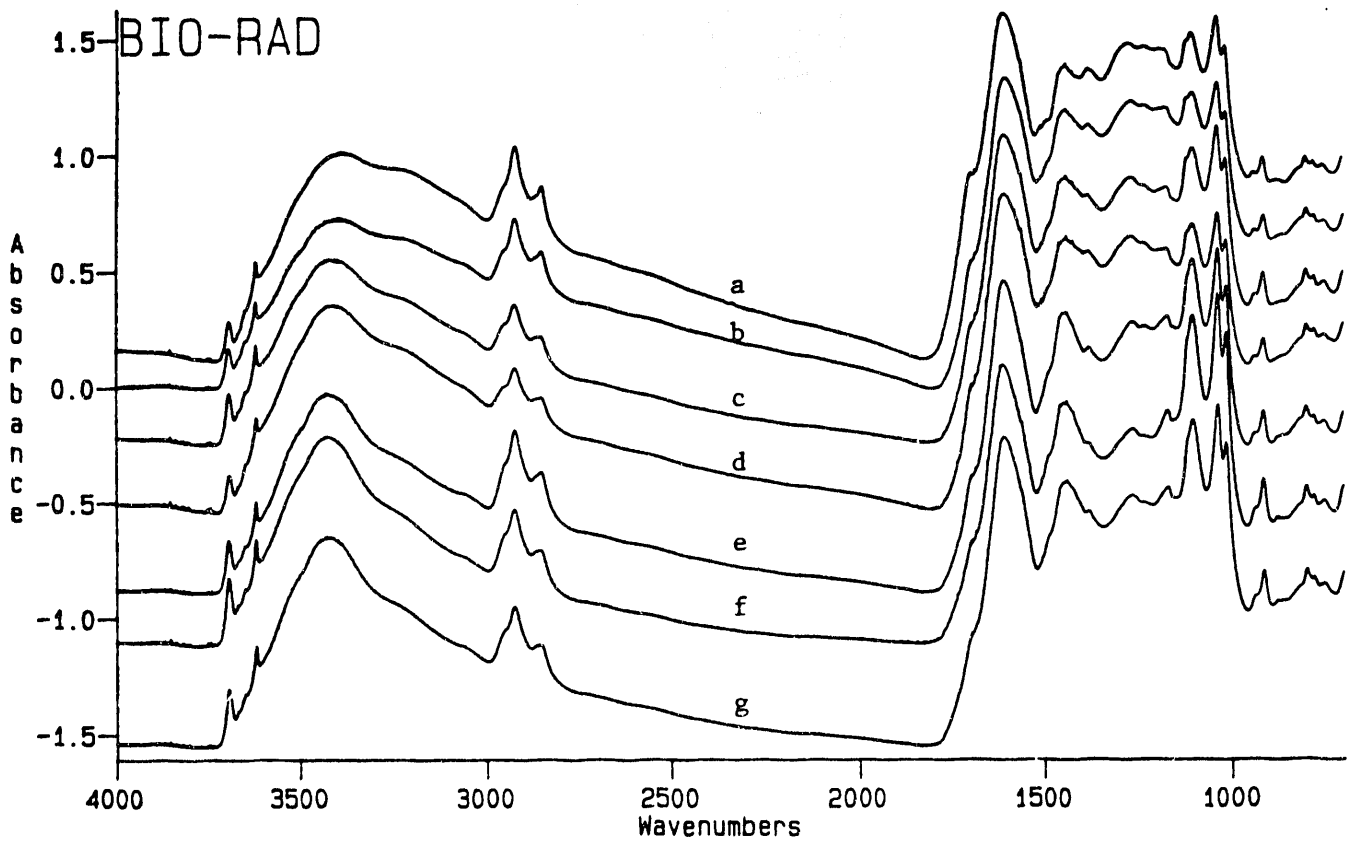

Figure 41. FTIR spectra of the THF-extracted coal dried in air for 2 h at 100 °C; a) unreacted; and reacted at 350 °C without catalyst; b) solvent free; c) with tetralin; d) with 1-methylnaphthalene; and in presence of catalyst; e) solvent free; f) with tetralin; g) with 1-methyl-naphthalene.

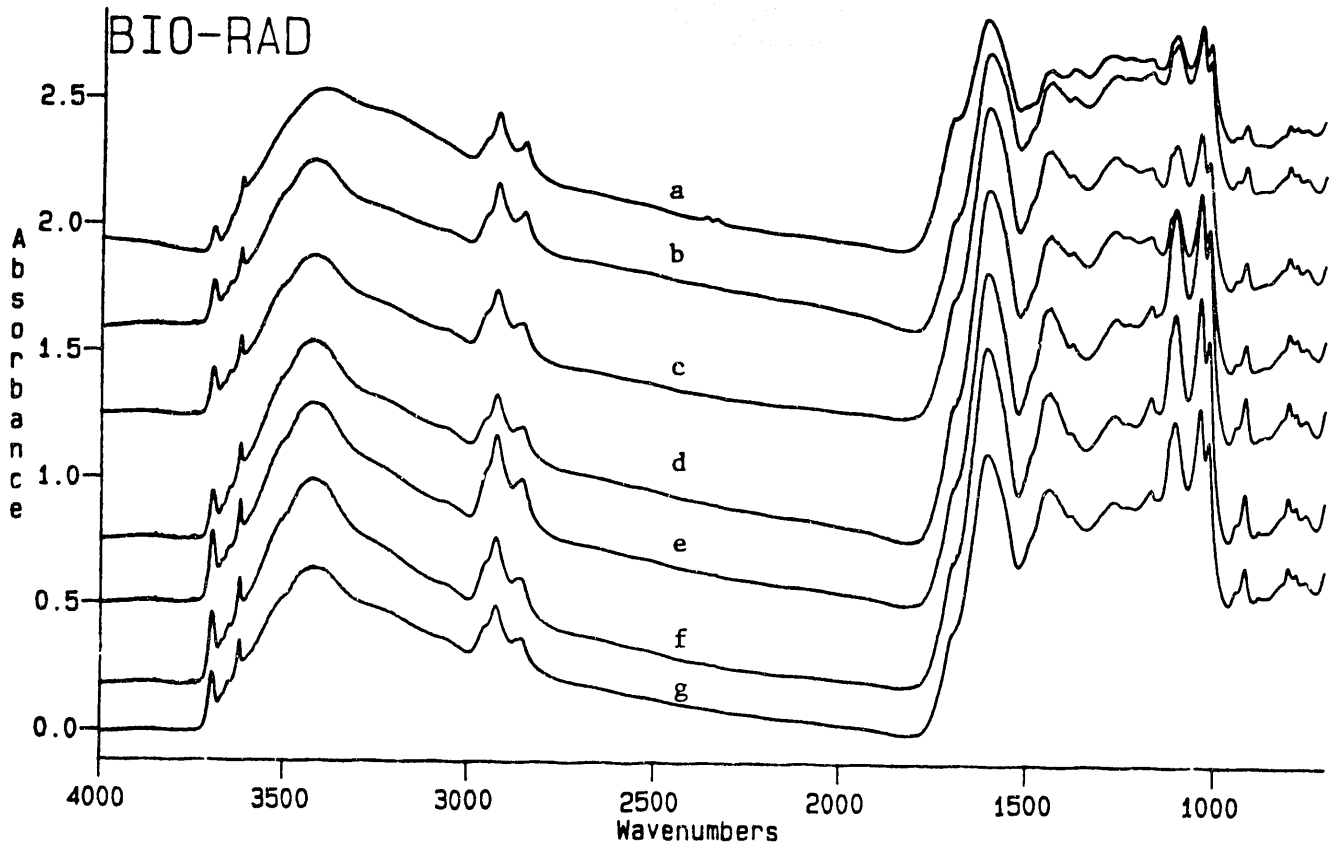

Figure 42. FTIR spectra of the THF-extracted coal dried in air for 20 h at 100 °C; a) unreacted; and reacted at 350 °C without catalyst; b) solvent free; c) with tetralin; d) with 1-methylnaphthalene; and in presence of catalyst; e) solvent free; f) with tetralin, g) with 1-methyl-naphthalene.

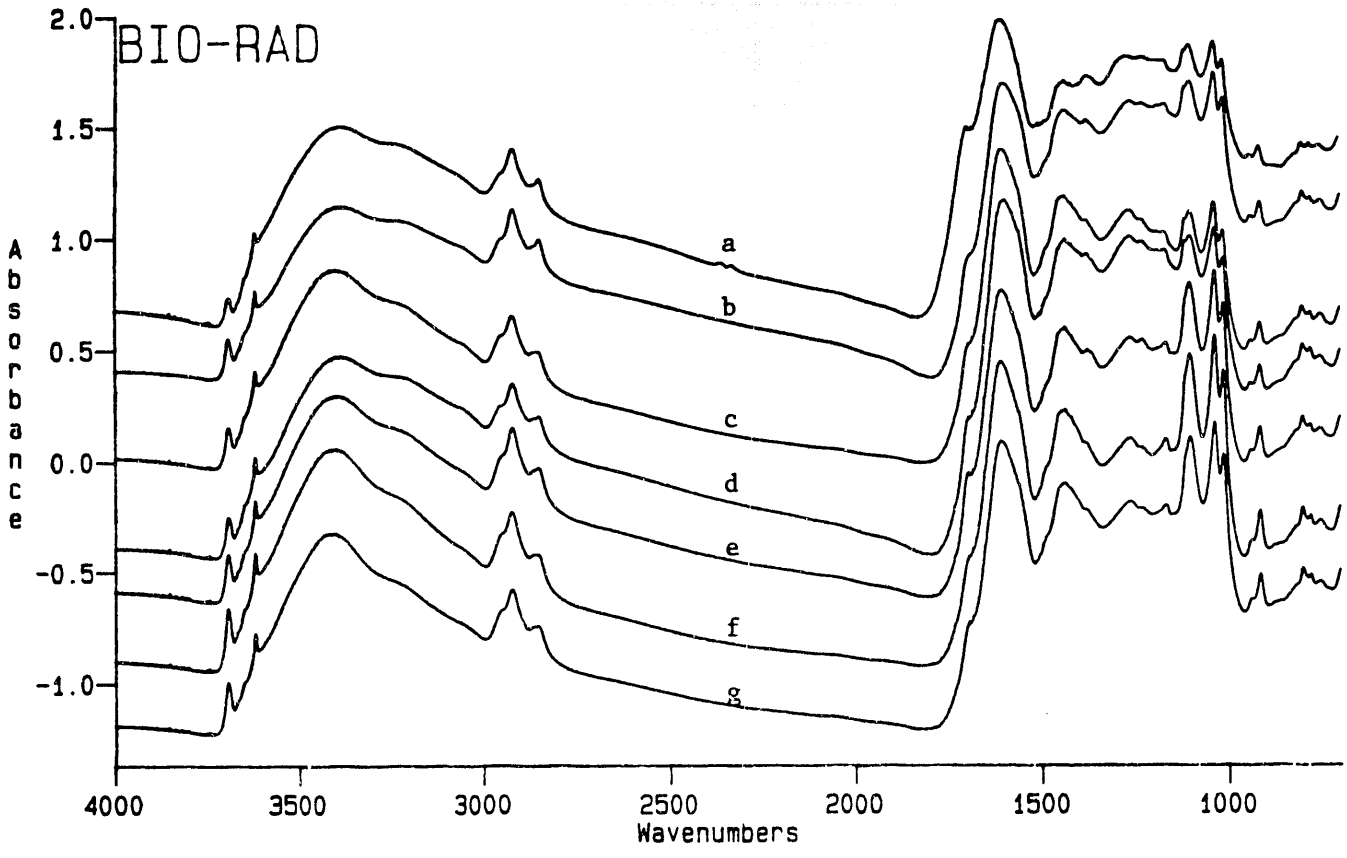

Figure 43. FTIR spectra of the THF-extracted coal dried in air for 100 h at 100 °C;a) unreacted; and reacted at 350 °C without catalyst; o) solvent free; c) with tetralin; d) with 1-methylnaphthalene; and in presence of catalyst ; e) solvent free; f) with tetralin; g) with 1-methyl-naphthalene.

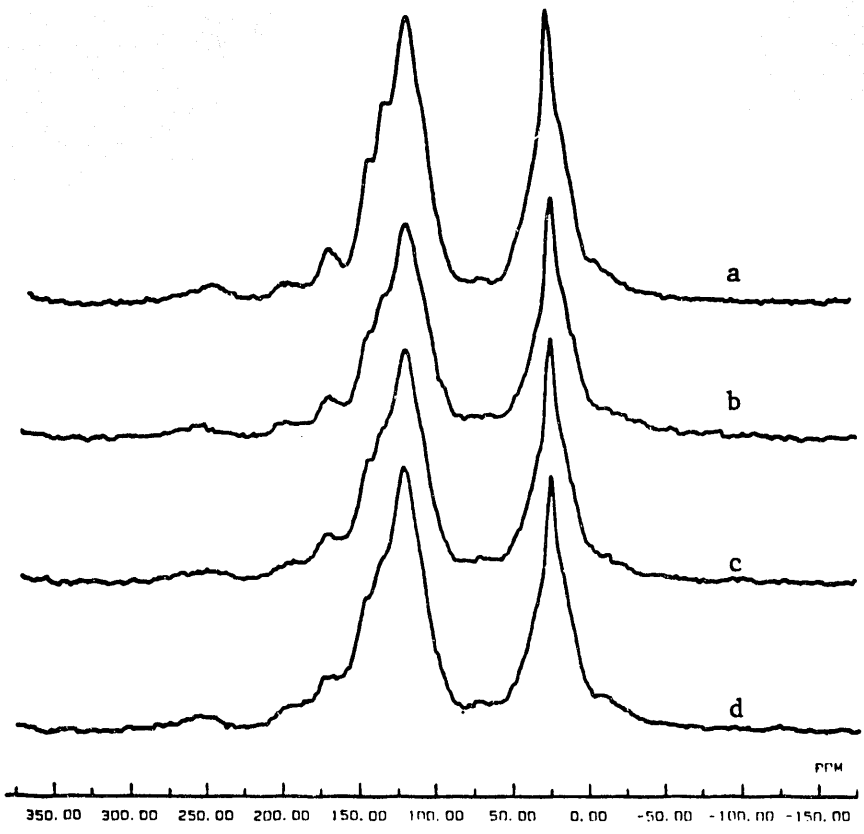

Figure 44. CPMAS ^{13}C NMR spectra of the coal a) raw as received; dried in air at 100 °C for; b) 2 h; c) 20 h; d) 100 h.

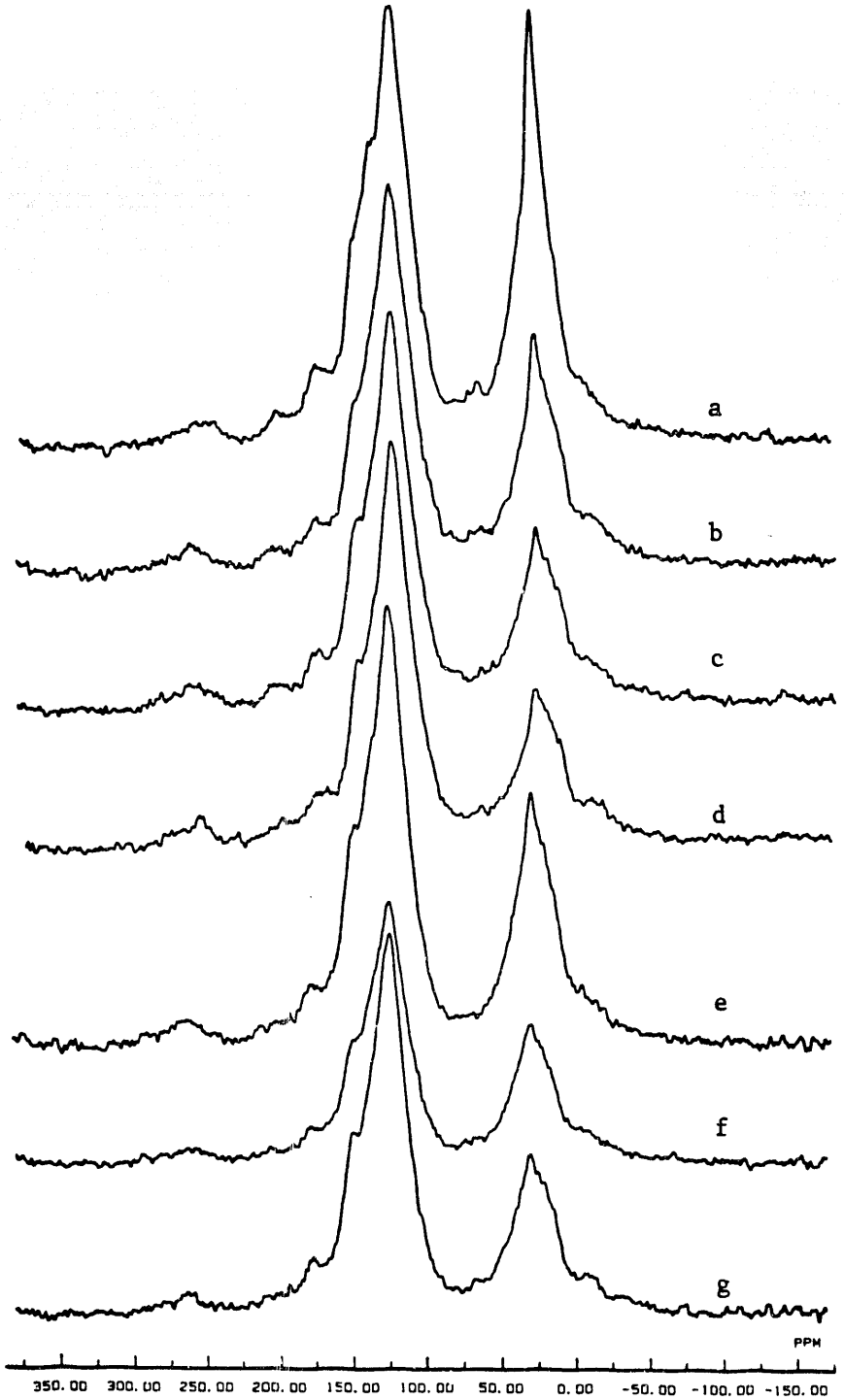

Figure 45. CPMAS ^{13}C NMR spectra of the THF-extracted coal dried in air for 2 h at 100 °C; a) unreacted; and reacted at 350 °C without catalyst; b) solvent free; c) with tetralin; d) with 1-methylnaphthalene; and in presence of catalyst; e) solvent free; f) with tetralin; g) with 1-methylnaphthalene.

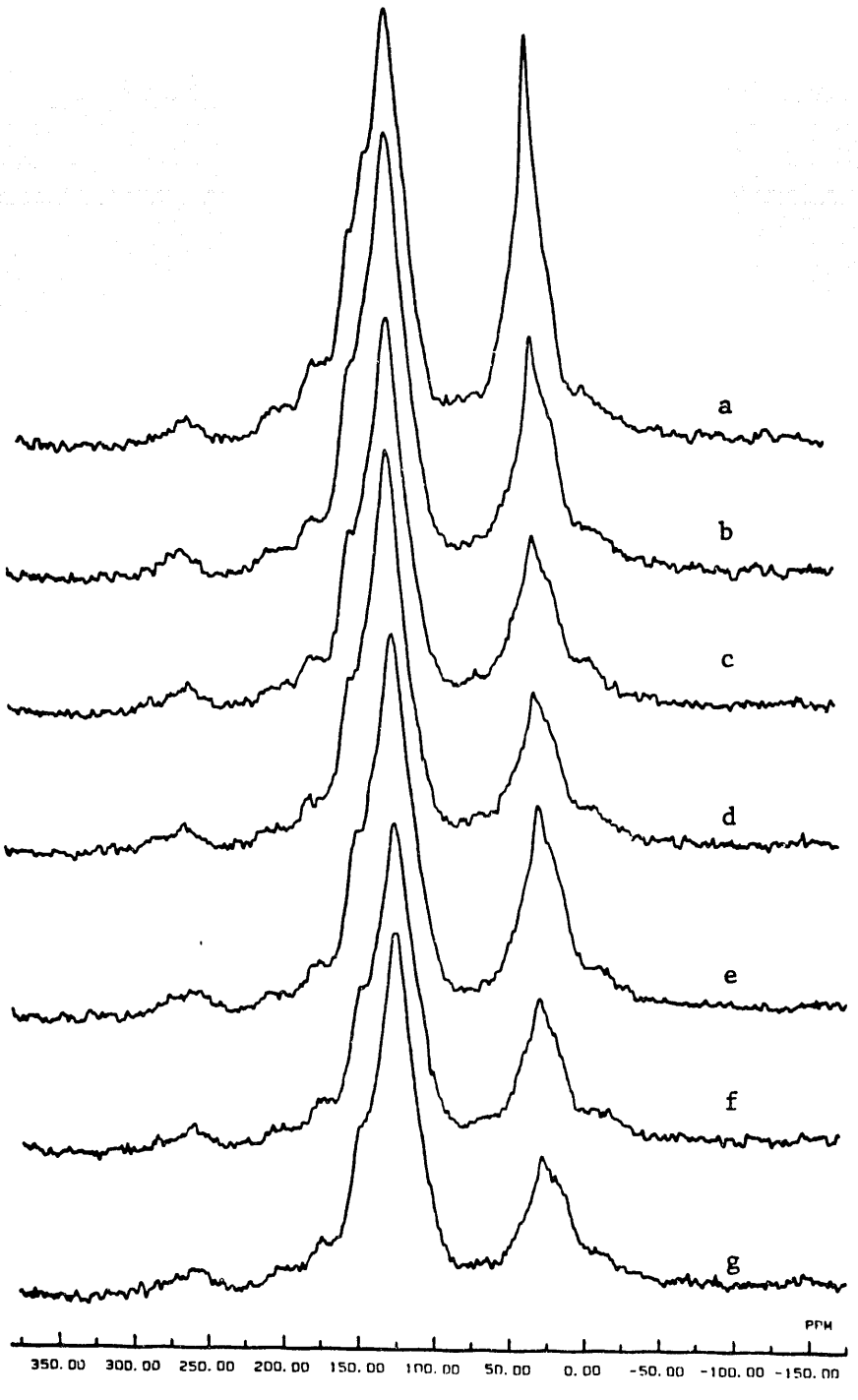

Figure 46. CPMAS ^{13}C NMR spectra of the THF-extracted coal dried in air for 20 h at 100 °C; a) unreacted; and reacted at 350 °C without catalyst; b) solvent free; c) with tetralin; d) with 1-methylnaphthalene; and in presence of catalyst; e) solvent free; f) with tetralin; g) with 1-methyl-naphthalene.

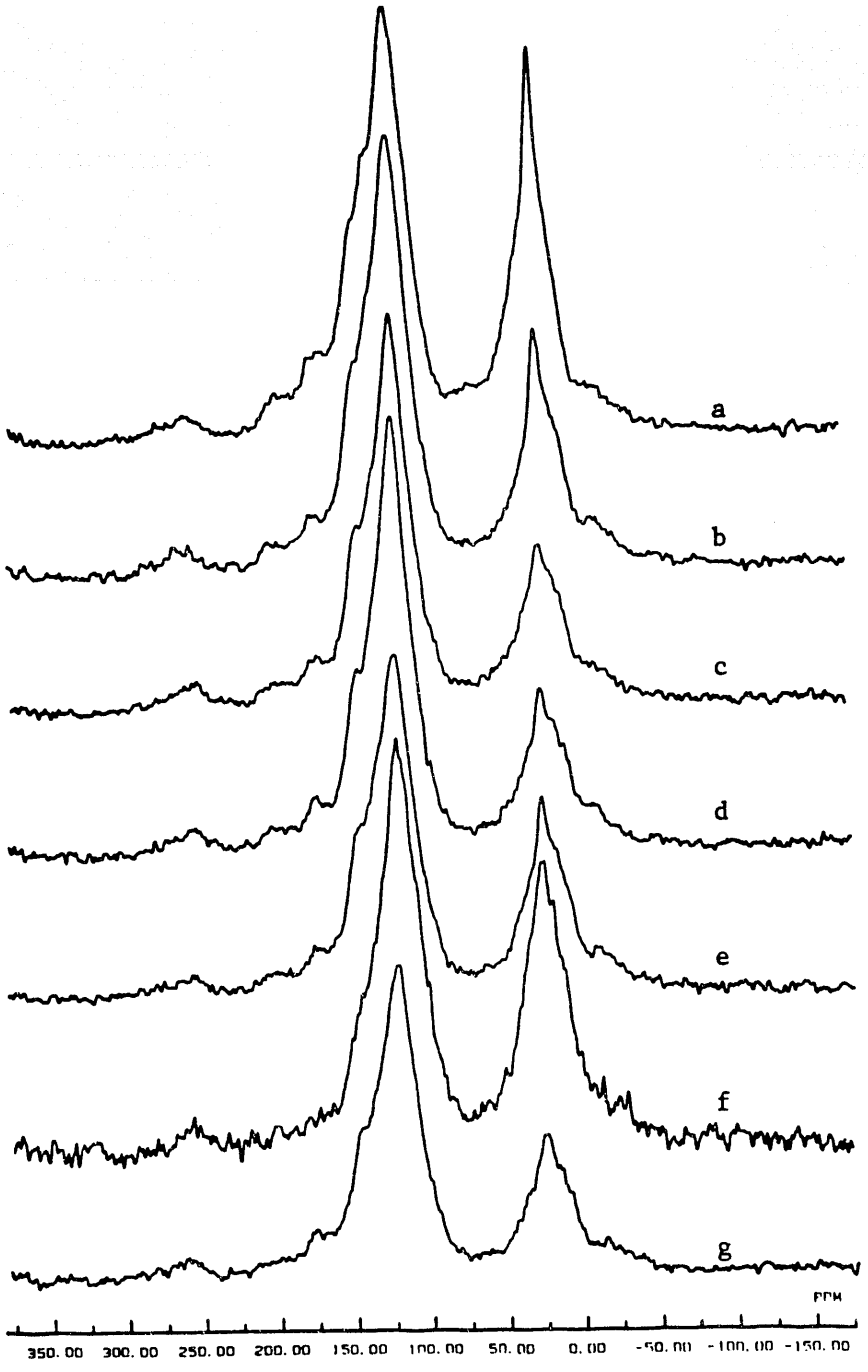

Figure 47. CPMAS ^{13}C NMR spectra of the THF-extracted coal dried in air for 100 h at 100 °C; a) unreacted; and reacted at 350 °C without catalyst; b) solvent free; c) with tetralin; d) with 1-methylnaphthalene; and in presence of catalyst; e) solvent free; f) with tetralin; g) with 1-methyl-naphthalene.

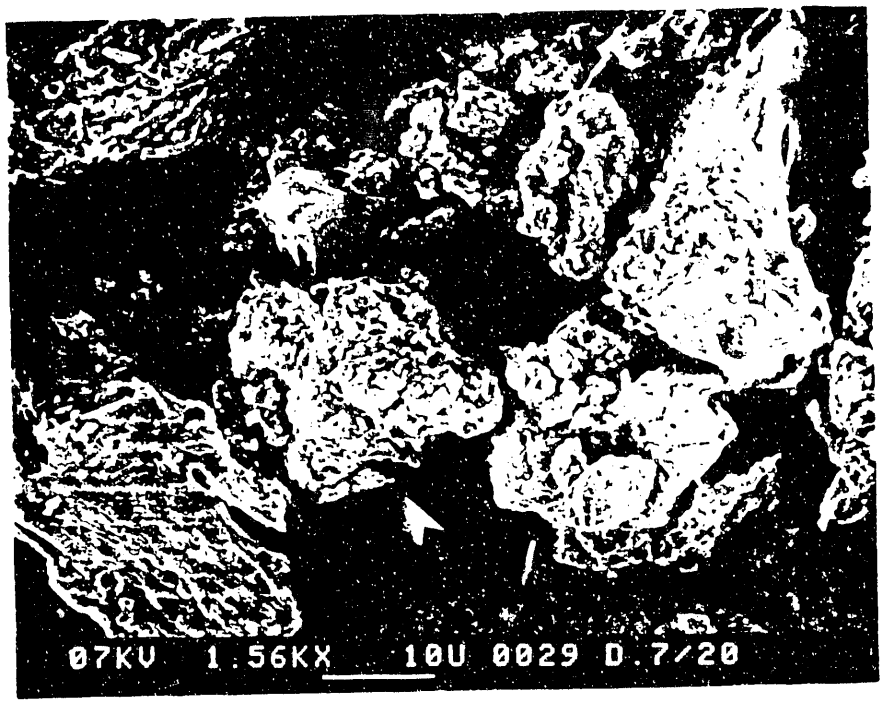

(a)

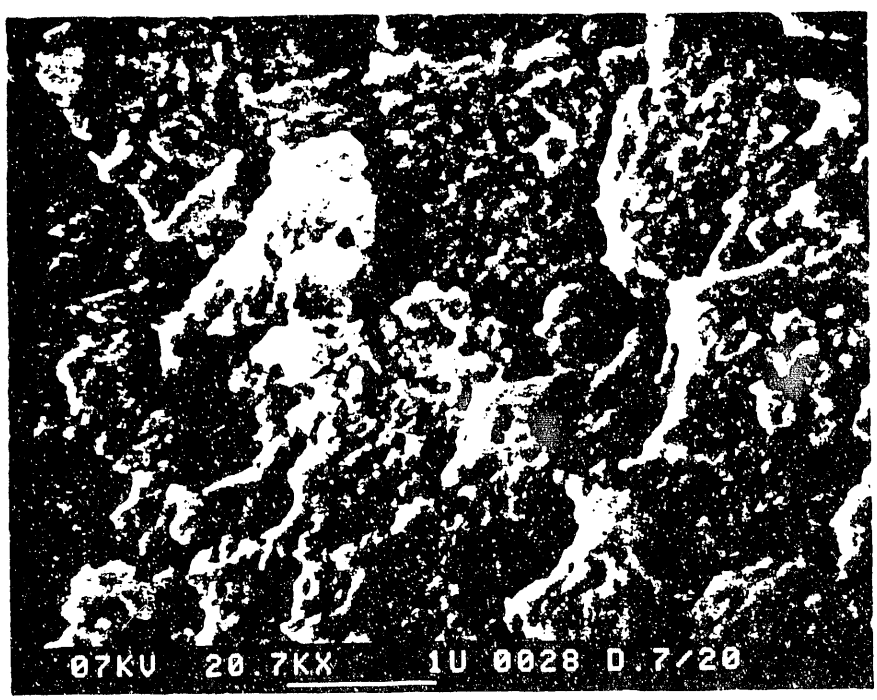

(b)

Figure 48. SEM micrograph of dried DECS-9. (a) several coal particles under low magnification; (b) higher magnification of the particle pointed by an arrow in (a).

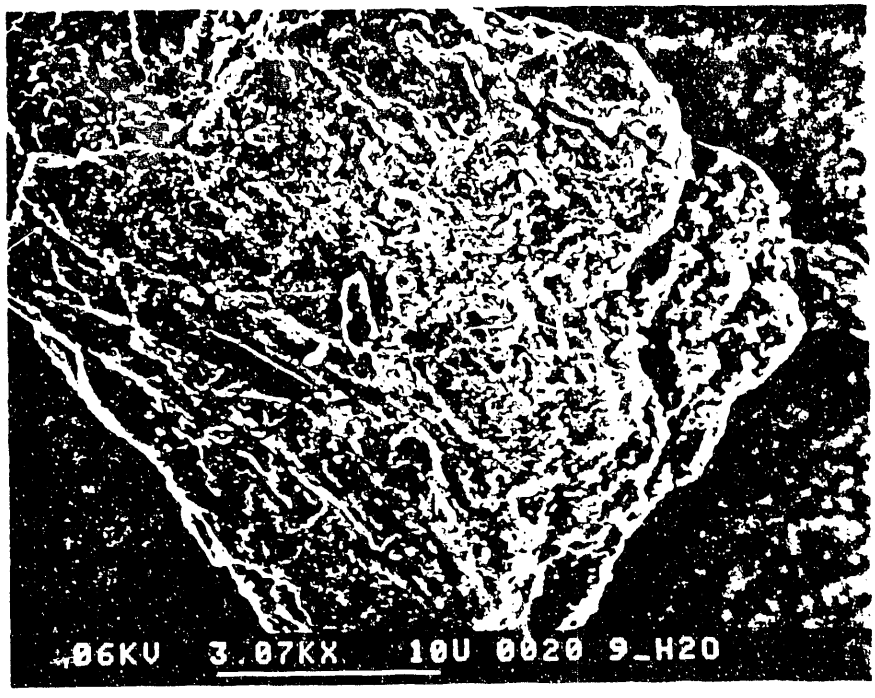

(a)

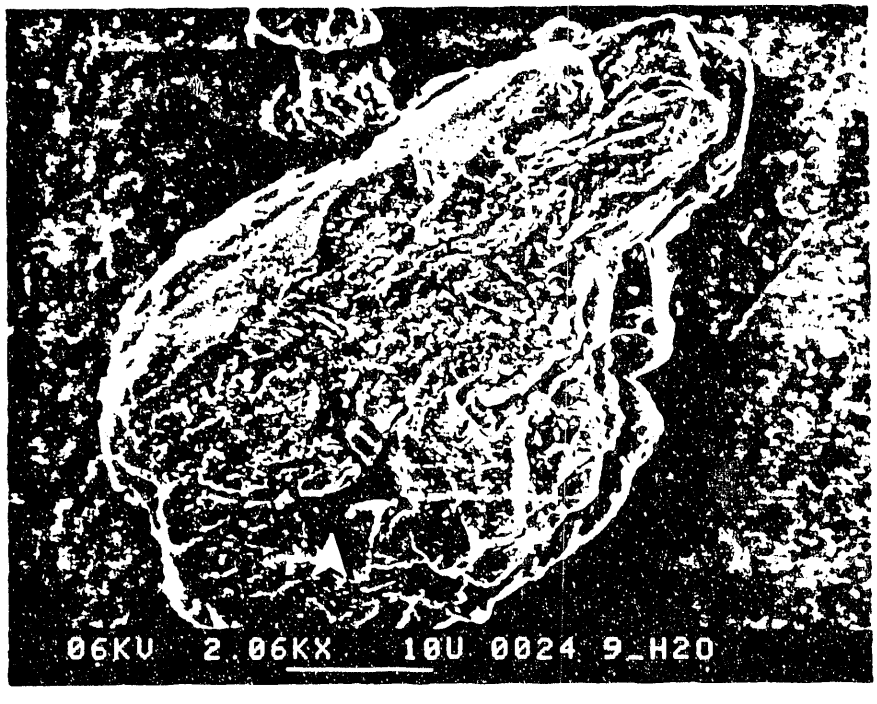

(b)

Figure 49. SEM micrograph of catalytic DECS-9 coal sample prepared by incipient wetness method using aqueous solution. (a) and (b) are two different particles.

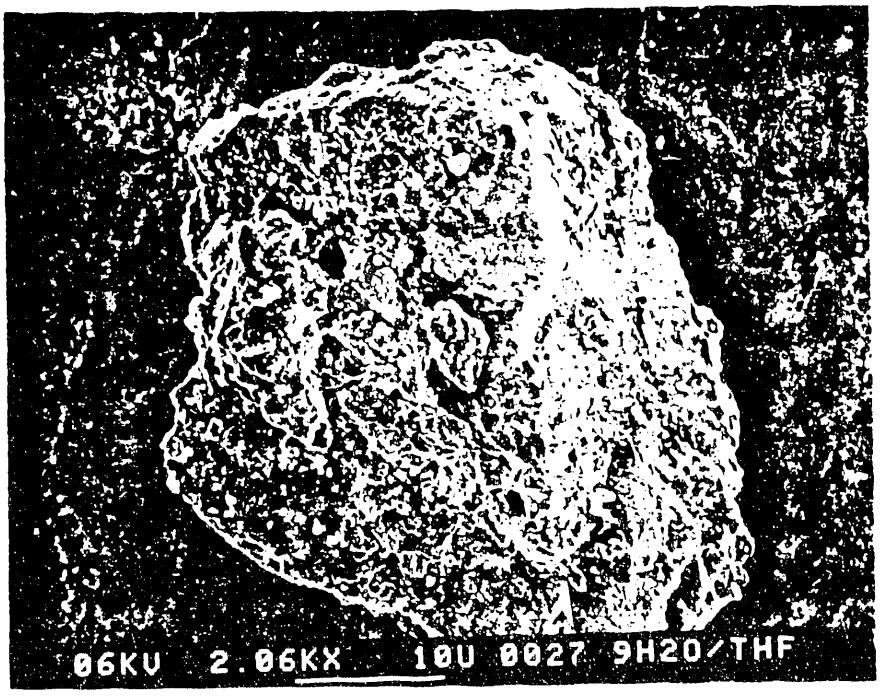

Figure 50. SEM micrograph of catalytic DECS-9 coal sample prepared by incipient wetness method using H_2O/THF solution.

END DATE

1-15-93